

Real-ESSI Simulator

Modeling and Simulation Examples

Yuan Feng, Han Yang, José Abell,
Sumeet Kumar Sinha, Fatemah Behbehani, Hexiang Wang
and
Boris Jeremić

University of California, Davis, CA. USA



Version: 3Jul2025, 10:20

<http://real-essi.us/>

This document is an excerpt from: <http://sokocalo.engr.ucdavis.edu/~jeremic/LectureNotes/>

please use google-chrome to view this PDF so that hyperlinks work



Contents

I	Modeling and Simulation Examples	11
1	Constitutive, Material Behaviour Examples	
	(2016-2017-2019-2023-)	12
1.1	Chapter Summary and Highlights	13
1.2	Elastic Solid Constitutive Examples	14
1.2.1	Linear Elastic Constitutive Examples	14
	Pure Shear, Monotonic Loading	14
	Pure Shear, Cyclic Loading	15
	Uniaxial Strain, Monotonic Loading	16
	Uniaxial Strain, Cyclic Loading	17
1.2.2	Nonlinear Elastic Constitutive Examples	18
	Triaxial Uniform Pressure, Monotonic Loading	18
1.3	Elastic Plastic Solid Constitutive Examples	19
1.3.1	Elastic Perfectly Plastic Constitutive Examples	19
	Pure Shear	19
	Uniaxial Strain	20
1.3.2	Elastic Plastic, Isotropic Hardening, Constitutive Examples	21
	Pure Shear, Monotonic Loading	21
	Pure Shear, Cyclic Loading	22
	Uniaxial Strain, Monotonic Loading	23
	Uniaxial Strain, Cyclic Loading	24
1.3.3	Elastic Plastic, Kinematic Hardening, Constitutive Examples	25
	Pure Shear, Monotonic Loading	25
	Pure Shear, Cyclic Loading	26
	Uniaxial Strain, Monotonic Loading	27
	Uniaxial Strain, Cyclic Loading	28

1.3.4	Elastic Plastic, Armstrong-Frederick, von-Mises, Constitutive Examples	29
	Pure Shear, Cyclic Loading	29
1.3.5	Elastic Plastic, Armstrong-Frederick, Drucker-Prager, Constitutive Examples	30
	Pure Shear, Cyclic Loading	30
1.3.6	Elastic Plastic, SaniSAND, Constitutive Examples	31
	Bardet Constraint Examples	31
1.4	Stiffness Reduction and Damping Curves Modeling	32
1.4.1	Multi-yield-surface von-Mises	32
	Model description	32
	Real-ESSI input file	32
1.4.2	Multi-yield-surface Drucker-Prager	35
	Problem description	35
	Real-ESSI input file:	35
1.4.3	Simulate Stiffness Reduction using von-Mises Armstrong-Frederick	38
	Model description	38
	Real-ESSI input file:	38
1.5	Cosserat, Micropolar Material Modeling	39
1.5.1	Cosserat, Micropolar Elastic Material Model <small>(example in development)</small>	40
1.5.2	Cosserat, Micropolar Elastic-Plastic von Mises Material Model <small>(example in development)</small>	41
1.5.3	Cosserat, Micropolar Elastic-Plastic Druekcr Prager Material Model <small>(example in development)</small>	42
2	Static Examples	
	<small>(2016-2017-2019-2021-)</small>	43
2.1	Chapter Summary and Highlights	43
2.2	Static Elastic Solid Examples	43
2.2.1	Statics, Bricks, with Nodal Forces	43
	Statics, 8 Node Brick, with Nodal Forces	43
	Statics, 27 Node Brick, with Nodal Forces	44
	Statics, 8-27 Node Brick, with Nodal Forces	45
2.2.2	Statics, Bricks, with Surface Loads	46
	Statics, 8 Node Brick, with Surface Forces	46
	Statics, 27 Node Brick, with Surface Forces	46
2.2.3	Statics, Bricks, with Body Forces	47
	Statics, 8 Node Brick, with Body Forces	47
	Statics, 27 Node Brick, with Body Forces	49

Statics, 8-27 Node Brick, with Body Forces	50
2.3 Static Elastic Structural Examples	51
2.3.1 Statics, Truss, with Nodal Forces	51
2.3.2 Statics, Elastic Beam, with Nodal Forces	52
2.3.3 Statics, Elastic Beam, with Body Forces	53
2.3.4 Statics, ShearBeam Element	54
Problem description	54
Results	54
2.3.5 Statics, Elastic Shell, with Nodal Forces	55
ANDES Shell, out of Plane Force	55
ANDES Shell, Perpendicular to Plane, bending	55
ANDES Shell, In-plane Force	55
2.3.6 Statics, Elastic Shell, with Body Forces	57
ANDES shell under the out-of-Plane Body Force	57
ANDES Shell, In-plane Body Force	57
2.4 Statics, Interface/Contact Elements	59
2.4.1 Statics, Two Bar Normal Interface/Contact Problem Under Monotonic Loading.	59
2.4.2 Statics, Four Bar Interface/Contact Problem With Normal and Shear Force Under Monotonic Loading	60
2.4.3 Statics, 3-D Truss example with normal confinement and Shear Loading	62
2.4.4 Statics, Six Solid Blocks Example With Interface/Contact	64
2.5 Static Inelastic Solid Examples	65
2.5.1 Statics, Bricks, Elastic-Plastic, von Mises, with Nodal Forces	65
2.5.2 Statics, Bricks, Elastic-Plastic, Drucker Prager, with Nodal Forces	65
2.6 Static Inelastic Shell Examples <small>(example in development)</small>	68
2.7 Statics, Elastic Single Solid Finite Element Examples	68
2.7.1 Statics, Linear Elastic, Solid Examples	68
Statics, Pure Shear, Monotonic Loading	68
Pure Shear, Cyclic Loading	69
Uniaxial Strain, Monotonic Loading	69
Uniaxial Strain, Cyclic Loading	70
2.7.2 Statics, Nonlinear Elastic, Duncan-Chang, Pure Shear, Solid Examples	70
Pure Shear, Monotonic Loading	70
Pure Shear, Cyclic Loading	71
2.8 Statics, Elastic-Plastic Single Solid Finite Element Examples	72

2.8.1	Statics, Elastic Perfectly Plastic, Cyclic Loading, Pure Shear Solid Examples	72
	Statics, von-Mises Yield Function, Isotropic Hardening	73
	Statics, von Mises Yield Function, Kinematic Hardening	74
	Statics, Drucker Prager Yield Function, von-Mises Plastic Potential Function, Perfectly Plastic Hardening Rule	75
	Statics, Drucker Prager Yield Function, Drucker Prager Plastic Potential Function, Perfectly Plastic Hardening Rule	77
2.8.2	Statics, Drucker Prager with Armstrong Frederick Nonlinear Kinematic Hardening Ma- terial Model	78
2.9	Statics, Elastic, Fiber Cross Section Beam Finite Element Examples	80
2.9.1	Statics, Linear Elastic, Normal Loading and Pure Bending Fiber Cross Section Beam Finite Element Examples	80
	Linear Elastic Normal Loading, Fiber Cross Section Beam Finite Element Examples . .	80
	Linear Elastic Pure Bending, Fiber Cross Section Beam Finite Element Examples . . .	81
2.10	Statics, Elastic-Plastic, Fiber Cross Section Beam Finite Element Examples	82
2.10.1	Statics, Elastic-Plastic, Normal Loading and Pure Bending Fiber Cross Section Beam Finite Element	82
	Elastic-Plastic Normal Loading, (Fiber Cross Section) Beam Finite Element Examples .	82
	Elastic-Plastic Pure Bending, (Fiber Cross Section) Beam Finite Element Examples . .	83
2.11	Statics, Elastic, Inelastic Wall Finite Element Examples	84
2.11.1	Statics, Linear Elastic, Wall Finite Element Examples	84
	Statics, Linear Elastic, Wall Finite Element Examples	84
	Linear Elastic, Bi-Axial, Wall Finite Element Examples	85
	Linear Elastic, Shear, (Fiber Cross Section) Wall Finite Element Examples	86
2.12	Statics, Elastic-Plastic Wall Finite Element Examples	87
2.12.1	Statics, Elastic-Plastic, in Plane, Wall Finite Element Examples	87
	Elastic-Plastic, Uni-Axial, Wall Finite Element Examples	87
	Elastic-Plastic, Bi-Axial, Wall Finite Element Examples	88
	Elastic-Plastic, Shear, Wall Finite Element Examples	89
2.13	Statics, Solution Advancement Control	90
2.13.1	Increments: Load Control	90
	Solids Example, Elastic Plastic Isotropic Hardening	90
	Solids Example, Elastic Plastic Kinematic Hardening	91
	Inelastic Beam Example, Steel and Reinforced Concrete	92
2.13.2	Statics, Increments: Displacement Control	92

Statics, Single Displacement Control	92
Solids Example, Elastic-Perfectly Plastic	92
Solids Example, Elastic Plastic Isotropic Hardening	93
Solids Example, Elastic Plastic Kinematic Hardening	94
Inelastic Beam Example, Steel and Reinforced Concrete	94
2.13.3 Statics, Solution Algorithms	96
Statics, Solution Algorithm: No Convergence Check	96
Statics, Solution Algorithm: Newton Algorithm	97
Statics, Solution Algorithm: Newton Algorithm with Line Search	98
2.13.4 Statics, Solution Advancement Control, Iterations: Convergence Criteria	99
Statics, Solution Advancement Control, Convergence Criteria: Unbalanced Force	99
Statics, Solution Advancement Control, Convergence Criteria: Displacement Increment	100
2.13.5 Statics, Solution Advancement Control, Different Convergence Tolerances <small>(Examples in preparation)</small>	101
2.14 Statics, Small Practical Examples	102
2.14.1 Statics, Elastic Beam Element for a Simple Frame Structure	102
Problem Description	102
2.14.2 Statics, 4NodeANDES Square Plate, Four Edges Clamped	103
Problem description	103
Numerical model	103
2.14.3 Statics, Six Solid Blocks Example With Interface/Contact	105
3 Dynamic Examples	
(2016-2017-2018-2019-2021-)	107
3.1 Chapter Summary and Highlights	107
3.2 Dynamic Solution Advancement (in Time)	107
3.2.1 Dynamics: Newmark Method	107
Newmark Model Description	107
Newmark Results	108
3.2.2 Dynamics: Hilber-Hughes-Taylor (α) Method	108
HHT Model Description	108
HHT Results	108
3.3 Dynamics: Solution Advancement: Time Step Size	109
3.3.1 Dynamics: Solution Advancement: Equal Time Step	109
Model Description	109
Results	109

3.3.2	Dynamics Solution Advancement: Variable Time Step	110
	Model Description	110
	Results	111
3.4	Dynamics: Energy Dissipation, Damping	111
3.4.1	Dynamics: Energy Dissipation: Viscous Damping	111
	Dynamics: Energy Dissipation, Viscous Damping: Rayleigh Damping	111
	Dynamics: Energy Dissipation, Viscous Damping: Caughey Damping	112
3.4.2	Dynamics: Energy Dissipation: Material (Elastic-Plastic, Hysteretic) Damping	112
	Dynamics: Energy Dissipation, Material Damping: Elastic Perfectly Plastic Models	112
	Dynamics: Energy Dissipation, Material/Hysteretic Damping: Elastic Plastic Isotropic Hardening Models	114
	Dynamics: Energy Dissipation, Material/Hysteretic Damping: Elastic Plastic Kinematic Hardening Models	114
	Dynamics: Energy Dissipation, Material/Hysteretic Damping: Elastic Plastic Armstrong- Frederick Models	115
3.4.3	Dynamics: Energy Dissipation: Numerical Damping	116
	Energy Dissipation, Numerical Damping: Newmark Method	116
	Dynamics: Energy Dissipation, Numerical Damping: Hilber-Hughes-Taylor (α) Method	116
3.5	Dynamics: Elastic Solid Dynamic Examples	118
3.5.1	Model Description	118
3.5.2	Results	118
3.6	Dynamics: Elastic Structural Dynamic Examples	119
3.6.1	Model Description	119
3.6.2	Results	119
3.7	Dynamics: Interface/Contact Elements	121
3.7.1	Dynamics: Hard Interface/Contact: One Bar Normal Interface/Contact Dynamics	121
	Model Description	121
	Dynamics: No Viscous Damping	122
	Dynamics: Normal Viscous Damping Between Interface/Contact Node Pairs	122
	Dynamics: Explicit Simulation	123
3.7.2	Dynamics: Hard Interface/Contact: Frictional Single Degree of Freedom Problem	124
	Dynamics: No Viscous Damping	125
	Dynamics: Tangential Viscous Damping Between Interface/Contact Node Pairs	125
	Dynamics: Explicit Simulation	126
3.7.3	Dynamics: Soft Interface/Contact: One Bar Normal Interface/Contact Dynamics	127

Dynamics: No Viscous Damping	128
Dynamics: With Normal Viscous Damping Between Interface/Contact Node Pairs	128
Dynamics: Explicit Simulation	129
3.7.4 Dynamics: Soft Interface/Contact: Frictional Single Degree of Freedom Problem	130
Dynamics: No Viscous Damping	131
Dynamics: Tangential Viscous Damping Between Interface/Contact Node Pairs	131
Dynamics: Explicit Simulation	132
3.7.5 Dynamics: Split Beam	133
Model Description	133
Dynamics: Split Beam With Hard Interface/Contact	133
Dynamics: Split Beam With Soft Interface/Contact	134
3.7.6 Dynamics: Block on Soil ESSI	135
3.8 Dynamics: Inelastic Solid Examples	137
3.9 Dynamics: Inelastic Structural Examples	138
3.10 Dynamics: Domain Reduction Method (DRM)	139
3.10.1 Dynamics: DRM One Dimensional (1D) Model	139
3.10.2 Dynamics: Three Dimensional (3D) DRM Model	143
3.10.3 Dynamics: DRM Model with Structure	145
3.11 Dynamics: Eigen Analysis	146
3.12 Dynamics: Fully Coupled u-p-U and u-p Elements	147
3.13 Dynamics: Partially Saturated / Unsaturated u-p-U Element <small>(example in development)</small>	148
3.14 Dynamics: Coupled Interface/Contact Element <small>(example in development)</small>	149
3.15 Dynamics: Buoyant Forces <small>(example in development)</small>	150
3.16 Chapter Summary and Highlights	151

4 Stochastic Examples

<small>(2018-2019-2020-2021-)</small>	152
4.1 Probabilistic Constitutive Modeling	152
4.1.1 Probabilistic Constitutive Modeling: Linear Elastic	152
4.1.2 Probabilistic Constitutive Modeling: Elasto-Plastic	152
4.2 Probabilistic Characterization of Seismic Motions	153
4.3 1D Stochastic Seismic Wave Propagation	154
4.3.1 1D Stochastic Seismic Wave Propagation: Linear Elastic	154
4.3.2 1D Stochastic Seismic Wave Propagation: Elasto-Plastic	155
4.4 1D Stochastic Seismic Wave Propagation: Sobol Sensitivity Analysis	158

5 Large Scale, Realistic Examples

(2016-2018-)

159

6 Short Course Examples

(2017-2023-)

160

6.1	Nonlinear Analysis Steps	161
6.1.1	Free Field 1C	161
6.1.2	Free Field 3C	165
6.1.3	Soil-Foundation Interaction 3D	169
6.1.4	Soil-Structure Interaction 3D	172
6.1.5	Analysis of a Structure without Soil	179
	Eigen Analysis	179
	Imposed Motion	181
6.2	Day 1: Overview	184
6.2.1	Nuclear Power Plant with 3C motions from SW4	184
6.2.2	Nuclear Power Plant with 1C motions from Deconvolution	186
6.2.3	Nuclear Power Plant with 3×1C motions from Deconvolution	188
6.2.4	Single Element Models: Illustration of the Elastic-Plastic Behavior	190
6.2.5	Pushover for Nonlinear Frame	192
6.2.6	Pre-Processing examples with Gmsh	194
	Cantilever Example	194
	Brick-shell-beam Example	195
	DRM 2D Example	196
	DRM 3D Example	197
6.2.7	Post-processing examples with ParaView	198
	Slice Visualization	198
	Stress Visualization	199
	Pore Pressure Visualization with upU Element	200
	Eigen Visualization	201
6.2.8	Check Model and Visualization of Boundary Conditions	202
6.2.9	Restart Simulation	203
	Restart in the next stage	203
	Restart inside the stage	204
6.3	Day 2: Seismic Motions	205
6.3.1	Deconvolution and Propagation of 1C Motions, 1D Model	205

6.3.2	Convolution and Propagation of 1C Motions, 1D Model	205
6.3.3	Convolution, Deconvolution and Propagation of 1C Motions, 2D Model	205
	ESSI 3D building model, deconvolution 1C model, shell model with DRM	207
6.3.4	Deconvolution 3×1C Motions	209
	Free field 1C model, deconvolution 3×1C motion, model with DRM	209
	Free field 3D model, deconvolution 3×1C motion, model with DRM	211
	ESSI 3D building model, deconvolution 3×1C motion, shell model with DRM	212
6.3.5	Mesh Dependence of Wave Propagation Frequencies	214
6.3.6	Application of 3C Motions from SW4	216
	3C Seismic Motion from SW4	216
	Free field 3D model, 3C motion, model with DRM	218
	ESSI 3D building model, 3C motion, shell model with DRM	220
6.4	Day 3: Inelastic, Nonlinear Analysis	221
6.4.1	Single Element Models: Illustration of the Elastic-Plastic Behavior	221
	von-Mises Perfectly Plastic Material Model.	221
	von-Mises Armstrong-Frederick Material Model.	221
	von-Mises G/Gmax Material Model	223
	Drucker-Prager Perfectly Plastic Material Model	225
	Drucker-Prager Armstrong-Frederick Non-Associated Material Model	225
	Drucker-Prager G/Gmax Non-Associated Material Model	226
6.4.2	Wave Propagation Through Elasto-plastic Soil	228
6.4.3	Contact/Interface/Joint Examples	229
	Axial Behavior: Stress-Based Hard Contact/Interface/Joint Example	229
	Axial Behavior: Stress-Based Soft Contact/Interface/Joint Example	229
	Shear behavior: Stress-Based Elastic Perfectly Plastic Contact/Interface/Joint	230
	Shear behavior: Stress-Based Elastic-Hardening Contact/Interface/Joint	230
	Shear behavior: Stress-Based Elastic-Hardening-Softening Contact/Interface/Joint	230
	Force Based Contact/Interface/Joint Example: Base Isolator	232
6.4.4	Inelastic Frame Pushover	233
6.4.5	Inelastic Wall Pushover	236
6.4.6	Viscous Nonlinear behavior	238
6.4.7	Numerical Damping Example	240
6.4.8	Nuclear Power Plant Example with Nonlinearities	242
6.4.9	Buildings, ATC-144/FEMA-P-2091 Examples	244

Part I

Modeling and Simulation Examples

Chapter 1

Constitutive, Material Behaviour Examples

(2016-2017-2019-2023-)

(In collaboration with Dr. Yuan Feng and Dr. Han Yang)

1.1 Chapter Summary and Highlights

In this Chapter constitutive behavior of elastic-plastic material is illustrated through a number of examples.

All the examples described here, and many more, organized in sub-directories, for constitutive behavior, static and dynamic behavior can be directly downloaded from a repository at: http://sokocalo.engr.ucdavis.edu/~jeremic/lecture_notes_online_material/Real-ESSI_Examples/education_examples. These examples can then be tried, analyzed using Real-ESSI Simulator that is available on Amazon Web Services (AWS) computers around the world. Login to AWS market place and search for Real-ESSI...

1.2 Elastic Solid Constitutive Examples

1.2.1 Linear Elastic Constitutive Examples

Pure Shear, Monotonic Loading

The Real-ESSI input files for this example are available [HERE](#). The compressed package of Real-ESSI input files and postprocessing results for this example is available [HERE](#).

Material properties in Real-ESSI input:

```
1 model name "test";
2 add material # 1 type linear_elastic_isotropic_3d
3   mass_density = 2E3 * kg/m^3
4   elastic_modulus = 2E7 * Pa
5   poisson_ratio= 0.0 ;
6 simulate constitutive testing strain control pure shear monotonic ←
7   loading use material # 1
8   confinement_strain = 0.001
9   strain_increment_size = 0.0001
10  number_of_increment = 100;
11  bye;
```

Material Response:

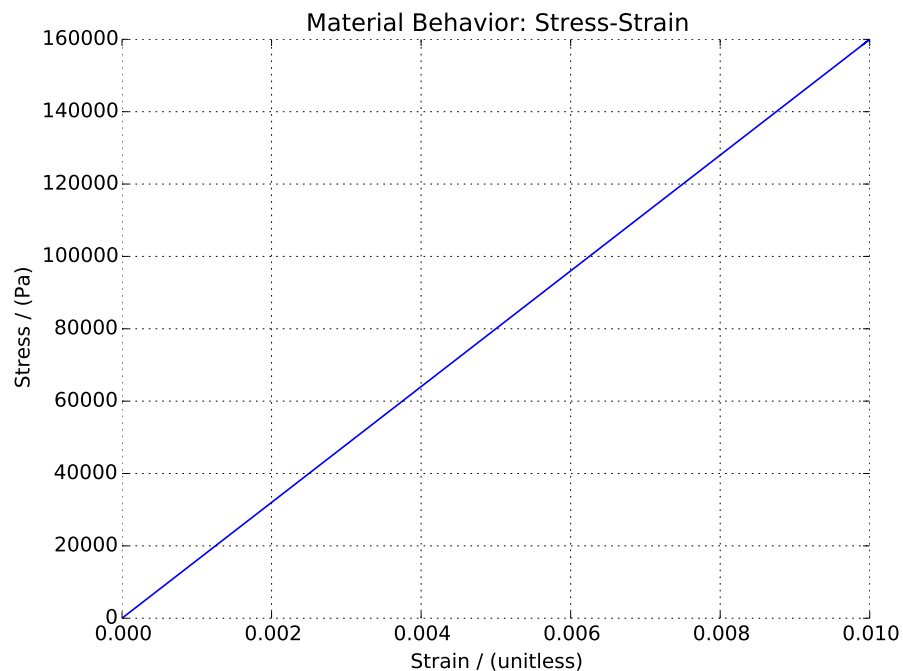


Figure 1.1: Linear Elastic Pure Shear Monotonic Loading

Pure Shear, Cyclic Loading

The Real-ESSI input files for this example are available [HERE](#). The compressed package of Real-ESSI input files and postprocessing results for this example is available [HERE](#).

Material properties in Real-ESSI input:

```
1 model name "test";
2 add material # 1 type linear_elastic_isotropic_3d
3   mass_density = 2E3 * kg/m^3
4   elastic_modulus = 2E7 * Pa
5   poisson_ratio= 0.25 ;
6 simulate constitutive testing strain control pure shear cyclic ↔
   loading use material # 1
7   confinement_strain = 0.001
8   strain_increment_size = 0.0001
9   maximum_strain = 0.01
10  number_of_cycles = 1;
11 bye;
```

Material Response:

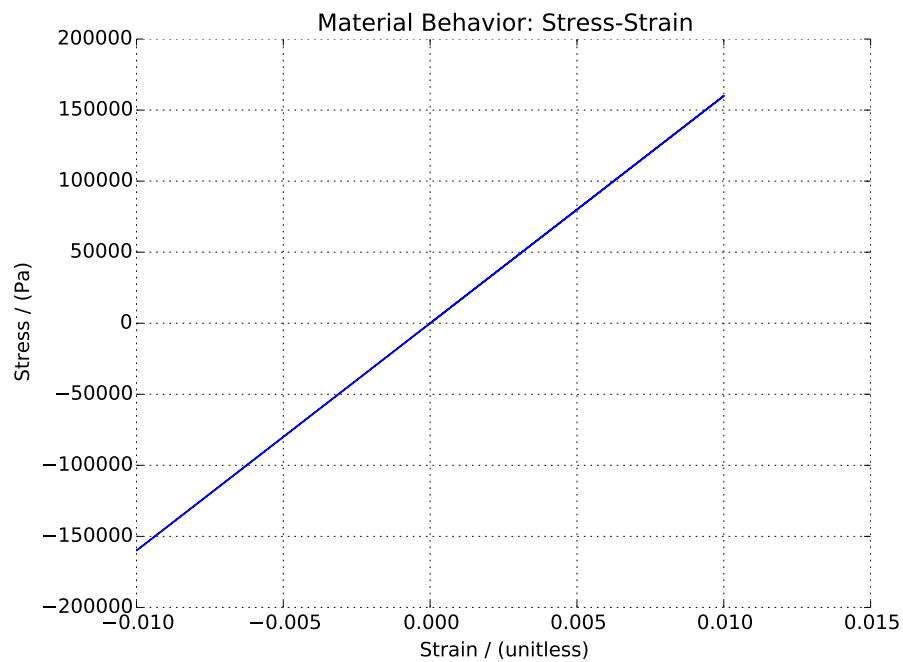


Figure 1.2: Linear Elastic Pure Shear Cyclic Loading.

Uniaxial Strain, Monotonic Loading

The Real-ESSI input files for this example are available [HERE](#). The compressed package of Real-ESSI input files and postprocessing results for this example is available [HERE](#).

Material properties in Real-ESSI input:

```
1 model name "test";
2 add material # 1 type linear_elastic_isotropic_3d
3   mass_density = 2E3 * kg/m^3
4   elastic_modulus = 2E7 * Pa
5   poisson_ratio= 0.0 ;
6 simulate constitutive testing strain control uniaxial monotonic ←
   loading use material # 1
7   confinement_strain = 0.001
8   strain_increment_size = 0.0001
9   number_of_increment = 100;
10 bye;
```

Material Response:

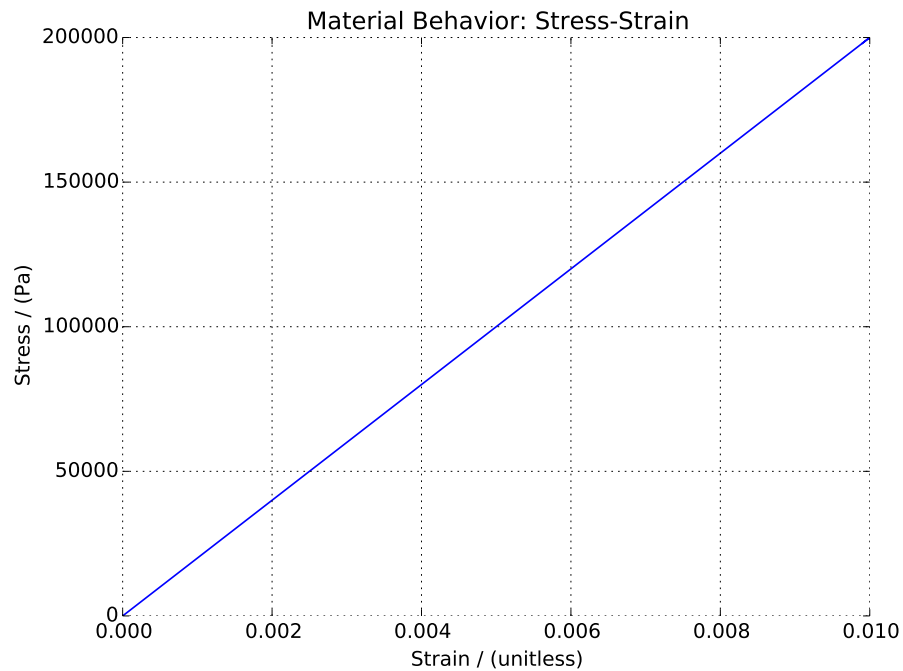


Figure 1.3: Linear Elastic Uniaxial Monotonic Loading

Uniaxial Strain, Cyclic Loading

The Real-ESSI input files for this example are available [HERE](#). The compressed package of Real-ESSI input files and postprocessing results for this example is available [HERE](#).

Material properties in Real-ESSI input:

```
1 model name "test";
2 add material # 1 type linear_elastic_isotropic_3d
3   mass_density = 2E3 * kg/m^3
4   elastic_modulus = 2E7 * Pa
5   poisson_ratio= 0.25 ;
6 simulate constitutive testing strain control pure shear cyclic ↔
   loading use material # 1
7   confinement_strain = 0.001
8   strain_increment_size = 0.0001
9   maximum_strain = 0.01
10  number_of_cycles = 1;
11 bye;
```

Material Response:

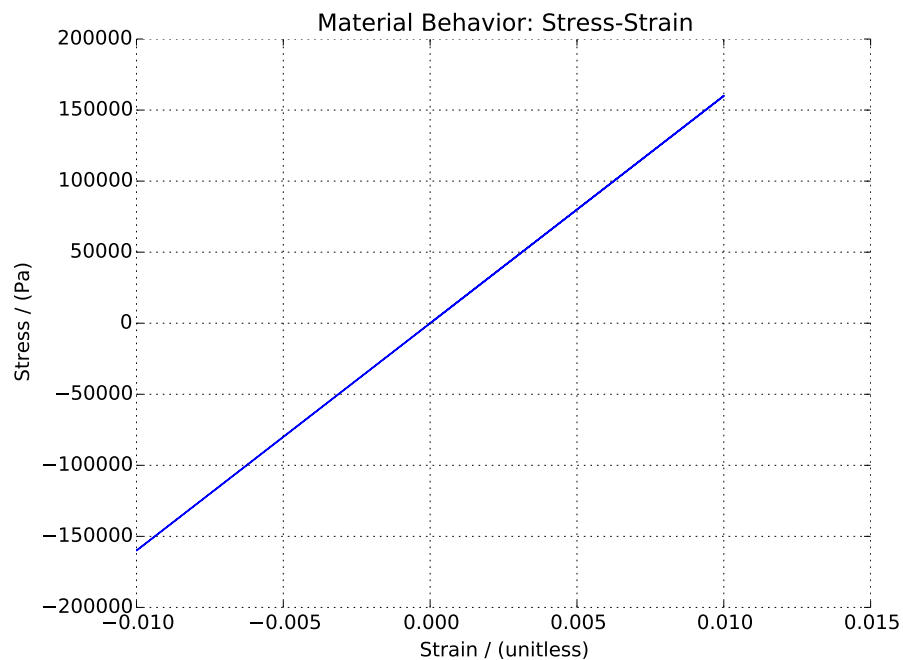


Figure 1.4: Linear Elastic Uniaxial Cyclic Loading

1.2.2 Nonlinear Elastic Constitutive Examples

Triaxial Uniform Pressure, Monotonic Loading

The Real-ESSI input files for this example are available [HERE](#). The compressed package of Real-ESSI input files and postprocessing results for this example is available [HERE](#).

The Duncan-Chang nonlinear elastic materials:

$$E = K p_a \left(\frac{\sigma_3}{p_a} \right)^n \quad (1.1)$$

where K and n are material constants. And pressure p_a is atmospheric pressure. And stress σ_3 is the minor principal stress.

Material properties in Real-ESSI input:

```

1 model name "test";
2 add material # 1 type Duncan_Chang_nonlinear_elastic_isotropic_3d_LT
3   mass_density = 2E3 * kg/m^3
4   initial_elastic_modulus = 3E5 * Pa
5   poisson_ratio= 0.15
6   DuncanChang_K = 1E3
7   DuncanChang_pa = 1E5 * Pa
8   DuncanChang_n = 0.5 ;
9 simulate constitutive testing strain control triaxial confinement ←
   loading use material # 1
10   strain_increment_size = 0.00001
11   maximum_strain = 0.01
12   number_of_increment = 2000;
13 bye;
```

Material Response:

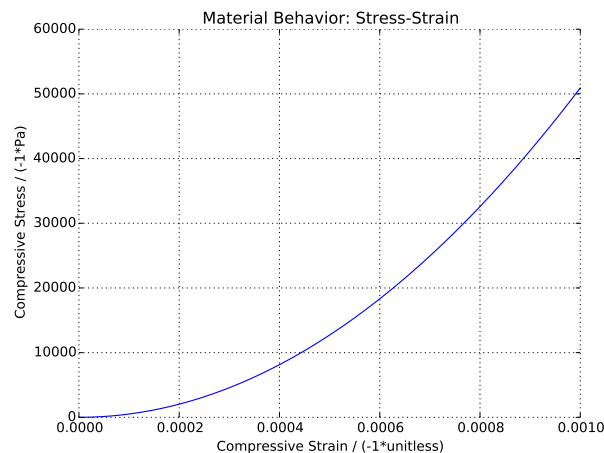


Figure 1.5: Results of Duncan-Chang Nonlinear Elastic Monotonic Loading

1.3 Elastic Plastic Solid Constitutive Examples

1.3.1 Elastic Perfectly Plastic Constitutive Examples

Pure Shear

The Real-ESSI input files for this example are available [HERE](#). The compressed package of Real-ESSI input files and postprocessing results for this example is available [HERE](#).

Material properties in Real-ESSI input:

```

1 model name "test";
2 add material # 1 type VonMises
3   mass_density = 2E3*kg/m^3
4   elastic_modulus = 2E7 * Pa
5   poisson_ratio=0.25
6   von_mises_radius = 1E5*Pa
7   kinematic_hardening_rate = 0.0 *Pa
8   isotropic_hardening_rate = 0.0*Pa ;
9 define NDMaterial constitutive integration algorithm Backward_Euler
10  yield_function_relative_tolerance = 1E-2
11  stress_relative_tolerance = 1E-3
12  maximum_iterations = 30;
13 simulate constitutive testing strain control pure shear cyclic ↔
14   loading use material # 1
15   confinement_strain = 0.001
16   strain_increment_size = 0.0001
17   maximum_strain = 0.01
18   number_of_cycles = 1;
18 bye;
```

Material Response:

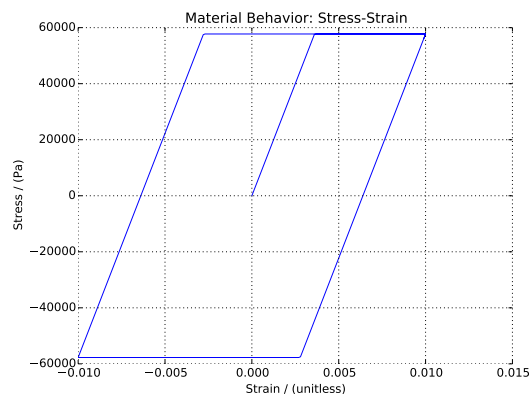


Figure 1.6: Perfectly Plastic Pure Shear Cyclic Loading.

Uniaxial Strain

The Real-ESSI input files for this example are available [HERE](#). The compressed package of Real-ESSI input files and postprocessing results for this example is available [HERE](#).

Material properties in Real-ESSI input:

```
1 model name "test";
2 add material # 1 type VonMises
3   mass_density = 2E3*kg/m^3
4   elastic_modulus = 2E7 * Pa
5   poisson_ratio=0.25
6   von_mises_radius = 1E5*Pa
7   kinematic_hardening_rate = 0.0 *Pa
8   isotropic_hardening_rate = 0.0*Pa ;
9 define NDMaterial constitutive integration algorithm Backward_Euler
10  yield_function_relative_tolerance = 1E-2
11  stress_relative_tolerance = 1E-3
12  maximum_iterations = 30;
13 simulate constitutive testing strain control uniaxial cyclic loading ↔
14   use material # 1
15   confinement_strain = 0.001
16   strain_increment_size = 0.0001
17   maximum_strain = 0.01
18   number_of_cycles = 1;
18 bye;
```

Material Response:

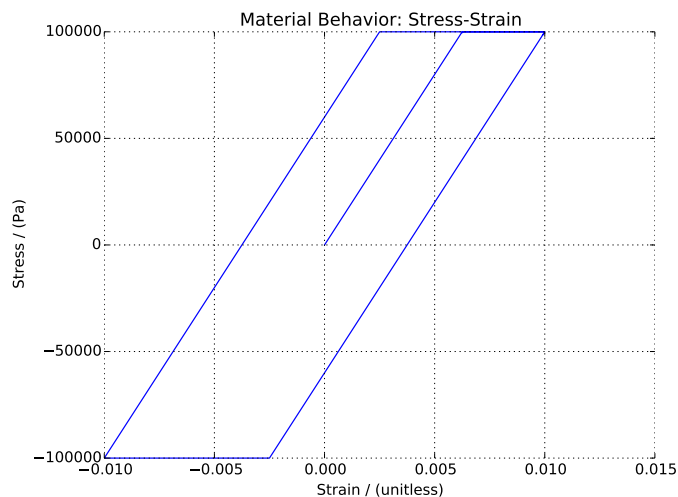


Figure 1.7: Perfectly Plastic Uniaxial Cyclic Loading

1.3.2 Elastic Plastic, Isotropic Hardening, Constitutive Examples

Pure Shear, Monotonic Loading

The Real-ESSI input files for this example are available [HERE](#). The compressed package of Real-ESSI input files and postprocessing results for this example is available [HERE](#).

Material properties in Real-ESSI input:

```

1 model name "test";
2 add material # 1 type VonMises
3   mass_density = 2E3*kg/m^3
4   elastic_modulus = 2E7 * Pa
5   poisson_ratio=0.25
6   von_mises_radius = 1E5*Pa
7   kinematic_hardening_rate = 0.0*Pa
8   isotropic_hardening_rate = 2E6 *Pa ;
9 define NDMaterial constitutive integration algorithm Backward_Euler
10  yield_function_relative_tolerance = 1E-2
11  stress_relative_tolerance = 1E-3
12  maximum_iterations = 30;
13 simulate constitutive testing strain control pure shear monotonic ←
14   loading use material # 1
15   confinement_strain = 0.001
16   strain_increment_size = 0.0001
17   number_of_increment = 99;
18 bye;
```

Material Response:

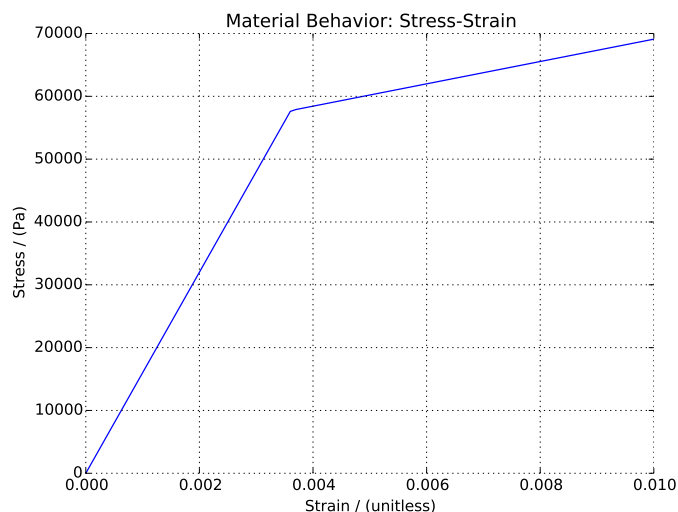


Figure 1.8: Isotropic Hardening Pure Shear Monotonic Loading

Pure Shear, Cyclic Loading

The Real-ESSI input files for this example are available [HERE](#). The compressed package of Real-ESSI input files and postprocessing results for this example is available [HERE](#).

Material properties in Real-ESSI input:

```

1 model name "test";
2 add material # 1 type VonMises
3   mass_density = 2E3*kg/m^3
4   elastic_modulus = 2E7 * Pa
5   poisson_ratio=0.25
6   von_mises_radius = 1E5*Pa
7   kinematic_hardening_rate = 0.0*Pa
8   isotropic_hardening_rate = 2E6 *Pa ;
9 define NDMaterial constitutive integration algorithm Backward_Euler
10  yield_function_relative_tolerance = 1E-2
11  stress_relative_tolerance = 1E-3
12  maximum_iterations = 30;
13 simulate constitutive testing strain control pure shear cyclic ↔
14   loading use material # 1
15   confinement_strain = 0.001
16   strain_increment_size = 0.0001
17   maximum_strain = 0.01
18   number_of_cycles = 1;
18 bye;

```

Material Response:

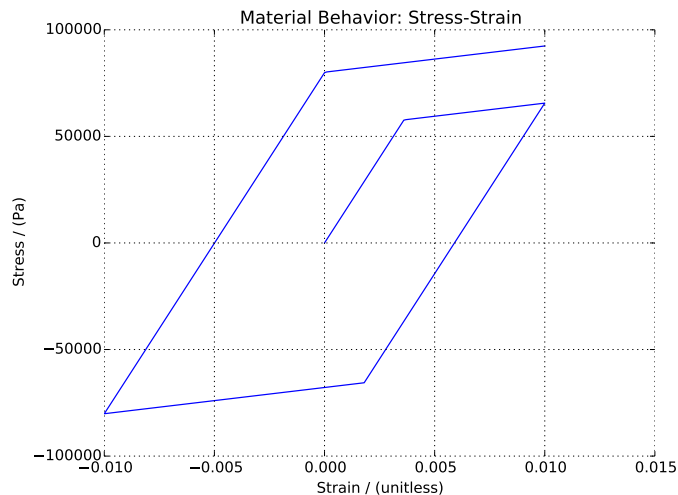


Figure 1.9: Isotropic Hardening Pure Shear Cyclic Loading.

Uniaxial Strain, Monotonic Loading

The Real-ESSI input files for this example are available [HERE](#). The compressed package of Real-ESSI input files and postprocessing results for this example is available [HERE](#).

Material properties in Real-ESSI input:

```

1 model name "test";
2 add material # 1 type VonMises
3   mass_density = 2E3*kg/m^3
4   elastic_modulus = 2E7 * Pa
5   poisson_ratio=0.25
6   von_mises_radius = 5E4*Pa
7   kinematic_hardening_rate = 0.0*Pa
8   isotropic_hardening_rate = 2E6 *Pa ;
9 define NDMaterial constitutive integration algorithm Backward_Euler
10  yield_function_relative_tolerance = 1E-2
11  stress_relative_tolerance = 1E-3
12  maximum_iterations = 30;
13 simulate constitutive testing strain control uniaxial monotonic ←
14   loading use material # 1
15   confinement_strain = 0.001
16   strain_increment_size = 0.0001
17   number_of_increment = 99;
17 bye;

```

Material Response:

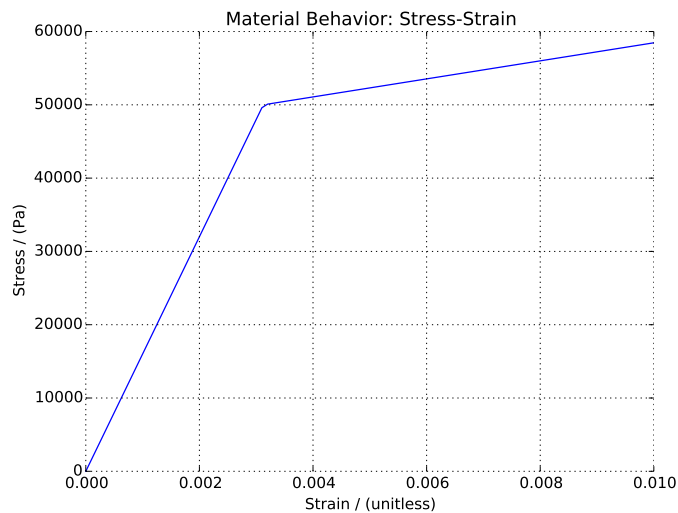


Figure 1.10: Isotropic Hardening Uniaxial Monotonic Loading

Uniaxial Strain, Cyclic Loading

The Real-ESSI input files for this example are available [HERE](#). The compressed package of Real-ESSI input files and postprocessing results for this example is available [HERE](#).

Material properties in Real-ESSI input:

```

1 model name "test";
2 add material # 1 type VonMises
3   mass_density = 2E3*kg/m^3
4   elastic_modulus = 2E7 * Pa
5   poisson_ratio=0.25
6   von_mises_radius = 5E4*Pa
7   kinematic_hardening_rate = 0.0*Pa
8   isotropic_hardening_rate = 2E6 *Pa ;
9 define NDMaterial constitutive integration algorithm Backward_Euler
10  yield_function_relative_tolerance = 1E-2
11  stress_relative_tolerance = 1E-3
12  maximum_iterations = 30;
13 simulate constitutive testing strain control uniaxial cyclic loading ←
14   use material # 1
15   confinement_strain = 0.001
16   strain_increment_size = 0.0001
17   maximum_strain = 0.01
18   number_of_cycles = 1;
18 bye;
```

Material Response:

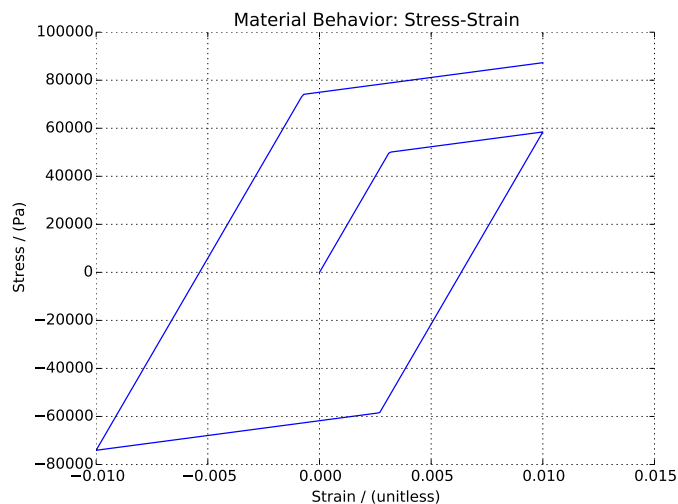


Figure 1.11: Isotropic Hardening Uniaxial Cyclic Loading

1.3.3 Elastic Plastic, Kinematic Hardening, Constitutive Examples

Pure Shear, Monotonic Loading

The Real-ESSI input files for this example are available [HERE](#). The compressed package of Real-ESSI input files and postprocessing results for this example is available [HERE](#).

Material properties in Real-ESSI input:

```

1 model name "test";
2 add material # 1 type VonMises
3   mass_density = 2E3*kg/m^3
4   elastic_modulus = 2E7 * Pa
5   poisson_ratio=0.25
6   von_mises_radius = 1E5*Pa
7   kinematic_hardening_rate = 2E6*Pa
8   isotropic_hardening_rate = 0.0*Pa ;
9 define NDMaterial constitutive integration algorithm Backward_Euler
10  yield_function_relative_tolerance = 1E-2
11  stress_relative_tolerance = 1E-3
12  maximum_iterations = 30;
13 simulate constitutive testing strain control pure shear monotonic ←
14   loading use material # 1
15   confinement_strain = 0.001
16   strain_increment_size = 0.0001
17   number_of_increment = 99;
18 bye;
```

Material Response:

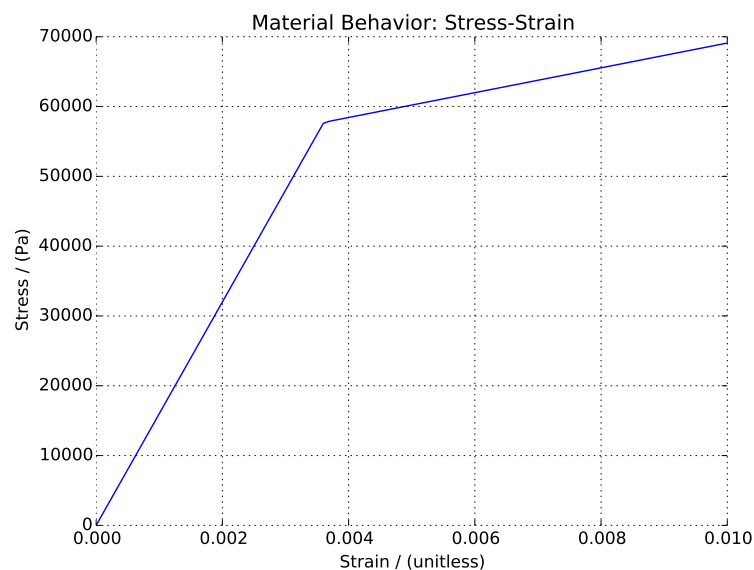


Figure 1.12: Kinematic Hardening Monotonic Cyclic Loading

Pure Shear, Cyclic Loading

The Real-ESSI input files for this example are available [HERE](#). The compressed package of Real-ESSI input files and postprocessing results for this example is available [HERE](#).

Material properties in Real-ESSI input:

```

1 model name "test";
2 add material # 1 type VonMises
3   mass_density = 2E3*kg/m^3
4   elastic_modulus = 2E7 * Pa
5   poisson_ratio=0.25
6   von_mises_radius = 1E5*Pa
7   kinematic_hardening_rate = 2E6*Pa
8   isotropic_hardening_rate = 0.0*Pa ;
9 define NDMaterial constitutive integration algorithm Backward_Euler
10  yield_function_relative_tolerance = 1E-2
11  stress_relative_tolerance = 1E-3
12  maximum_iterations = 30;
13 simulate constitutive testing strain control pure shear cyclic ↔
14   loading use material # 1
15   confinement_strain = 0.001
16   strain_increment_size = 0.0001
17   maximum_strain = 0.01
18   number_of_cycles = 1;
18 bye;

```

Material Response:

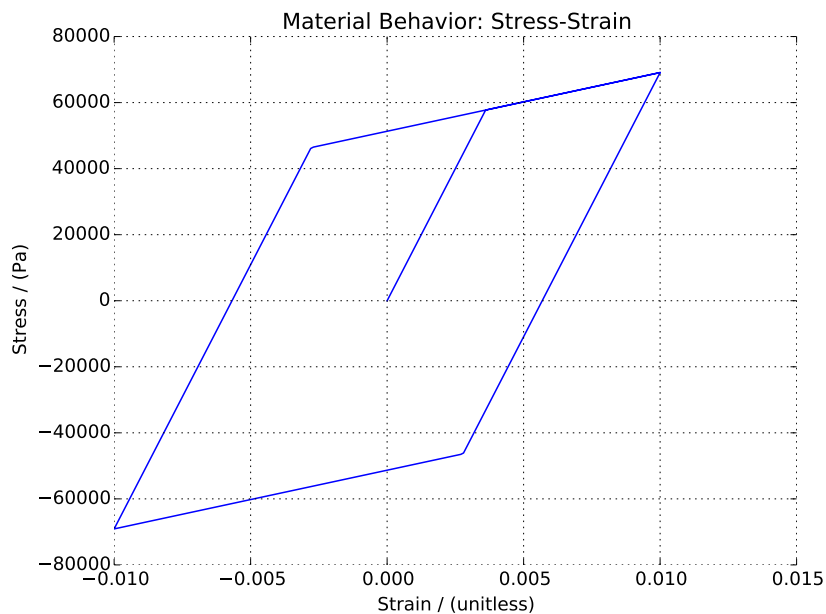


Figure 1.13: Kinematic Hardening Pure Shear Cyclic Loading.

Uniaxial Strain, Monotonic Loading

The Real-ESSI input files for this example are available [HERE](#). The compressed package of Real-ESSI input files and postprocessing results for this example is available [HERE](#).

Material properties in Real-ESSI input:

```
1 model name "test";
2 add material # 1 type VonMises
3   mass_density = 2E3*kg/m^3
4   elastic_modulus = 2E7 * Pa
5   poisson_ratio=0.25
6   von_mises_radius = 5E4*Pa
7   kinematic_hardening_rate = 2E6*Pa
8   isotropic_hardening_rate = 0.0*Pa ;
9 define NDMaterial constitutive integration algorithm Backward_Euler
10  yield_function_relative_tolerance = 1E-2
11  stress_relative_tolerance = 1E-3
12  maximum_iterations = 30;
13 simulate constitutive testing strain control uniaxial monotonic ↔
14   loading use material # 1
15   confinement_strain = 0.001
16   strain_increment_size = 0.0001
17   number_of_increment = 99;
17 bye;
```

Material Response:

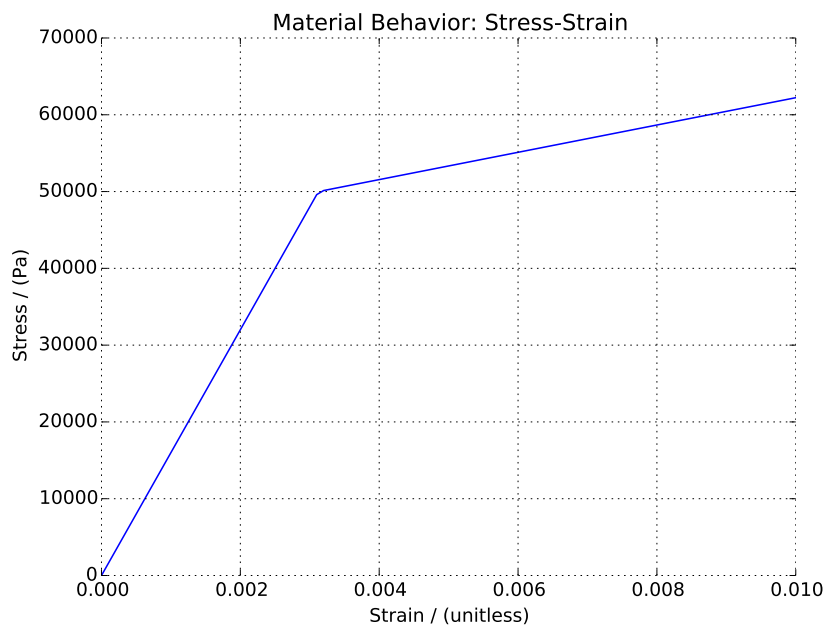


Figure 1.14: Kinematic Hardening Uniaxial Monotonic Loading

Uniaxial Strain, Cyclic Loading

The Real-ESSI input files for this example are available [HERE](#). The compressed package of Real-ESSI input files and postprocessing results for this example is available [HERE](#).

Material properties in Real-ESSI input:

```

1 model name "test";
2 add material # 1 type VonMises
3   mass_density = 2E3*kg/m^3
4   elastic_modulus = 2E7 * Pa
5   poisson_ratio=0.25
6   von_mises_radius = 5E4*Pa
7   kinematic_hardening_rate = 2E6*Pa
8   isotropic_hardening_rate = 0.0*Pa ;
9 define NDMaterial constitutive integration algorithm Backward_Euler
10  yield_function_relative_tolerance = 1E-2
11  stress_relative_tolerance = 1E-3
12  maximum_iterations = 30;
13 simulate constitutive testing strain control uniaxial cyclic loading ←
14   use material # 1
15   confinement_strain = 0.001
16   strain_increment_size = 0.0001
17   maximum_strain = 0.01
18   number_of_cycles = 1;
18 bye;

```

Material Response:

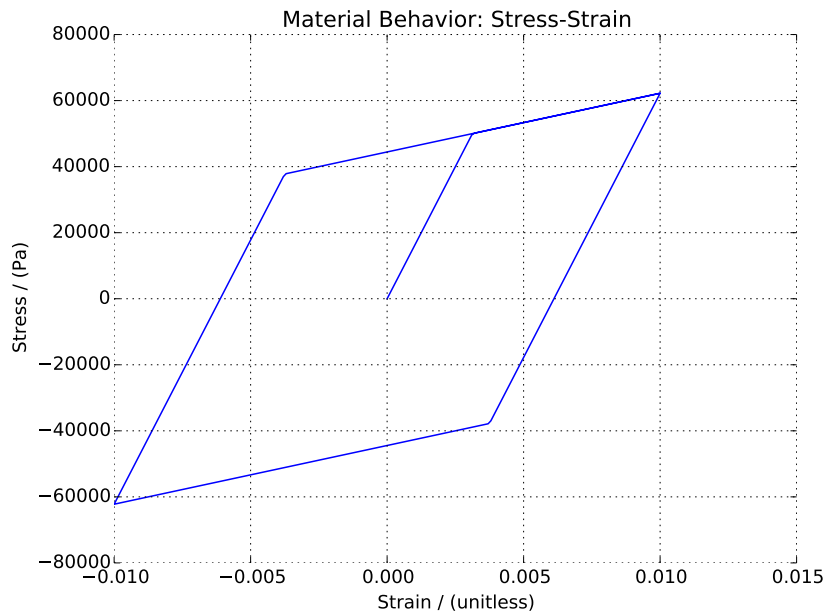


Figure 1.15: Kinematic Hardening Uniaxial Cyclic Loading

1.3.4 Elastic Plastic, Armstrong-Frederick, von-Mises, Constitutive Examples

Pure Shear, Cyclic Loading

The Real-ESSI input files for this example are available [HERE](#). The compressed package of Real-ESSI input files and postprocessing results for this example is available [HERE](#).

Material properties in Real-ESSI input:

```

1 model name "vmaf";
2 add material # 1 type vonMisesArmstrongFrederick
3   mass_density = 0.0*kg/m^3
4   elastic_modulus = 2E7*N/m^2
5   poisson_ratio = 0.0
6   von_mises_radius = 100 * Pa
7   armstrong_frederick_ha = 2E7*N/m^2
8   armstrong_frederick_cr = 1000
9   isotropic_hardening_rate = 0*Pa ;
10 define NDMaterial constitutive integration algorithm Backward_Euler
11   yield_function_relative_tolerance = 1E-6
12   stress_relative_tolerance = 1E-6
13   maximum_iterations = 30;
14 simulate constitutive testing strain control pure shear cyclic ←
15   loading use material # 1
16   confinement_strain = 0.001
17   strain_increment_size = 0.0001
18   maximum_strain = 0.01
19   number_of_cycles = 1;
19 bye;

```

Material Response:

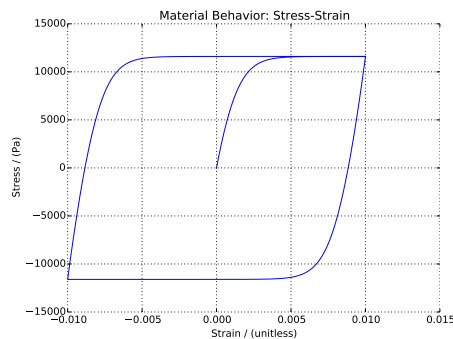


Figure 1.16: Material von-Mises Armstrong-Frederick under Pure Shear Cyclic Loading.

1.3.5 Elastic Plastic, Armstrong-Frederick, Drucker-Prager, Constitutive Examples

Pure Shear, Cyclic Loading

The Real-ESSI input files for this example are available [HERE](#). The compressed package of Real-ESSI input files and postprocessing results for this example is available [HERE](#).

Material properties in Real-ESSI input:

```

1 model name "test";
2 phi = 5;
3 phirad = pi*phi/180;
4 eta = 6*sin(phirad)/(3-sin(phirad));
5 add material # 1 type DruckerPragerNonAssociateArmstrongFrederick
6   mass_density = 0.0*kg/m^3
7   elastic_modulus = 2E7*N/m^2
8   poisson_ratio = 0.0
9   druckerprager_k = eta
10  armstrong_frederick_ha = 2E7*N/m^2
11  armstrong_frederick_cr = 100
12  isotropic_hardening_rate = 0*Pa
13  initial_confining_stress = 1*Pa
14  plastic_flow_xi = 0.0
15  plastic_flow_kd = 0.0 ;
16 define NDMaterial constitutive integration algorithm Backward_Euler
17   yield_function_relative_tolerance = 1E-6
18   stress_relative_tolerance = 1E-6
19   maximum_iterations = 30;
20 simulate constitutive testing strain control pure shear cyclic ←
21   loading use material # 1
22   confinement_strain = 0.001
23   strain_increment_size = 0.0001
24   maximum_strain = 0.01
25   number_of_cycles = 1;
26 bye;

```

Material Response:

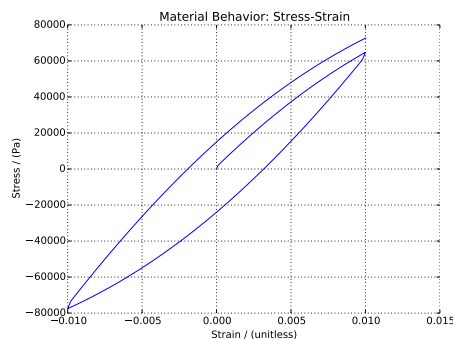


Figure 1.17: Drucker-Prager Armstrong-Frederick under Pure Shear Cyclic Loading.

1.3.6 Elastic Plastic, SaniSAND, Constitutive Examples

Bardet Constraint Examples

The compressed package of Real-ESSI input files and postprocessing scripts and results for this example is available [HERE](#). Material Response is shown in Figure 1.18

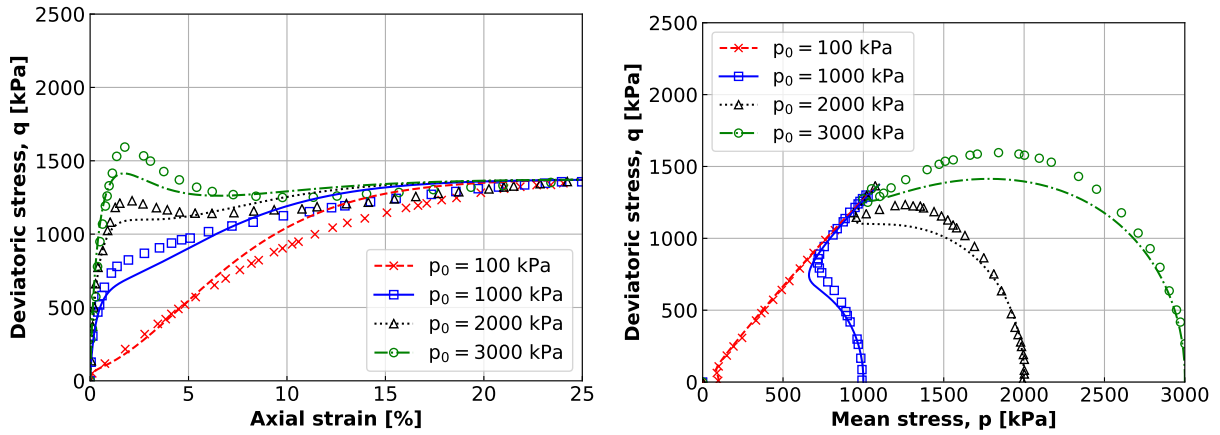


Figure 1.18: SaniSAND response.

1.4 Stiffness Reduction and Damping Curves Modeling

1.4.1 Multi-yield-surface von-Mises

The Real-ESSI input files for this example are available [HERE](#). The compressed package of Real-ESSI input files and postprocessing results for this example is available [HERE](#).

Model description

This model illustrates the G/Gmax input to multi-yield-surface von-Mises material. This example is based on one Gauss-point with multi-yield-surface von-Mises material. The G/Gmax is converted to material modeling parameters (yield-surface size and hardening parameter) inside the DSL.

Real-ESSI input file

```

1 model name "test";
2 add material # 1 type vonMisesMultipleYieldSurfaceGoverGmax
3   mass_density = 0.0*kg/m^3
4   initial_shear_modulus = 3E8 * Pa
5   poisson_ratio = 0.0
6   total_number_of_shear_modulus = 9
7   GoverGmax =
8   "1,0.995,0.966,0.873,0.787,0.467,0.320,0.109,0.063"
9   ShearStrainGamma =
10  "0,1E-6,1E-5,5E-5,1E-4, 0.0005, 0.001, 0.005, 0.01"
11  ;
12 define NDMaterial constitutive integration algorithm Backward_Euler
13   yield_function_relative_tolerance = 1E-6
14   stress_relative_tolerance = 1E-6
15   maximum_iterations = 30
16   ;
17 incr_size = 0.000001 ;
18 max_strain= 0.005 ;
19 num_of_increm = max_strain/incr_size -1 ;
20 simulate constitutive testing strain control pure shear use material ←
21   # 1
22   confinement_strain = 0.0
23   strain_increment_size = incr_size
24   maximum_strain = max_strain
25   number_of_increment = num_of_increm;
26 bye;

```

Material Response at Gauss Point:

Computed G/Gmax curve exactly matches the one used for input at control points.

The difference in G/Gmax between control points can be reduced by using more than just 9 control points as in this example.

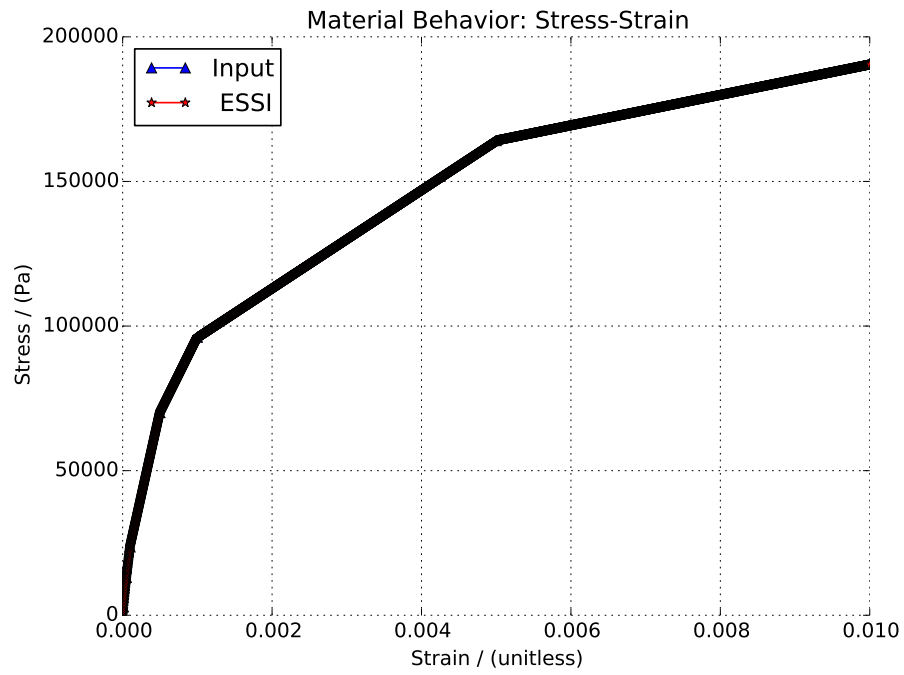


Figure 1.19: Stress-Strain Relationship

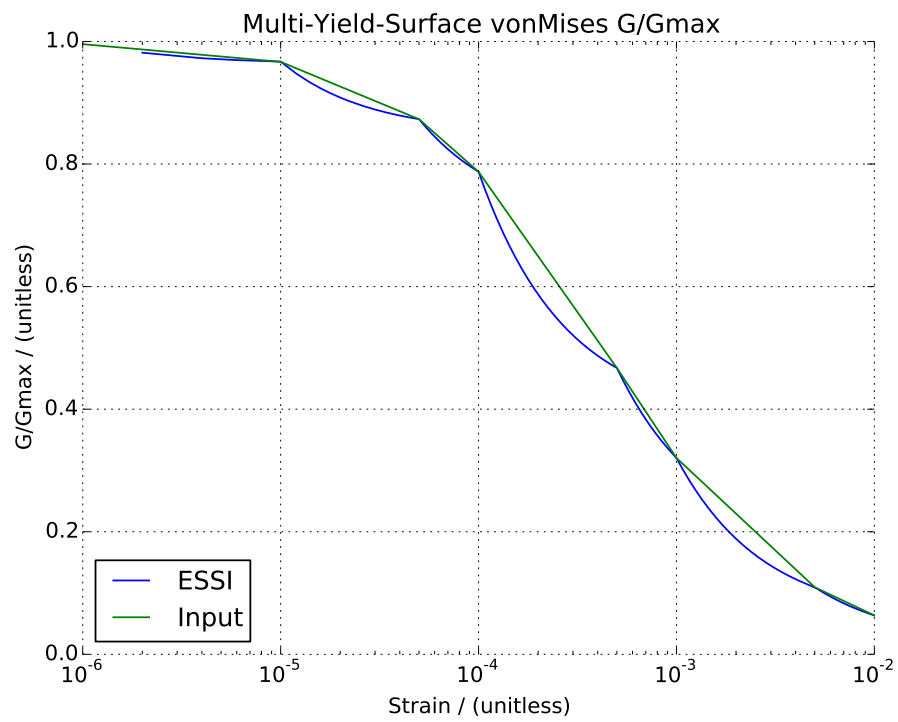


Figure 1.20: The G/Gmax results.

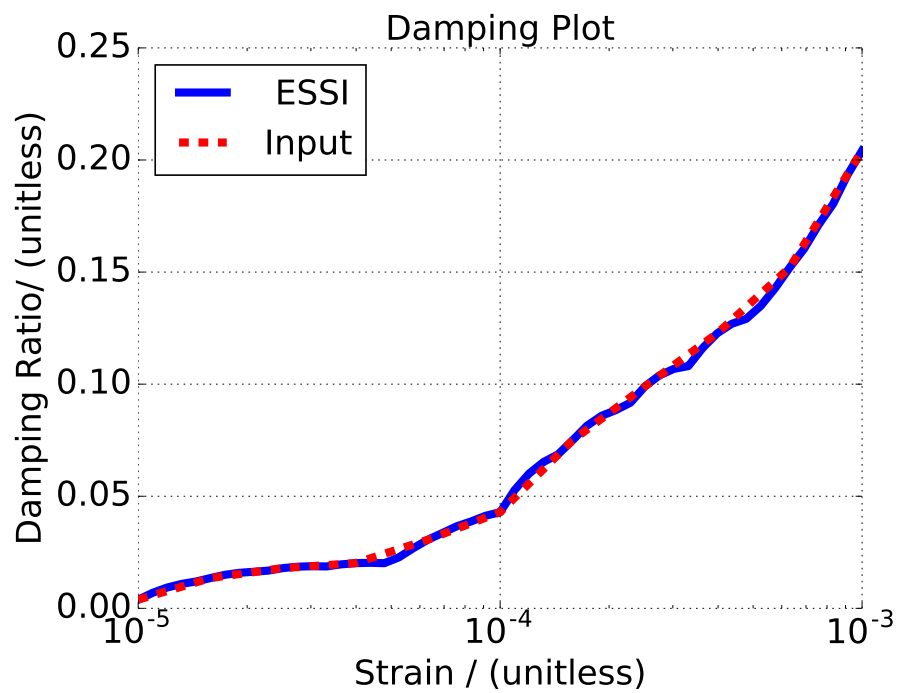


Figure 1.21: Damping Ratio Plot

1.4.2 Multi-yield-surface Drucker-Prager

The Real-ESSI input files for this example are available [HERE](#). The compressed package of Real-ESSI input files and postprocessing results for this example is available [HERE](#).

Problem description

This model illustrates the G/Gmax input to multi-yield-surface Drucker-Prager material. Purely deviatoric plastic flow is used in this material, which means that the parameter `dilation_scale` is set to zero. If user wants to model change of volume (dilation or compression) for this material, then G/Gmax curve need to be iterated upon manually by changing yield surface size directly, which is done using different `DruckerPragerMultipleYieldSurface` command. This example is based on one Gauss-point which use multi-yield-surface Drucker-Prager material. The G/Gmax is converted to the yield-surface size and hardening parameter inside the DSL.

Real-ESSI input file:

```

1 model name "test";
2
3 add material # 1 type DruckerPragerMultipleYieldSurfaceGoverGmax
4   mass_density = 0.0*kg/m^3
5   initial_shear_modulus = 3E8 * Pa
6   poisson_ratio = 0.0
7   initial_confining_stress = 1E5 * Pa
8   reference_pressure = 1E5 * Pa
9   pressure_exponential_n = 0.5
10  cohesion = 0. * Pa
11  dilation_angle_eta =1.0
12  dilation_scale = 0.0
13  total_number_of_shear_modulus = 9
14  GoverGmax =
15  "1,0.995,0.966,0.873,0.787,0.467,0.320,0.109,0.063"
16  ShearStrainGamma =
17  "0,1E-6,1E-5,5E-5,1E-4, 0.0005, 0.001, 0.005, 0.01"
18  ;
19 define NDMaterial constitutive integration algorithm Backward_Euler
20   yield_function_relative_tolerance = 1E-6
21   stress_relative_tolerance = 1E-6
22   maximum_iterations = 30;
23 simulate constitutive testing strain control pure shear use material ←
24   # 1
25   confinement_strain = 0.0
26   strain_increment_size = 0.000001
27   maximum_strain = 0.005
28   number_of_increment = 0.005 / 0.000001 -1 ;
29 bye;

```

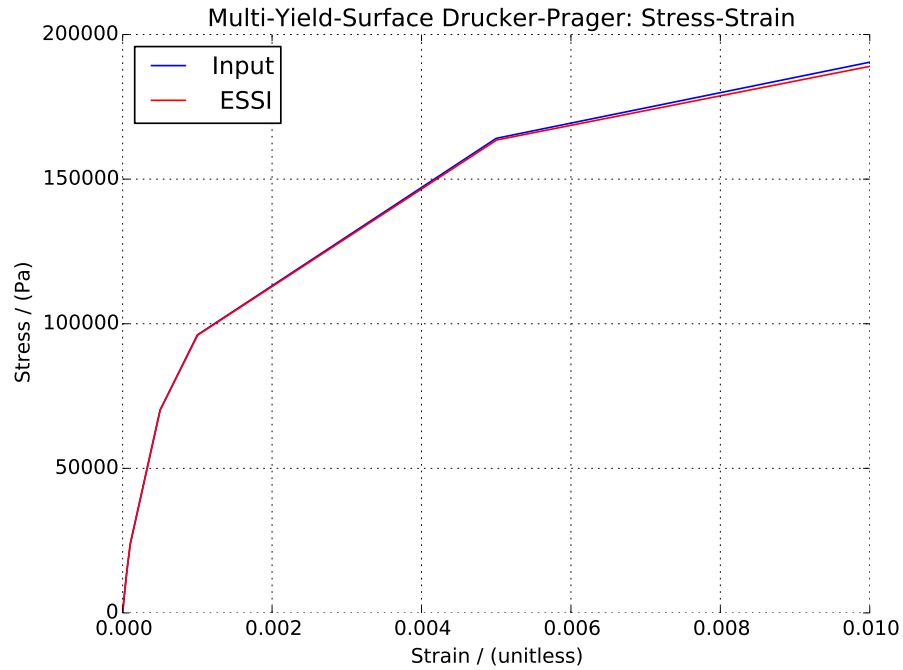


Figure 1.22: Nested-Yield-Surface Drucker-Prager Stress-Strain Relationship

Inside the DSL, the yield surface radius is calculated as $\sqrt{3}\sigma_y$, where σ_y is the yield stress of the corresponding yield surface. Then, the radius is divided by the confinement to obtain the slope (opening angle).

The hardening parameter is calculated as

$$\frac{1}{H'_i} = \frac{1}{H_i} - \frac{1}{2G} \quad (1.2)$$

where H'_i is the current hardening parameter corresponding to yield surface i . H_i is the current tangent shear modulus to surface i , namely, $H_i = 2(\tau_{i+1} - \tau_i)/(\gamma_{i+1} - \gamma_i)$. And G is the initial shear modulus.

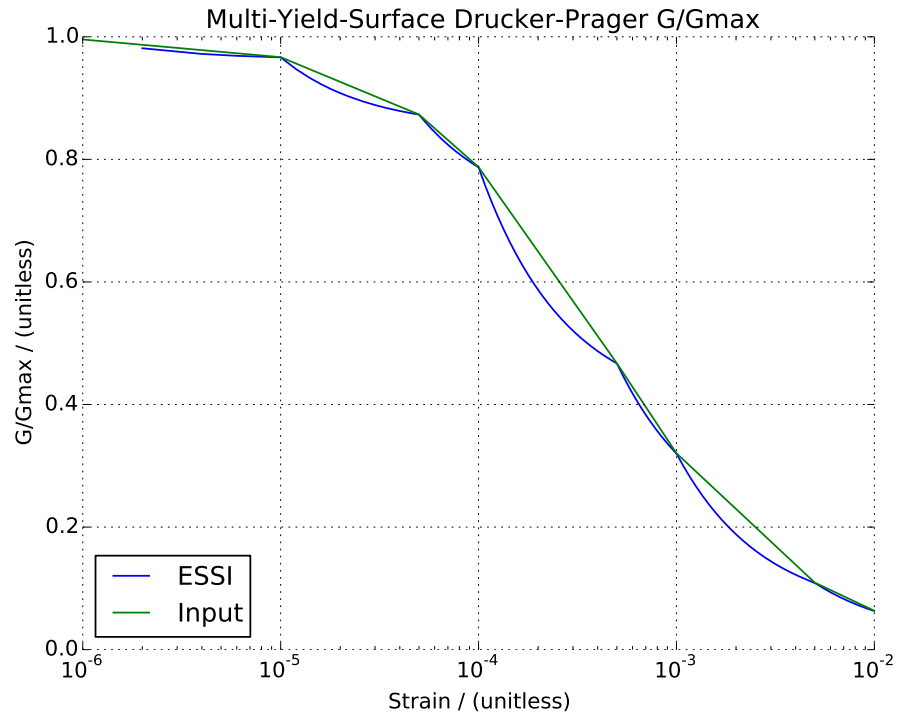


Figure 1.23: Nested-Yield-Surface Drucker-Prager G/Gmax results

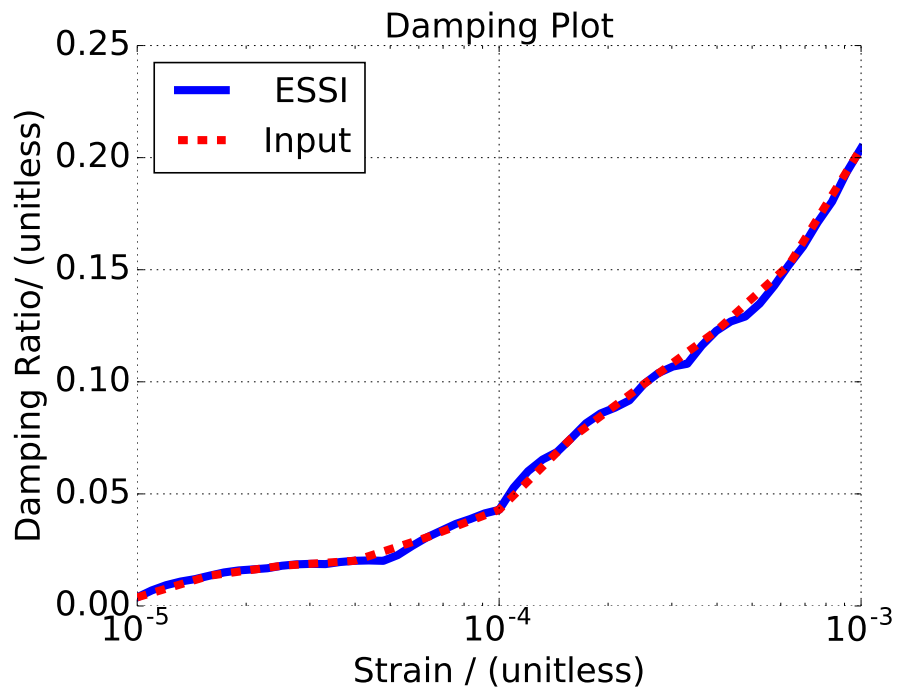


Figure 1.24: Damping Ratio Plot

1.4.3 Simulate Stiffness Reduction using von-Mises Armstrong-Frederick

The Real-ESSI input files for this example are available [HERE](#). The compressed package of Real-ESSI input files and postprocessing results for this example is available [HERE](#).

Model description

This model illustrates the simulation of stiffness reduction using von-Mises Armstrong-Frederick. This example is based on one Gauss-point.

Real-ESSI input file:

```
1 model name "test";
2
3 add material # 1 type vonMisesArmstrongFrederick
4     mass_density = 2500.0*kg/m^3
5     elastic_modulus = 3E7*N/m^2
6     poisson_ratio = 0.2
7     von_mises_radius = 300 * Pa
8     armstrong_frederick_ha = 5*3E7*N/m^2
9     armstrong_frederick_cr = 25000
10    isotropic_hardening_rate = 0*Pa
11    ;
12 define NDMaterial constitutive integration algorithm Backward_Euler
13     yield_function_relative_tolerance = 1E-6
14     stress_relative_tolerance = 1E-6
15     maximum_iterations = 30
16     ;
17 incr_size = 0.000001 ;
18 max_strain= 0.005 ;
19 num_of_increm = max_strain/incr_size -1 ;
20 simulate constitutive testing strain control pure shear use material ↔
21     # 1
22     confinement_strain = 0.0
23     strain_increment_size = incr_size
24     maximum_strain = max_strain
25     number_of_increment = num_of_increm;
26 bye;
```

The von-Mises Armstrong-Frederick material behavior matches the stiffness reduction curve.

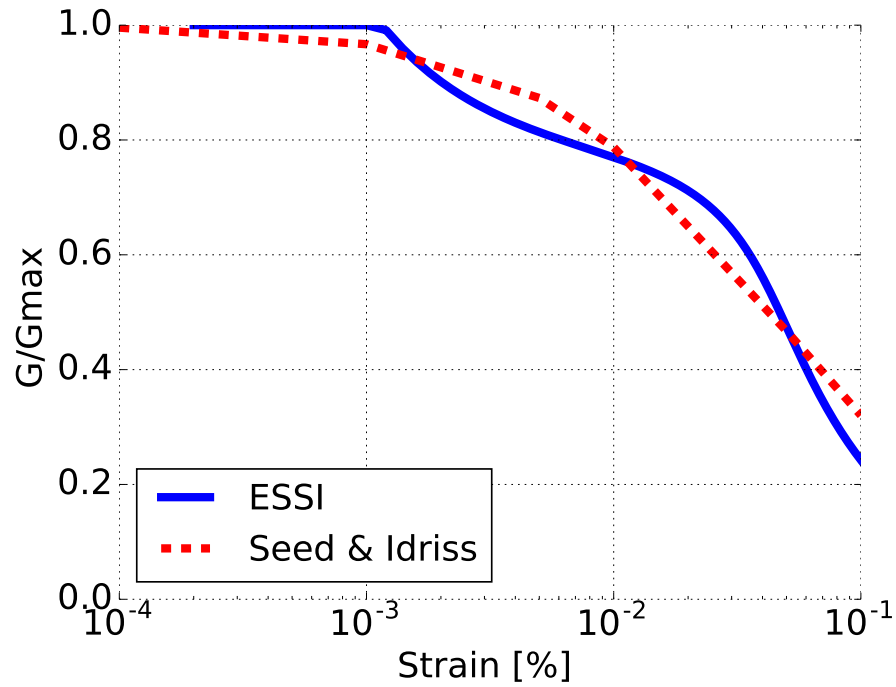


Figure 1.25: The stiffness reduction results.

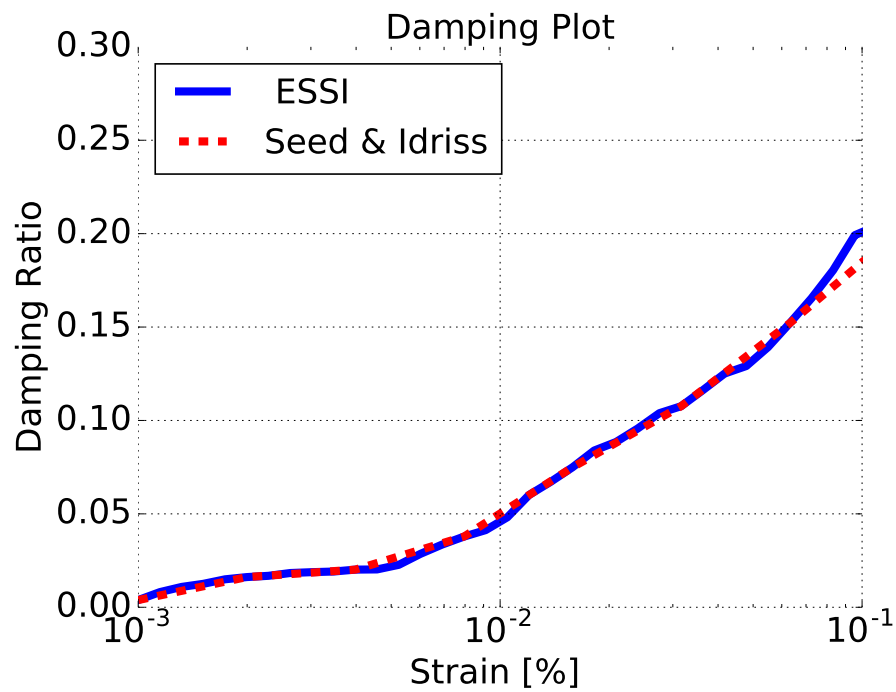


Figure 1.26: Damping Ratio Plot

1.5 Cosserat, Micropolar Material Modeling

1.5.1 Cosserat, Micropolar Elastic Material Model (example in development)

1.5.2 Cosserat, Micropolar Elastic-Plastic von Mises Material Model (example in development)

1.5.3 Cosserat, Micropolar Elastic-Plastic Druekcr Prager Material Model (example in development)

Chapter 2

Static Examples

(2016-2017-2019-2021-)

(In collaboration with Prof. José Abell, Dr. Yuan Feng, Mr. Sumeet Kumar Sinha, and Dr. Han Yang)

2.1 Chapter Summary and Highlights

In this Chapter static modeling and simulation of solids and structures is illustrated through a number of examples.

All the examples described here, and many more, organized in sub-directories, for constitutive behavior, static and dynamic behavior can be directly downloaded from a repository at: http://sokocalo.engr.ucdavis.edu/~jeremic/lecture_notes_online_material/Real-ESSI_Examples/education_examples. These examples can then be tried, analyzed using Real-ESSI Simulator that is available on Amazon Web Services (AWS) computers around the world. Login to AWS market place and search for Real-ESSI...

2.2 Static Elastic Solid Examples

2.2.1 Statics, Bricks, with Nodal Forces

Statics, 8 Node Brick, with Nodal Forces

The Real-ESSI input files for this example are available [HERE](#). The compressed package of Real-ESSI input files and postprocessing results for this example is available [HERE](#).

Problem description: a cantilever with a nodal force at the tip. Length=6m, Width=1m, Height=1m, Force=100N, $E=1E8Pa$, $\nu = 0.0$. The force direction was shown in Figure (2.1).

The mesh is generated with elastic 8 node brick.

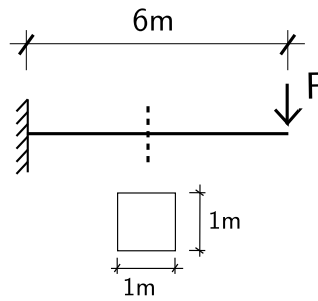


Figure 2.1: Problem description for cantilever beams.

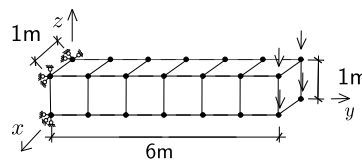


Figure 2.2: Six 8NodeBrick elements.

Statics, 27 Node Brick, with Nodal Forces

The Real-ESSI input files for this example are available [HERE](#). The compressed package of Real-ESSI input files and postprocessing results for this example is available [HERE](#).

Problem description: a cantilever with a nodal force at the tip. Length=6m, Width=1m, Height=1m, Force=100N, $E=1E8Pa$, $\nu = 0.0$. The force direction was shown in Figure (2.3).

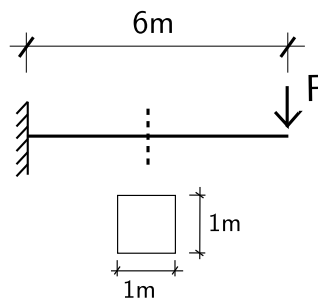


Figure 2.3: Problem description for cantilever beams.

The mesh is generated with elastic 27 node brick.

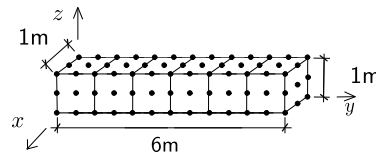


Figure 2.4: Six 27NodeBrick elements.

Statics, 8-27 Node Brick, with Nodal Forces

The Real-ESSI input files for this example are available [HERE](#). The compressed package of Real-ESSI input files and postprocessing results for this example is available [HERE](#).

Problem description: a cantilever with a nodal force at the tip. Length=2m, Width=2m, Height=2m, $\nu = 0.0$. The force direction was shown in Figure (2.5).

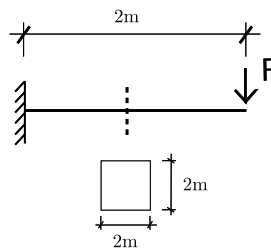


Figure 2.5: Problem description for cantilever beams.

The mesh is generated with an elastic 8-27 node brick. As shown in the Figure 2.16, some of the nodes are missing on purpose. The variable node brick element is usually used as the transition mesh between 8 node brick and 27 node brick.

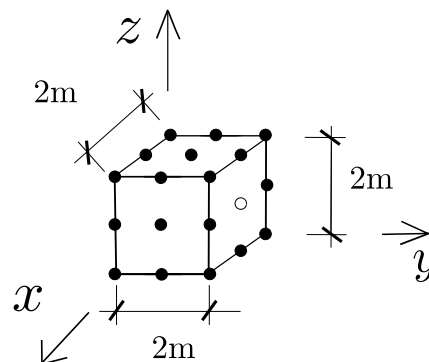


Figure 2.6: One 8-27 Node elements.

2.2.2 Statics, Bricks, with Surface Loads

Statics, 8 Node Brick, with Surface Forces

The Real-ESSI input files for this example are available [HERE](#). The compressed package of Real-ESSI input files and postprocessing results for this example is available [HERE](#).

Problem description: a cantilever with the load on one surface. Length=2m, Width=2m, Height=2m, $\nu = 0.0$. The force distribution was shown in Figure (2.7).

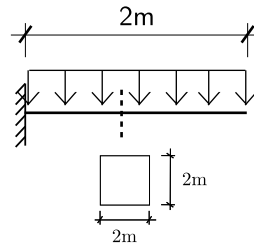


Figure 2.7: Problem description for cantilever beams.

The mesh is generated with an elastic 8 node brick.

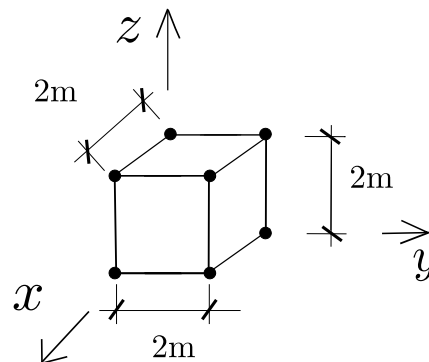


Figure 2.8: One element with surface load.

Statics, 27 Node Brick, with Surface Forces

The Real-ESSI input files for this example are available [HERE](#). The compressed package of Real-ESSI input files and postprocessing results for this example is available [HERE](#).

Problem description: a cantilever with the load on one surface. Length=2m, Width=2m, Height=2m. The force distribution was shown in Figure (2.9).

The mesh is generated with an elastic 27 node brick.

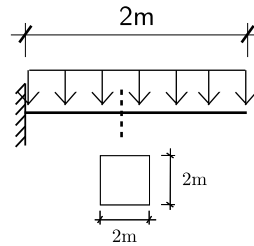


Figure 2.9: Problem description for cantilever beams.

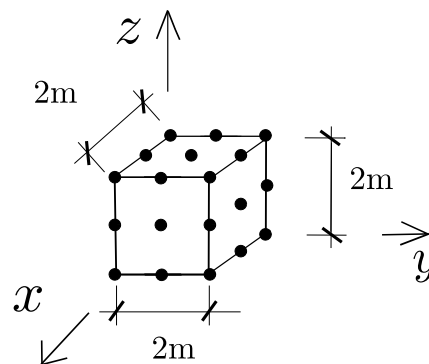


Figure 2.10: One element with surface load.

2.2.3 Statics, Bricks, with Body Forces

Statics, 8 Node Brick, with Body Forces

The Real-ESSI input files for this example are available [HERE](#). The compressed package of Real-ESSI input files and postprocessing results for this example is available [HERE](#).

Problem description: a cantilever with self weight on the whole element. Length=6m, Width=1m, Height=1m, $\nu = 0.3$. The force direction was shown in Figure (2.11).

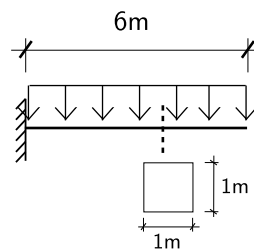


Figure 2.11: Problem description for cantilever beams.

The mesh is generated with an elastic 8 node brick.

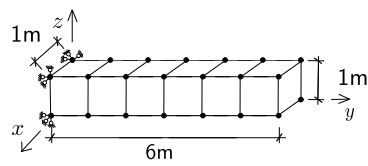


Figure 2.12: Six 8NodeBrick elements.

Statics, 27 Node Brick, with Body Forces

The Real-ESSI input files for this example are available [HERE](#). The compressed package of Real-ESSI input files and postprocessing results for this example is available [HERE](#).

Problem description: a cantilever with self weight on the whole element. Length=6m, Width=1m, Height=1m, $\nu = 0.3$. The force direction was shown in Figure (2.13).

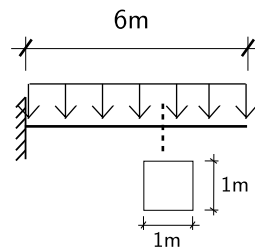


Figure 2.13: Problem description for cantilever beams.

The mesh is generated with an elastic 27 node brick.

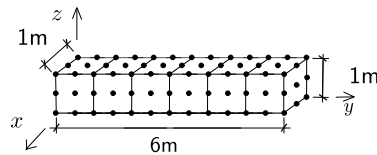


Figure 2.14: Six 27NodeBrick elements.

Statics, 8-27 Node Brick, with Body Forces

The Real-ESSI input files for this example are available [HERE](#). The compressed package of Real-ESSI input files and postprocessing results for this example is available [HERE](#).

Problem description: a cantilever with self weight on the whole element. Length=2m, Width=2m, Height=2m, $\nu = 0.3$. The force direction was shown in Figure (2.15).

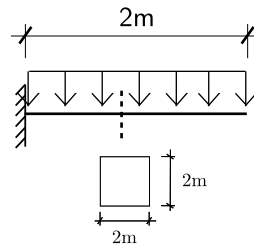


Figure 2.15: Problem description for cantilever beams.

The mesh is generated with an elastic 8-27 node brick. As shown in the Figure 2.16, some of the nodes are missing on purpose. The variable node brick element is usually used as the transition mesh between 8 node brick and 27 node brick.

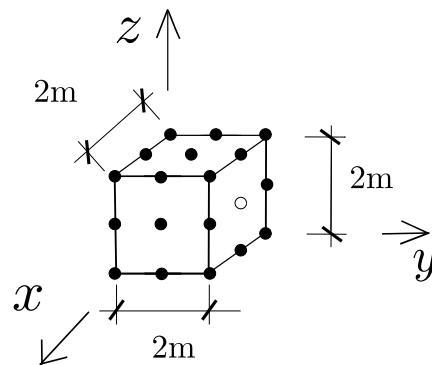


Figure 2.16: One variable Node Brick elements.

2.3 Static Elastic Structural Examples

2.3.1 Statics, Truss, with Nodal Forces

The Real-ESSI input files for this example are available [HERE](#). The compressed package of Real-ESSI input files and postprocessing results for this example is available [HERE](#).

Problem description: a cantilever with the nodal load on the tip. Length=1m, Cross Section= $1m^2$. The cross section shape is not necessarily a square. The force direction was shown in Figure (2.17). Truss only takes axial force.

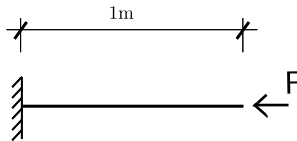


Figure 2.17: Problem description for a cantilever.

2.3.2 Statics, Elastic Beam, with Nodal Forces

The Real-ESSI input files for this example are available [HERE](#). The compressed package of Real-ESSI input files and postprocessing results for this example is available [HERE](#).

Problem description: a cantilever with nodal load on the tip. Length=1m, Width=1m, Height=1m, $E=1Pa$. The force direction was shown in Figure (2.18).

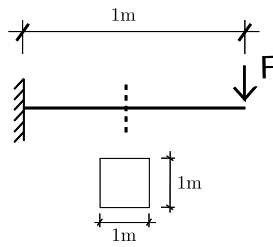


Figure 2.18: Problem description for cantilever beams.

2.3.3 Statics, Elastic Beam, with Body Forces

The Real-ESSI input files for this example are available [HERE](#). The compressed package of Real-ESSI input files and postprocessing results for this example is available [HERE](#).

Problem description: a cantilever with self weight. Length=1m, Width=1m, and Height=1m. The force direction was shown in Figure (2.19).

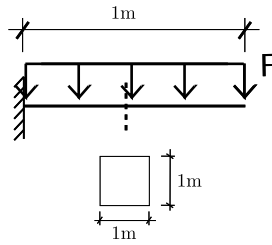


Figure 2.19: Problem description for cantilever beams.

2.3.4 Statics, ShearBeam Element

Problem description

The Real-ESSI input files for this example are available [HERE](#). The compressed package of Real-ESSI input files and postprocessing results for this example is available [HERE](#).

In the element type "ShearBeam", only one Gauss point exists. ShearBeam element was used here to test the von Mises Armstrong-Frederickó material model. Vertical force F_z was used to apply confinement to the element. Then, cyclic force F_x is used to load. Usually, pressure-dependent materials, like Drucker-Prager, require the confinement. The pressure-independent materials, like von Mises, do not require the confinement.

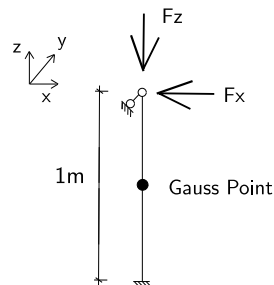


Figure 2.20: ShearBeam element.

Results

Resulting stress-strain relationship is shown in Fig.(2.21).

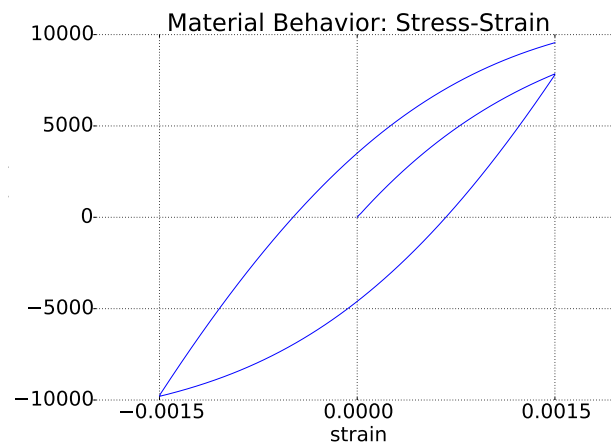


Figure 2.21: Shear stress-strain response.

2.3.5 Statics, Elastic Shell, with Nodal Forces

ANDES Shell, out of Plane Force

The Real-ESSI input files for this example are available [HERE](#). The compressed package of Real-ESSI input files and postprocessing results for this example is available [HERE](#).

Problem description: Length=6m, Width=1m, Height=1m, Force=100N, $E=1E8Pa$, $\nu = 0.0$.

The force direction was shown in Figure (2.22).

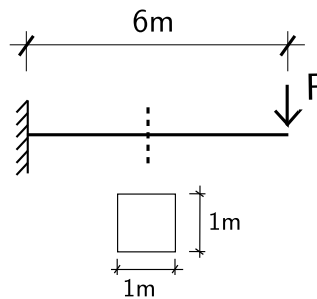


Figure 2.22: Problem description for cantilever beams.

ANDES Shell, Perpendicular to Plane, bending

The mesh and the out-of-plane force is shown in Fig. 2.23.

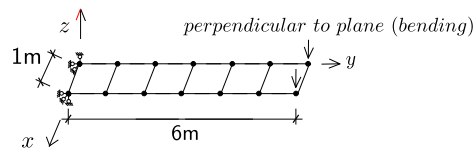


Figure 2.23: Six 4NodeANDES elements.

ANDES Shell, In-plane Force

The Real-ESSI input files for this example are available [HERE](#). The compressed package of Real-ESSI input files and postprocessing results for this example is available [HERE](#).

Problem description: a cantilever with a nodal force at the tip. Length=6m, Width=1m, Height=1m, Force=100N, $E=1E8Pa$, $\nu = 0.0$. The force direction was shown in Figure (2.24).

The mesh and the inplane force is shown in Fig. 2.25.

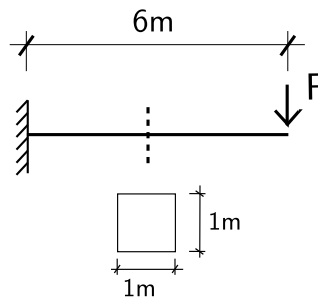


Figure 2.24: Problem description for cantilever beams.

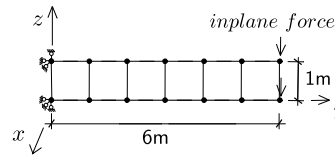


Figure 2.25: Six 4NodeANDES elements.

2.3.6 Statics, Elastic Shell, with Body Forces

ANDES shell under the out-of-Plane Body Force

The Real-ESSI input files for this example are available [HERE](#). The compressed package of Real-ESSI input files and postprocessing results for this example is available [HERE](#).

Problem description: Length=6m, Width=1m, Height=1m, Force=100N, $E=1E8Pa$, $\nu = 0.0$. The force direction was shown in Figure (2.26).

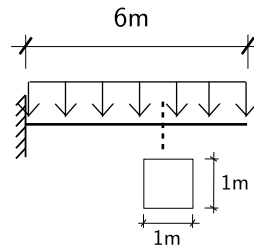


Figure 2.26: Problem description for cantilever beams.

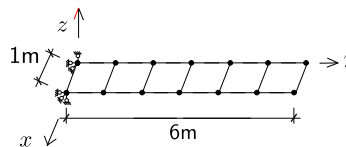


Figure 2.27: Six 4NodeANDES elements.

ANDES Shell, In-plane Body Force

The Real-ESSI input files for this example are available [HERE](#). The compressed package of Real-ESSI input files and postprocessing results for this example is available [HERE](#).

Problem description: a cantilever with a nodal force at the tip. Length=6m, Width=1m, Height=1m, Force=100N, $E=1E8Pa$, $\nu = 0.0$. The force direction was shown in Figure (2.28).

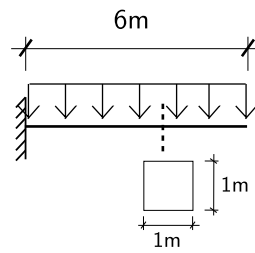


Figure 2.28: Problem description for cantilever beams.

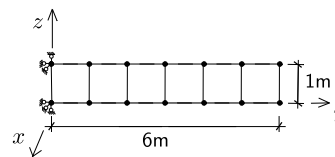


Figure 2.29: Six 4NodeANDES elements.

2.4 Statics, Interface/Contact Elements

2.4.1 Statics, Two Bar Normal Interface/Contact Problem Under Monotonic Loading.

The Real-ESSI input files for this example are available [HERE](#). The compressed package of Real-ESSI input files and postprocessing results for this example is available [HERE](#).

This is an example of normal monotonic loading on a 1-D contact/interface between two bars separated by an initial gap of 0.1 unit. An illustrative diagram of the problem statement is shown below.

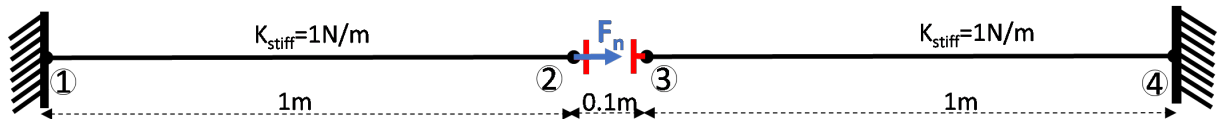


Figure 2.30: Illustration of Two Bar Normal Interface/Contact Problem under monotonic loading with initial gap.

The displacement output of *Node 2 and Node 3* are shown below.

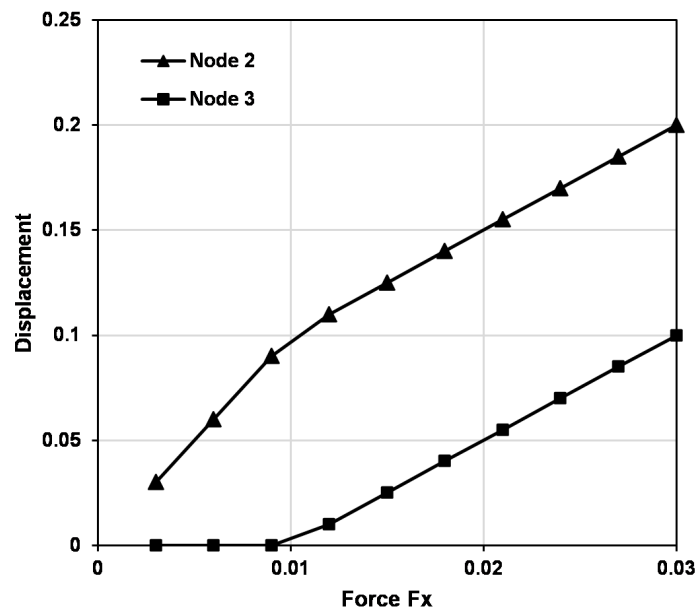


Figure 2.31: Displacement of Nodes 2 and 3.

2.4.2 Statics, Four Bar Interface/Contact Problem With Normal and Shear Force Under Monotonic Loading

The Real-ESSI input files for this example are available [HERE](#). The compressed package of Real-ESSI input files and postprocessing results for this example is available [HERE](#).

This is an example to show the normal and tangential behavior (stick and slip case) of contacts using four bars in 2-D plane. The bars in x-directions are in contact/interface (initial gap=0).

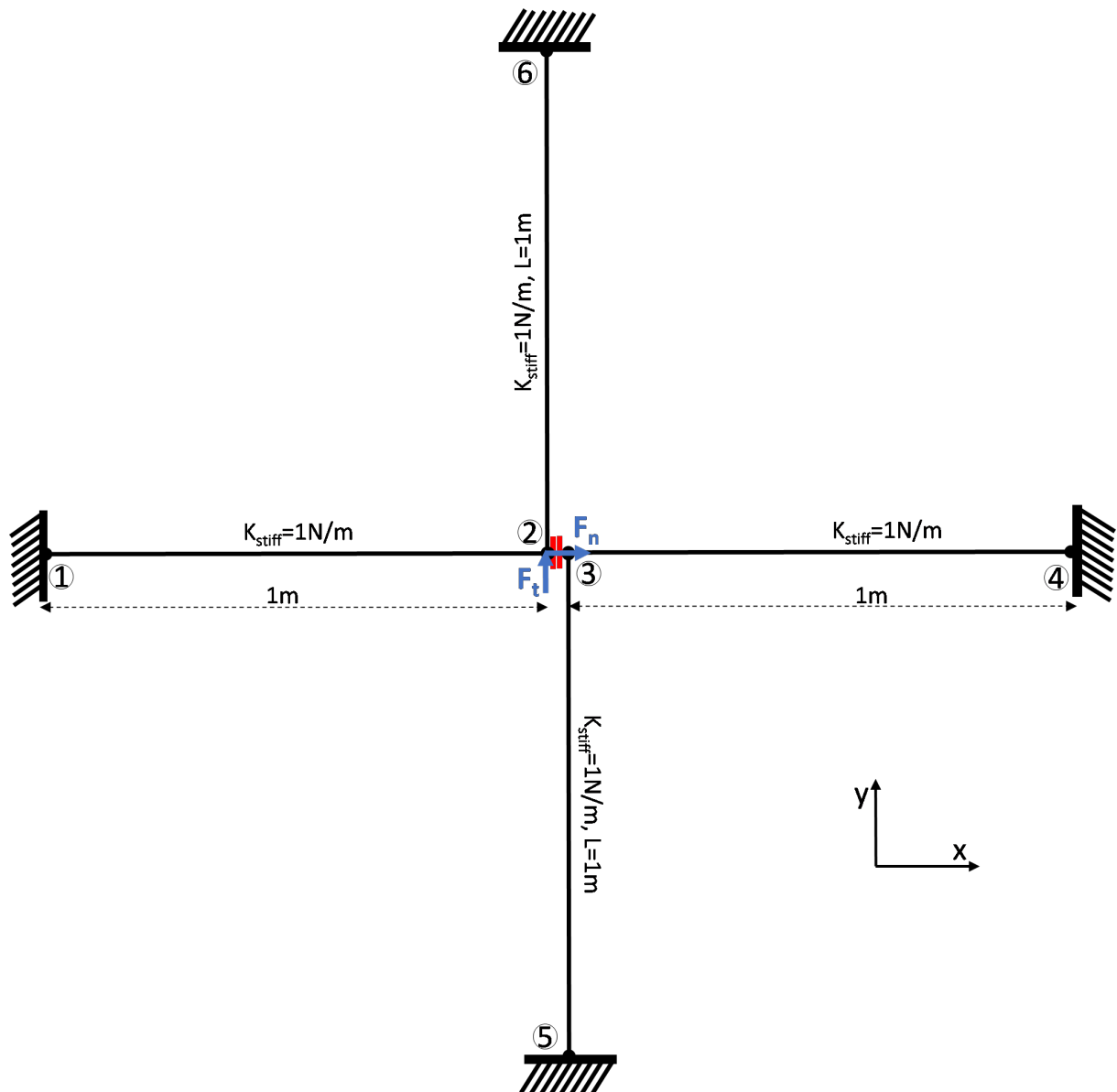


Figure 2.32: Illustration of Four Bar Normal Interface/Contact Problem With Normal and Shear Force Under Monotonic Loading with no initial gap.

The displacement output of *Node 2* and *Node 3* are shown below.

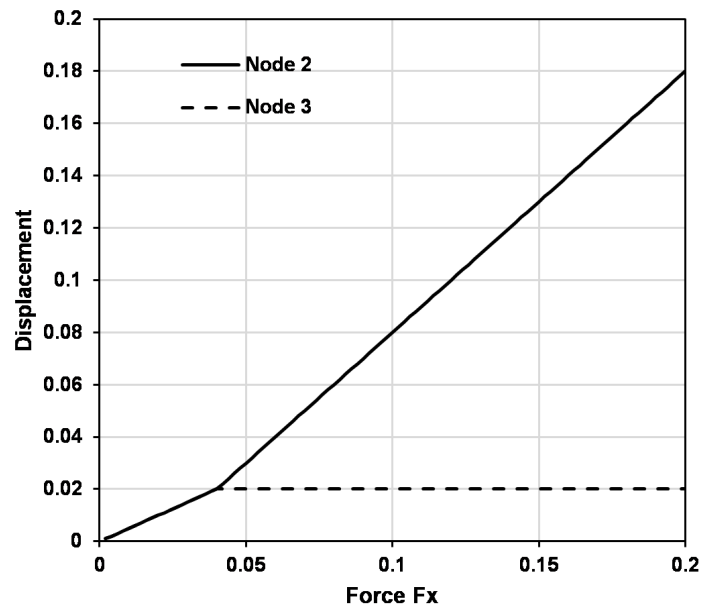


Figure 2.33: Displacement of Nodes 2 and 3 along y direction.

2.4.3 Statics, 3-D Truss example with normal confinement and Shear Loading

The Real-ESSI input files for this example are available [HERE](#). The compressed package of Real-ESSI input files and postprocessing results for this example is available [HERE](#).

A simple 3-D truss example with Normal confinement in z-direction of $F_N = 0.5N$, friction coefficient $\mu = 0.2$ and shear loading of magnitude $F_s = 0.5N$. Figure 2.34 below, shows the description of the problem.

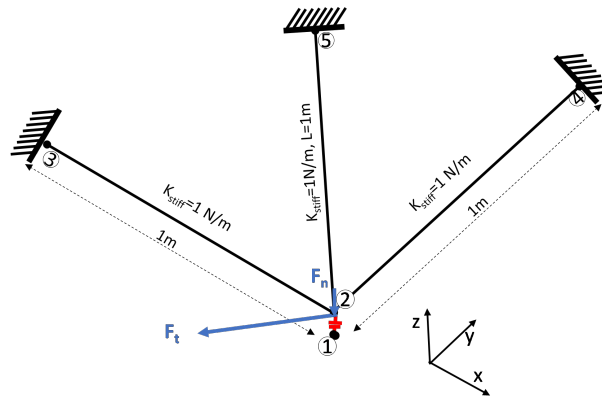


Figure 2.34: Illustration of 3-D Truss Problem with confinement loading in z-direction of 0.5N and then shear loading of 0.5N in x-y plane.

The generalized displacement response of the tangential loading stage is shown below.

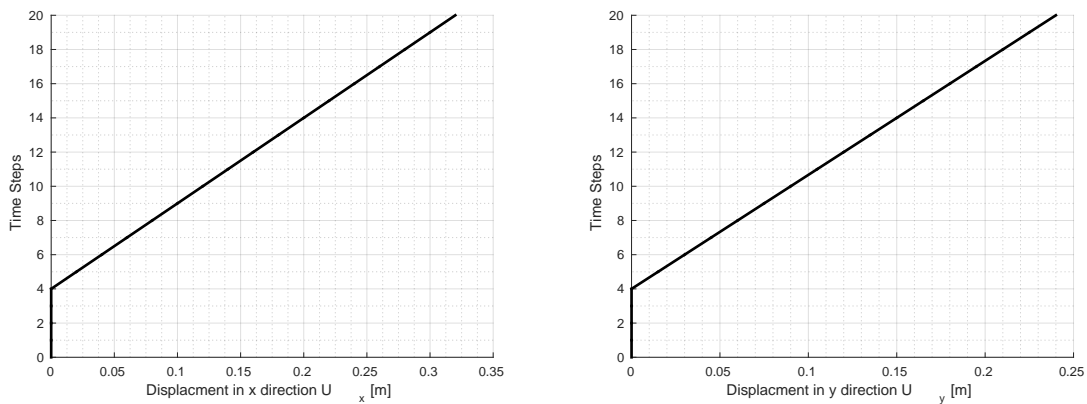


Figure 2.35: Displacements of Node 2 with applied shear tangential load step.

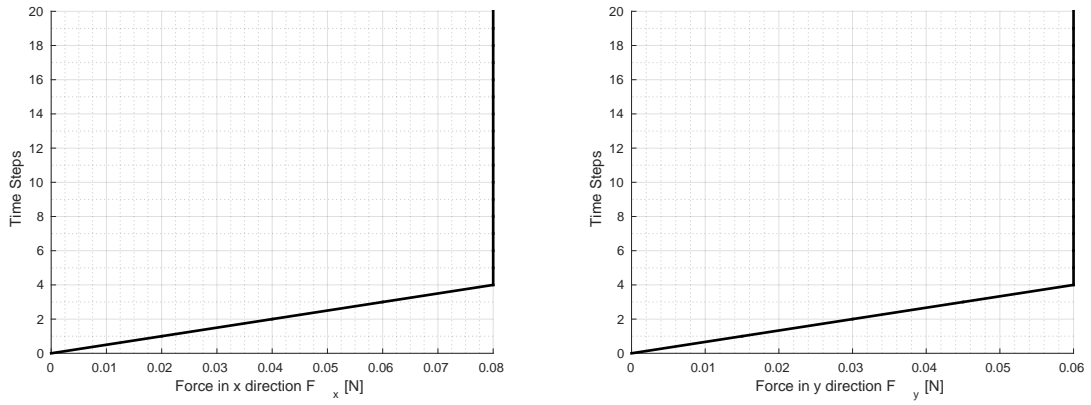


Figure 2.36: Resisting force by the contact/interface element with applied shear tangential load step.

2.4.4 Statics, Six Solid Blocks Example With Interface/Contact

The Real-ESSI input files for this example are available [HERE](#). The compressed package of Real-ESSI input files and postprocessing results for this example is available [HERE](#).

This is a 3-D solid block example with initial normal and then tangential load on different surfaces as shown below.

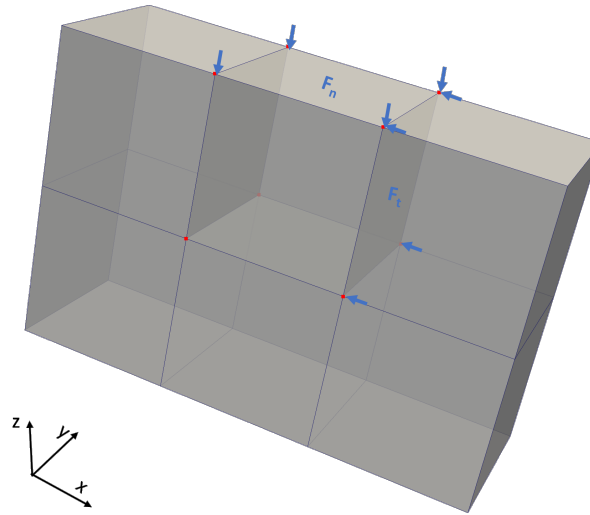


Figure 2.37: Illustration of Six Solid Blocks Example with Interface/Contact with first normal and then tangential loading stages.

The generalized displacement field of the two loading stages normal loading and *tangential loading* is shown below..

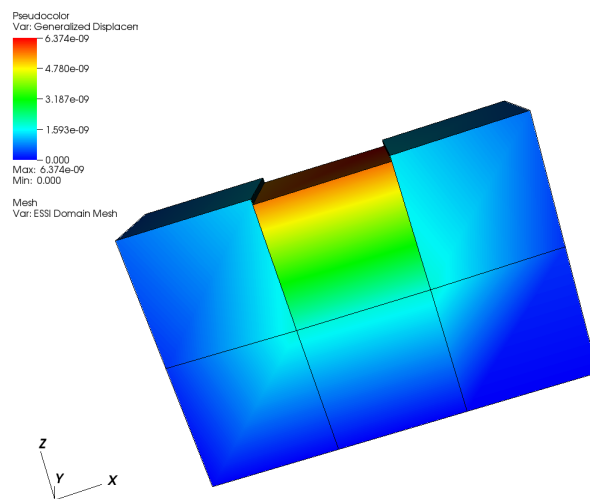


Figure 2.38: Generalized displacement magnitude visualization of normal loading.

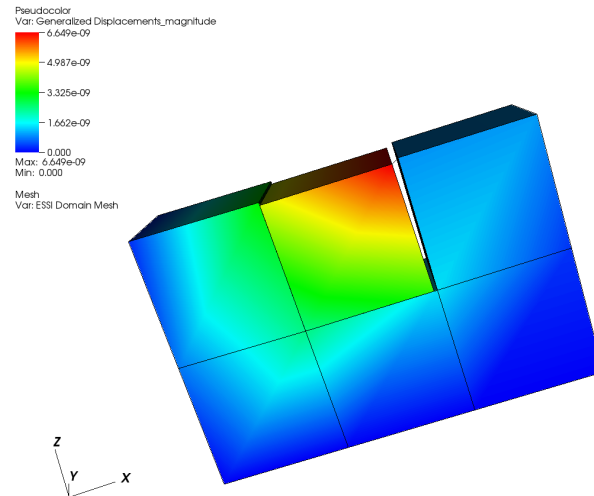


Figure 2.39: Generalized displacement magnitude visualization of tangential loading.

2.5 Static Inelastic Solid Examples

2.5.1 Statics, Bricks, Elastic-Plastic, von Mises, with Nodal Forces

The Real-ESSI input files for this example are available [HERE](#). The compressed package of Real-ESSI input files and postprocessing results for this example is available [HERE](#).

Model Description:

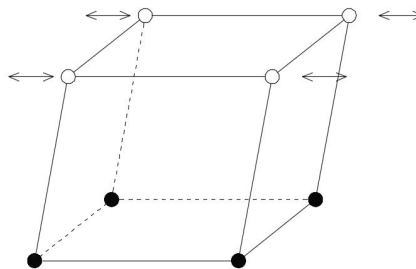


Figure 2.40: Perfectly Plastic Pure Shear Cyclic Loading.

Material Response at Gauss Point:

2.5.2 Statics, Bricks, Elastic-Plastic, Drucker Prager, with Nodal Forces

The Real-ESSI input files for this example are available [HERE](#). The compressed package of Real-ESSI input files and postprocessing results for this example is available [HERE](#).

Model Description:

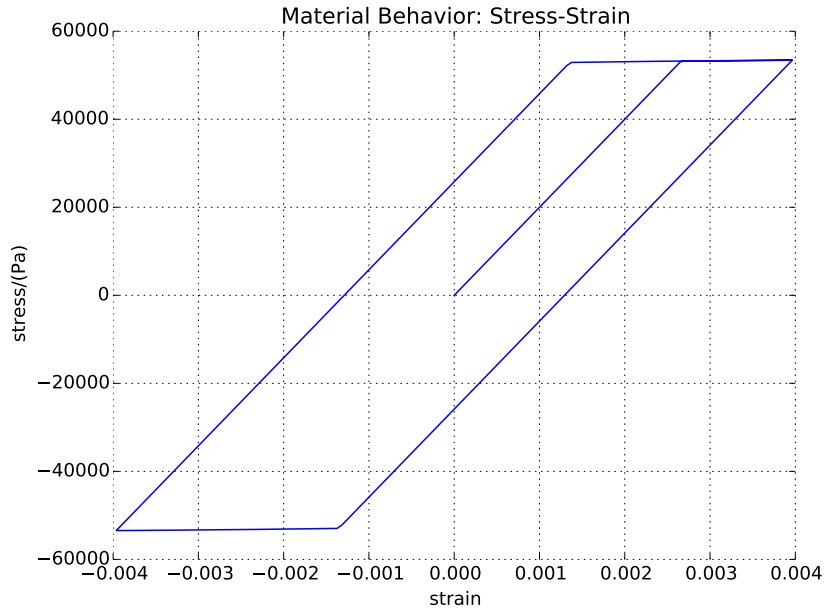


Figure 2.41: Results of Perfectly Plastic Pure Shear Cyclic Loading.

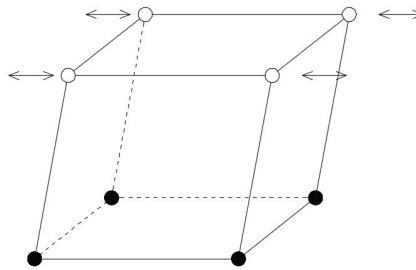


Figure 2.42: Diagram of Drucker-Prager Armstrong-Frederick Pure Shear Cyclic Loading.

Material Response at Gauss Point:

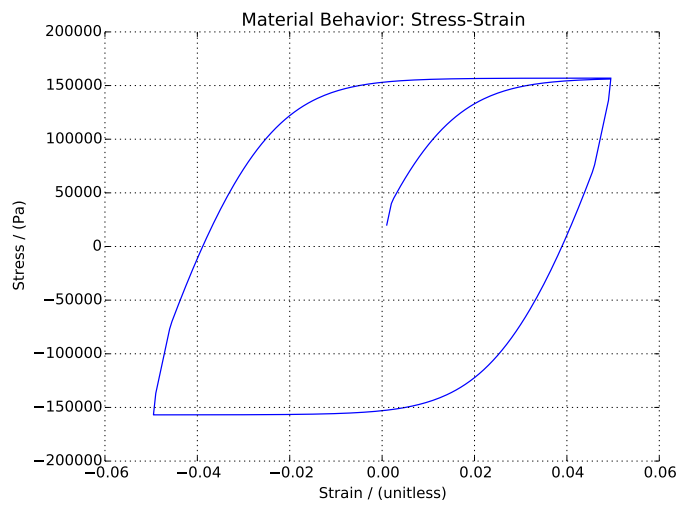


Figure 2.43: Result of Drucker-Prager Armstrong-Frederick Pure Shear Cyclic Loading.

2.6 Static Inelastic Shell Examples (example in development)

2.7 Statics, Elastic Single Solid Finite Element Examples

2.7.1 Statics, Linear Elastic, Solid Examples

Statics, Pure Shear, Monotonic Loading

The Real-ESSI input files for this example are available [HERE](#). The compressed package of Real-ESSI input files and postprocessing results for this example is available [HERE](#).

Model Description:

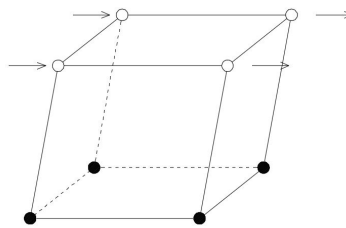


Figure 2.44: Diagram Linear Elastic Solid Pure Shear Monotonic Loading.

Material Response at Gauss Point:

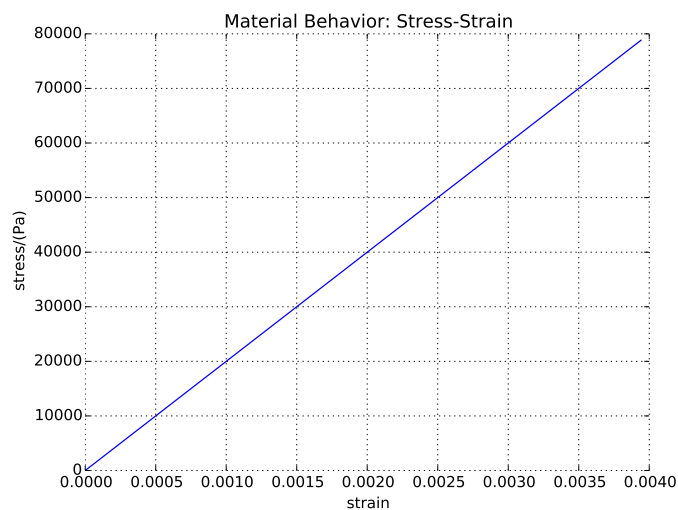


Figure 2.45: Results of Linear Elastic Solid Pure Shear Monotonic Loading.

Pure Shear, Cyclic Loading

The Real-ESSI input files for this example are available [HERE](#). The compressed package of Real-ESSI input files and postprocessing results for this example is available [HERE](#).

Model Description:

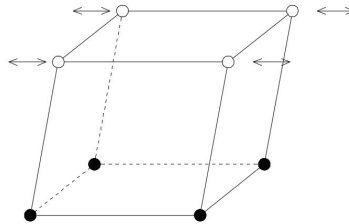


Figure 2.46: Diagram Linear Elastic Solid Pure Shear Cyclic Loading.

Material Response at Gauss Point:

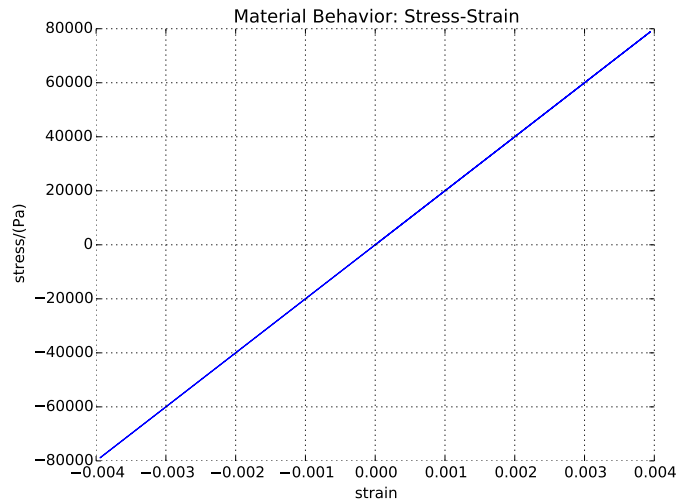


Figure 2.47: Results of Linear Elastic Solid Pure Shear Cyclic Loading.

Uniaxial Strain, Monotonic Loading

The Real-ESSI input files for this example are available [HERE](#). The compressed package of Real-ESSI input files and postprocessing results for this example is available [HERE](#).

Model Description:

Material Response at Gauss Point:

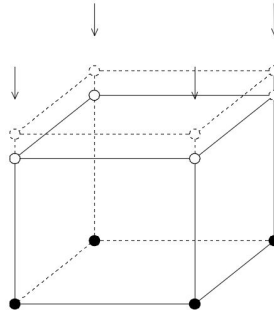


Figure 2.48: Diagram Linear Elastic Uniaxial Strain Solid Monotonic Loading.

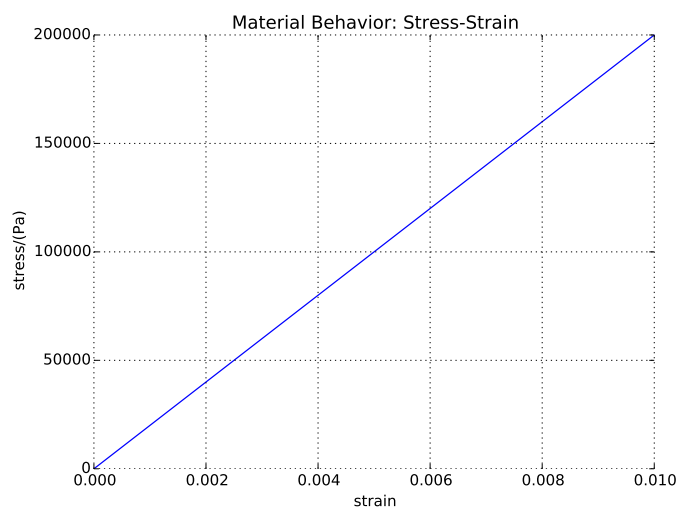


Figure 2.49: Results of Linear Elastic Pure Shear Monotonic Loading.

Uniaxial Strain, Cyclic Loading

The Real-ESSI input files for this example are available [HERE](#). The compressed package of Real-ESSI input files and postprocessing results for this example is available [HERE](#).

Model Description:

Material Response at Gauss Point:

2.7.2 Statics, Nonlinear Elastic, Duncan-Chang, Pure Shear, Solid Examples

Pure Shear, Monotonic Loading

The Real-ESSI input files for this example are available [HERE](#). The compressed package of Real-ESSI input files and postprocessing results for this example is available [HERE](#).

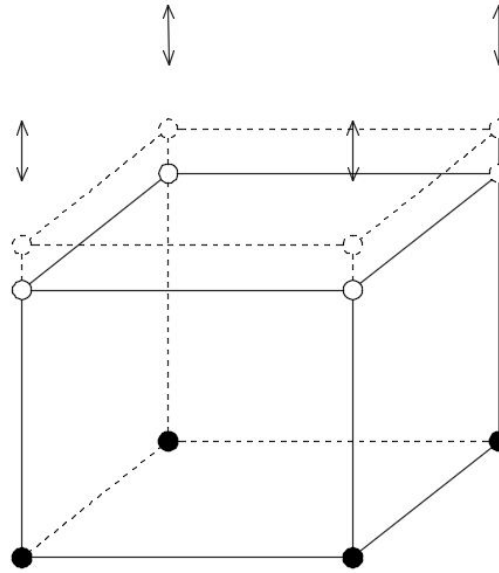


Figure 2.50: Linear Elastic Uniaxial Strain Cyclic Loading.

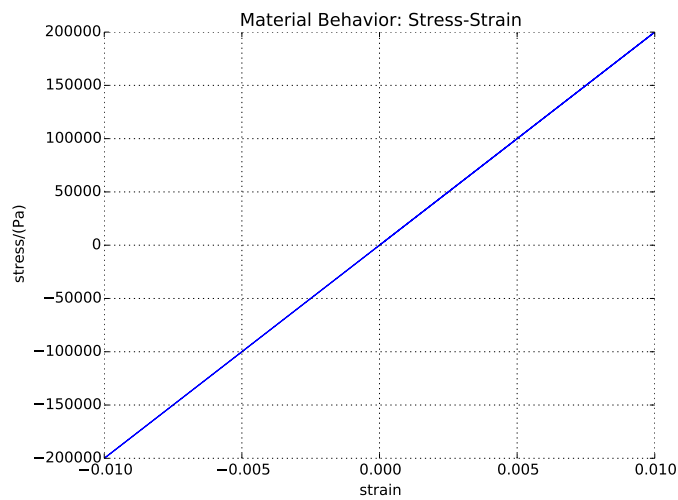


Figure 2.51: Results of Linear Elastic Pure Shear Cyclic Loading.

Model Description:

Material Response at Gauss Point:

Pure Shear, Cyclic Loading

The Real-ESSI input files for this example are available [HERE](#). The compressed package of Real-ESSI input files and postprocessing results for this example is available [HERE](#).

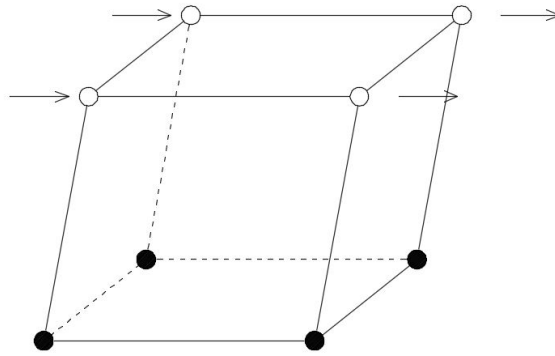


Figure 2.52: Nonlinear Elastic Uniaxial Strain Monotonic Loading.

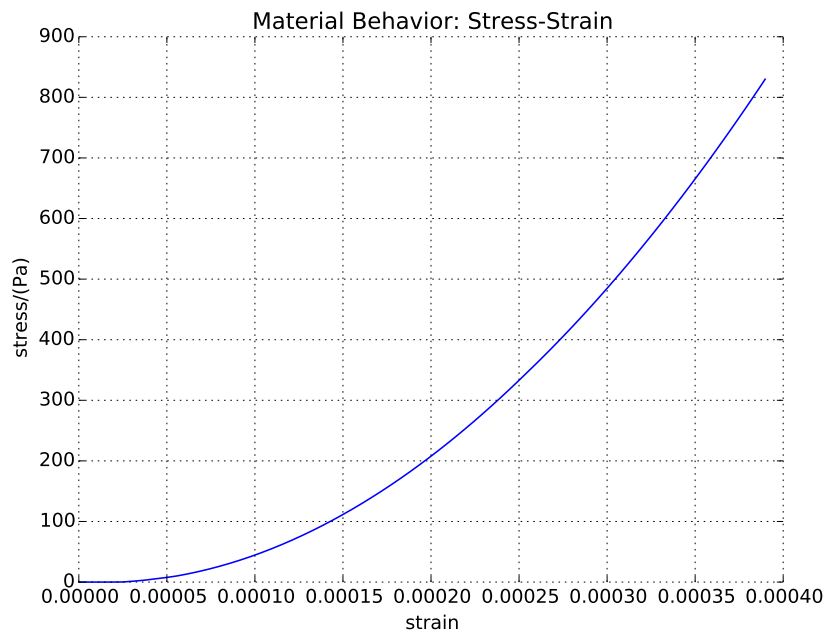


Figure 2.53: Results of Nonlinear Elastic Pure Shear Monotonic Loading.

Model Description:

Material Response at Gauss Point:

2.8 Statics, Elastic-Plastic Single Solid Finite Element Examples

2.8.1 Statics, Elastic Perfectly Plastic, Cyclic Loading, Pure Shear Solid Examples

The Real-ESSI input files for this example are available [HERE](#). The compressed package of Real-ESSI input files and postprocessing results for this example is available [HERE](#).

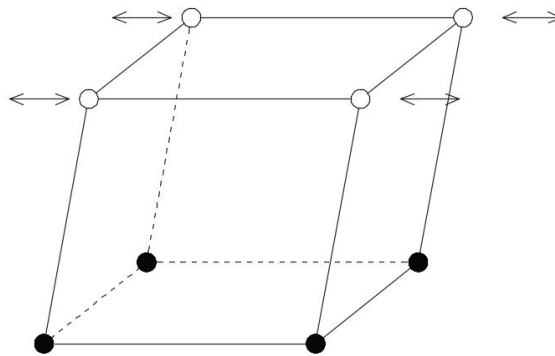


Figure 2.54: Nonlinear Elastic Uniaxial Strain Cyclic Loading.

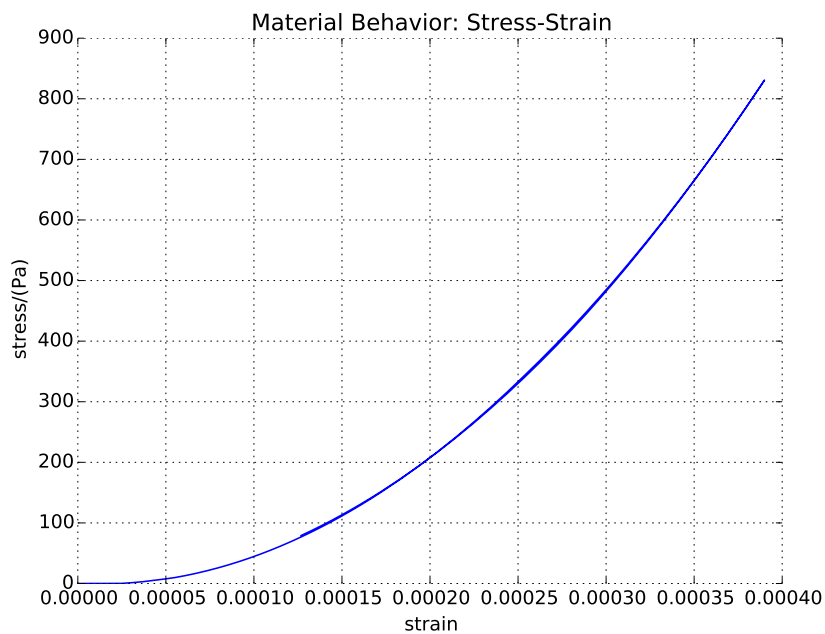


Figure 2.55: Results of Nonlinear Elastic Pure Shear Cyclic Loading.

Model Description:

Material Response at Gauss Point:

Statics, von-Mises Yield Function, Isotropic Hardening

The Real-ESSI input files for this example are available [HERE](#). The compressed package of Real-ESSI input files and postprocessing results for this example is available [HERE](#).

Model Description:

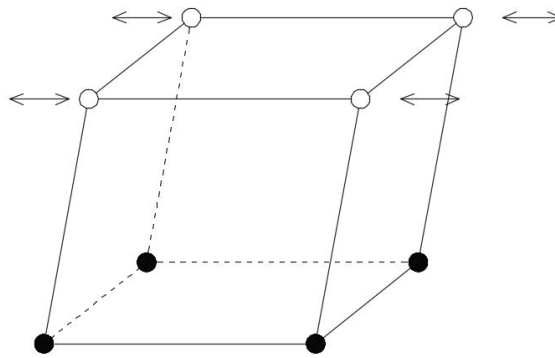


Figure 2.56: Perfectly Plastic Pure Shear Cyclic Loading.

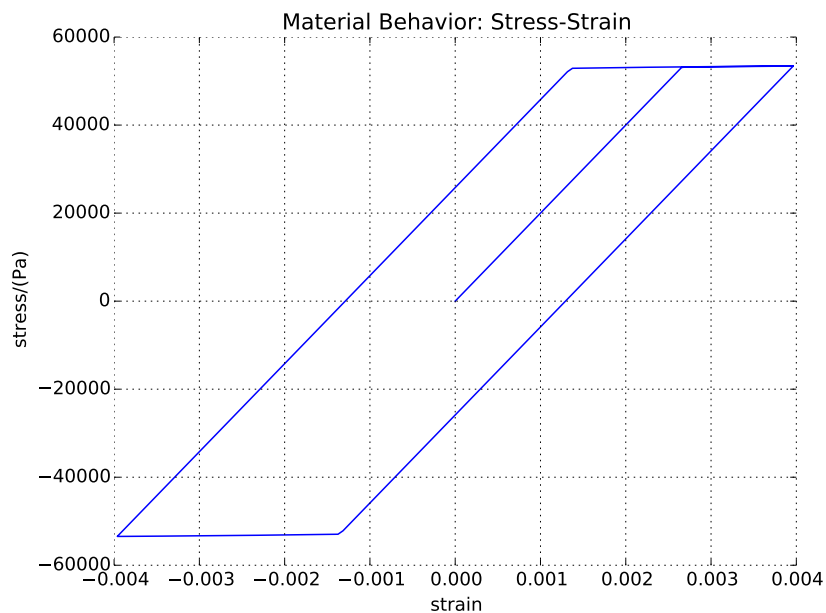


Figure 2.57: Results of Perfectly Plastic Pure Shear Cyclic Loading.

Material Response at Gauss Point:

Statics, von Mises Yield Function, Kinematic Hardening

The Real-ESSI input files for this example are available [HERE](#). The compressed package of Real-ESSI input files and postprocessing results for this example is available [HERE](#).

Model Description:

Material Response at Gauss Point:

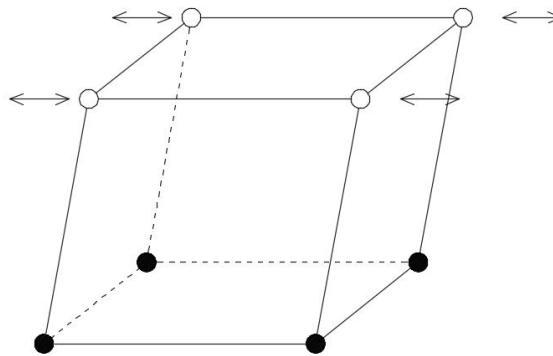


Figure 2.58: Pure Shear Cyclic Loading.

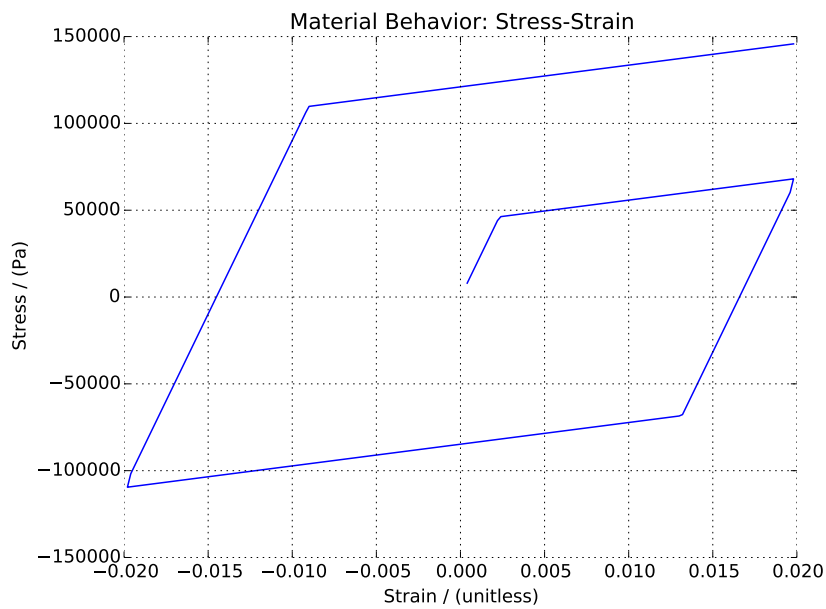


Figure 2.59: Material von-Mises Isotropic Hardening under Pure Shear Cyclic Loading.

Statics, Drucker Prager Yield Function, von-Mises Plastic Potential Function, Perfectly Plastic Hardening Rule

The Real-ESSI input files for this example are available [HERE](#). The compressed package of Real-ESSI input files and postprocessing results for this example is available [HERE](#).

Model Description:

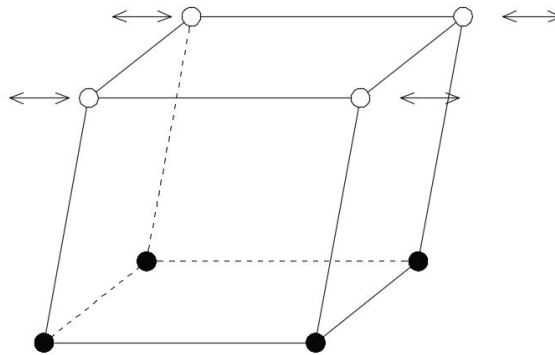


Figure 2.60: Pure Shear Cyclic Loading.

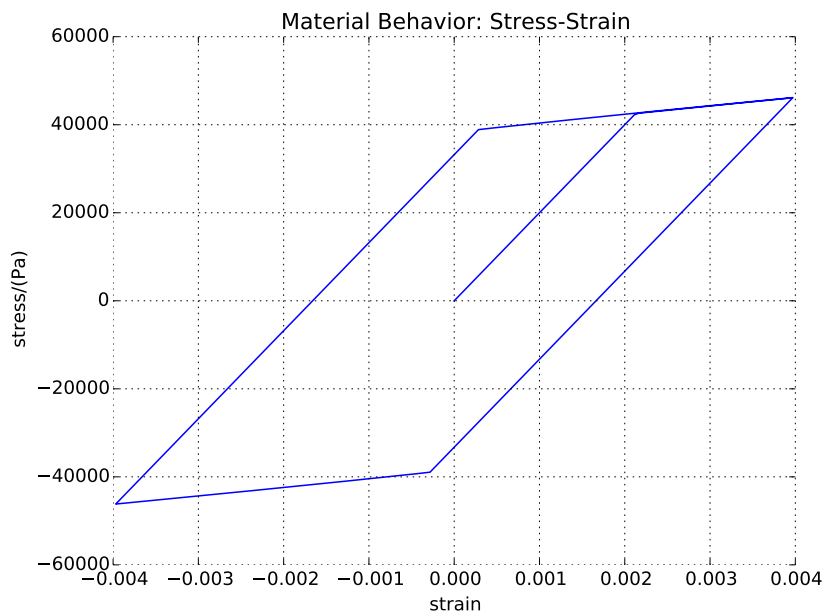


Figure 2.61: Results of von-Mises Kinematic Hardening Pure Shear Cyclic Loading.

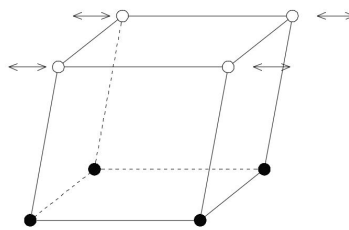


Figure 2.62: Pure Shear Cyclic Loading.

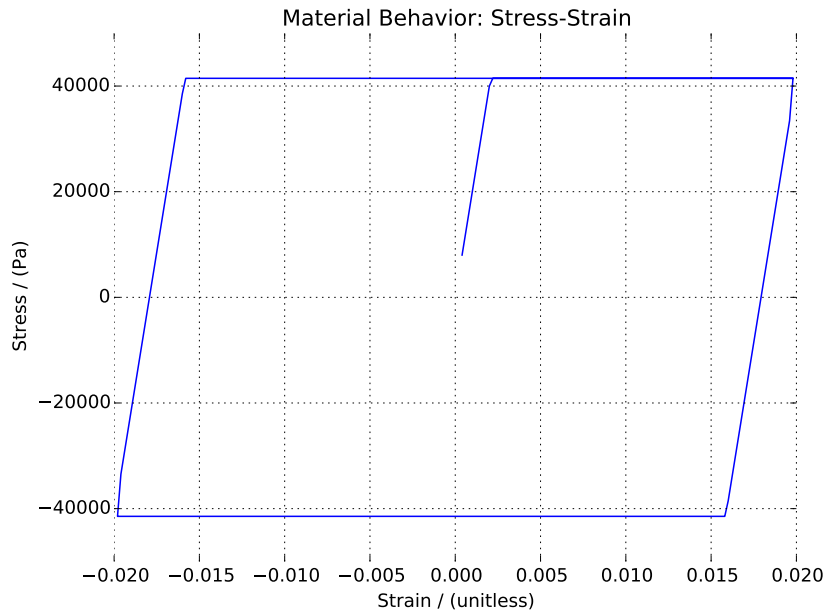


Figure 2.63: Results of Drucker Prager Yield Surface with Purely Deviatoric Plastic Flow under Pure Shear Cyclic Loading.

Statics, Drucker Prager Yield Function, Drucker Prager Plastic Potential Function, Perfectly Plastic Hardening Rule

The Real-ESSI input files for this example are available [HERE](#). The compressed package of Real-ESSI input files and postprocessing results for this example is available [HERE](#).

Model Description:

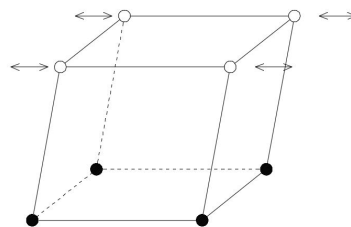


Figure 2.64: Pure Shear Cyclic Loading.

Material Response at Gauss Point:

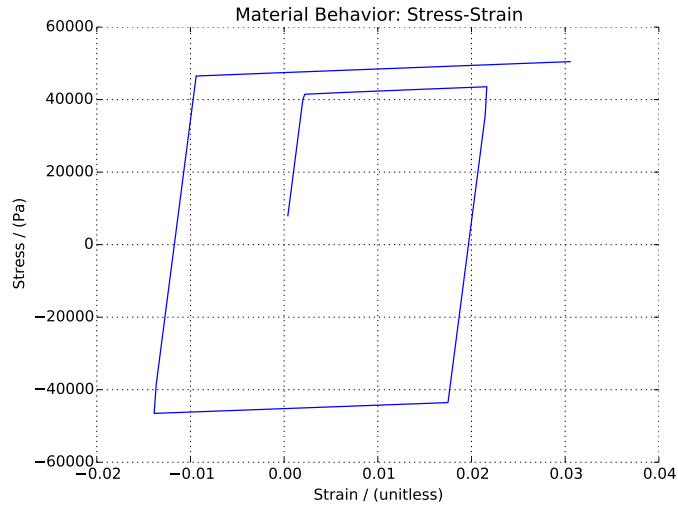


Figure 2.65: Results of Associative Drucker Prager Pure Shear Cyclic Loading.

2.8.2 Statics, Drucker Prager with Armstrong Frederick Nonlinear Kinematic Hardening Material Model

The Real-ESSI input files for this example are available [HERE](#). The compressed package of Real-ESSI input files and postprocessing results for this example is available [HERE](#).

Model Description:

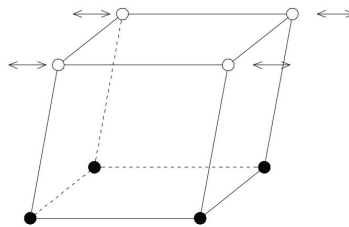


Figure 2.66: Pure Shear Cyclic Loading.

Material Response at Gauss Point:

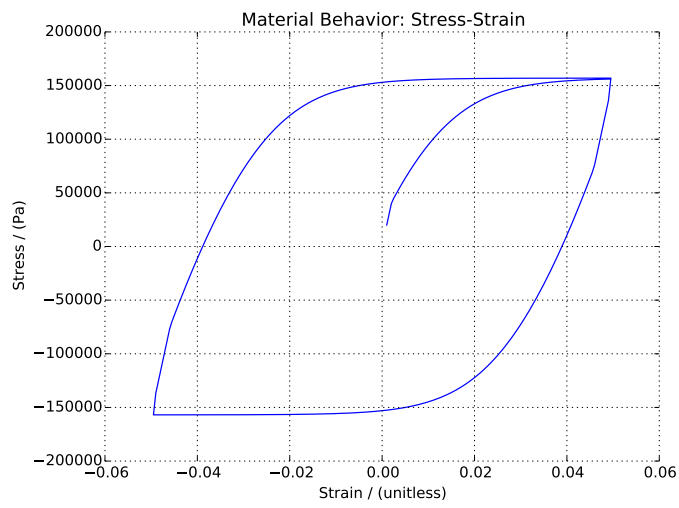


Figure 2.67: Result of Drucker-Prager Armstrong-Frederick Pure Shear Cyclic Loading.

2.9 Statics, Elastic, Fiber Cross Section Beam Finite Element Examples

2.9.1 Statics, Linear Elastic, Normal Loading and Pure Bending Fiber Cross Section Beam Finite Element Examples

Linear Elastic Normal Loading, Fiber Cross Section Beam Finite Element Examples

The Real-ESSI input files for this example are available [HERE](#). The compressed package of Real-ESSI input files and postprocessing results for this example is available [HERE](#).

The linear elastic beam is represented by the elastic section. This example is under the load of normal loading.



Figure 2.68: Normal Loading on the Fiber Beam with Elastic Section.

The elastic section represents the cross section properties of the beam.

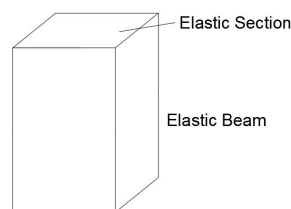


Figure 2.69: Diagram of the Fiber Beam with Elastic Section.

Linear Elastic Pure Bending, Fiber Cross Section Beam Finite Element Examples

The Real-ESSI input files for this example are available [HERE](#). The compressed package of Real-ESSI input files and postprocessing results for this example is available [HERE](#).

The linear elastic beam is represented by the elastic section. This example is under the bending load.

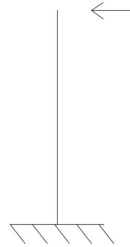


Figure 2.70: Bending on the Fiber Beam with Elastic Section.

The elastic section represents the cross section properties of the beam.

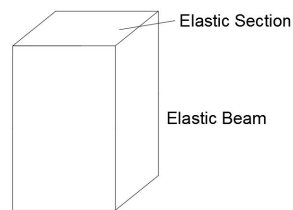


Figure 2.71: Diagram of the Fiber Beam with Elastic Section.

2.10 Statics, Elastic-Plastic, Fiber Cross Section Beam Finite Element Examples

2.10.1 Statics, Elastic-Plastic, Normal Loading and Pure Bending Fiber Cross Section Beam Finite Element

Elastic-Plastic Normal Loading, (Fiber Cross Section) Beam Finite Element Examples

The Real-ESSI input files for this example are available [HERE](#). The compressed package of Real-ESSI input files and postprocessing results for this example is available [HERE](#).

The Elastic-Plastic beam is represented by the fiber section. This example is under the load of normal loading.



Figure 2.72: Normal Loading on the Fiber Beam with Elastic-Plastic Section.

The fiber represents the rebar. The section of all fibers represents the cross section properties of the inelastic beam.

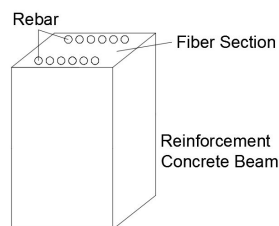


Figure 2.73: Diagram of the Fiber Beam with Elastic-Plastic Section.

Elastic-Plastic Pure Bending, (Fiber Cross Section) Beam Finite Element Examples

The Real-ESSI input files for this example are available [HERE](#). The compressed package of Real-ESSI input files and postprocessing results for this example is available [HERE](#).

The Elastic-Plastic beam is represented by the fiber section. This example is under the load of normal loading.

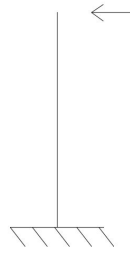


Figure 2.74: Bending on the Fiber Beam with Elastic-Plastic Section.

The fiber represents the rebar. The section of all fibers represents the cross section properties of the inelastic beam.

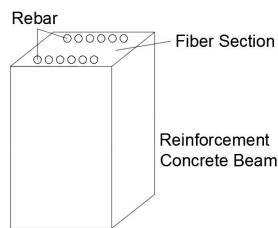


Figure 2.75: Diagram of the Fiber Beam with Elastic-Plastic Section.

2.11 Statics, Elastic, Inelastic Wall Finite Element Examples

2.11.1 Statics, Linear Elastic, Wall Finite Element Examples

Statics, Linear Elastic, Wall Finite Element Examples

Linear Elastic, Bi-Axial, Wall Finite Element Examples

Linear Elastic, Shear, (Fiber Cross Section) Wall Finite Element Examples

2.12 Statics, Elastic-Plastic Wall Finite Element Examples

2.12.1 Statics, Elastic-Plastic, in Plane, Wall Finite Element Examples

Elastic-Plastic, Uni-Axial, Wall Finite Element Examples

Elastic-Plastic, Bi-Axial, Wall Finite Element Examples

Elastic-Plastic, Shear, Wall Finite Element Examples

2.13 Statics, Solution Advancement Control

2.13.1 Increments: Load Control

When load-control is used as the solution advancement method, perfectly plastic model will fail immediately after the yield point. Load-control works with isotropic hardening and kinematic hardening.

Solids Example, Elastic Plastic Isotropic Hardening

The Real-ESSI input files for this example are available [HERE](#). The compressed package of Real-ESSI input files and postprocessing results for this example is available [HERE](#).

Model Description:

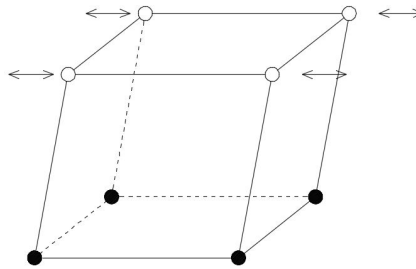


Figure 2.76: Pure Shear Cyclic Loading.

Material Response at Gauss Point:

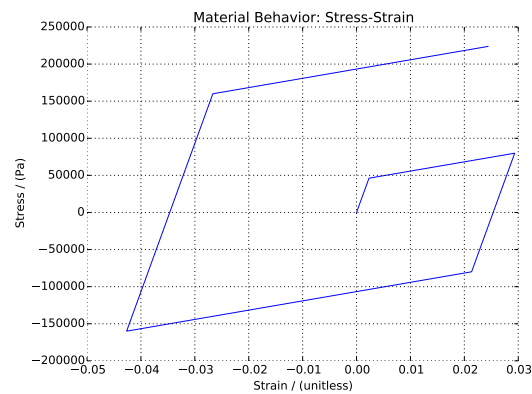


Figure 2.77: Material von-Mises Isotropic Hardening under Pure Shear Cyclic Loading.

Solids Example, Elastic Plastic Kinematic Hardening

The Real-ESSI input files for this example are available [HERE](#). The compressed package of Real-ESSI input files and postprocessing results for this example is available [HERE](#).

Model Description:

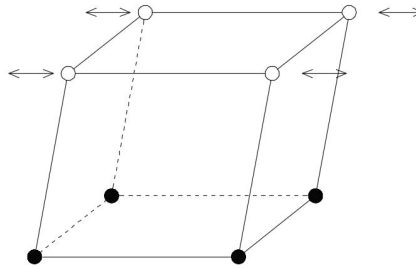


Figure 2.78: Pure Shear Cyclic Loading.

Material Response at Gauss Point:

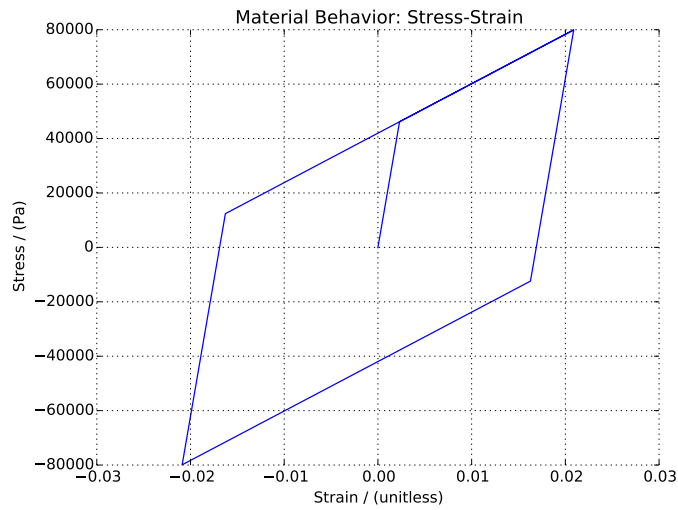


Figure 2.79: Material von-Mises Kinematic Hardening under Pure Shear Cyclic Loading.

Inelastic Beam Example, Steel and Reinforced Concrete

The Real-ESSI input files for this example are available [HERE](#).

The compressed package of Real-ESSI input files and postprocessing results for this example is available [HERE](#).

The Elastic-Plastic beam is represented by the fiber section. This example is under the load of normal loading.

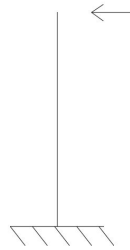


Figure 2.80: Normal Loading on the Beam with Fiber Section.

The fiber represents the rebar. The section of all fibers represents the cross section properties of the inelastic beam.

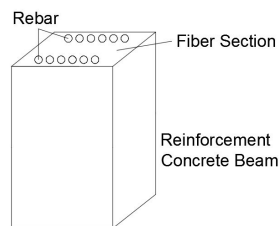


Figure 2.81: Diagram of the Beam with Fiber Section.

2.13.2 Statics, Increments: Displacement Control

Statics, Single Displacement Control

Solids Example, Elastic-Perfectly Plastic

The Real-ESSI input files for this example are available [HERE](#). The compressed package of Real-ESSI input files and postprocessing results for this example is available [HERE](#).

Model Description:

Material Response at Gauss Point:

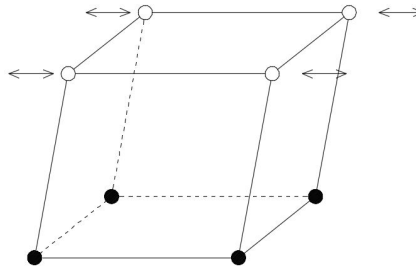


Figure 2.82: Pure Shear Cyclic Loading.

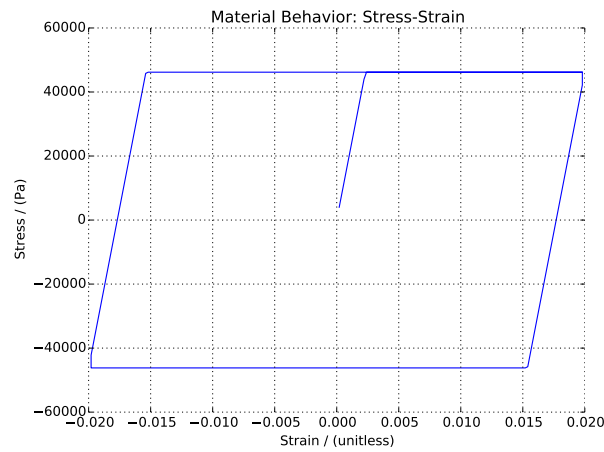


Figure 2.83: Displacement-Control of Perfectly Plastic Material under Pure Shear Cyclic Loading.

Solids Example, Elastic Plastic Isotropic Hardening

The Real-ESSI input files for this example are available [HERE](#). The compressed package of Real-ESSI input files and postprocessing results for this example is available [HERE](#).

Model Description:

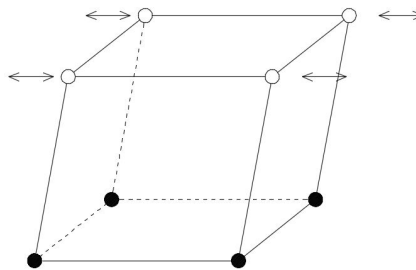


Figure 2.84: Pure Shear Cyclic Loading.

Material Response at Gauss Point:

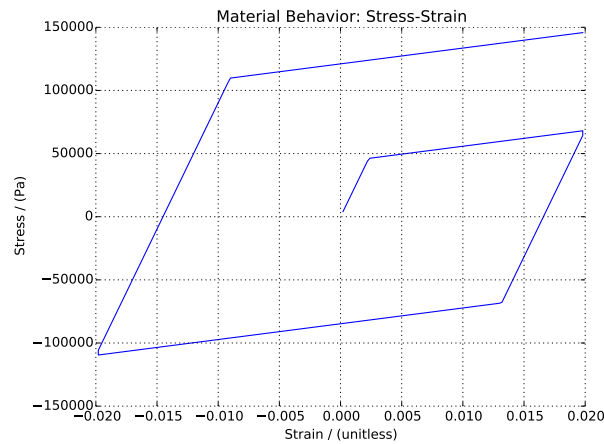


Figure 2.85: Displacement-Control of Isotropic Hardening Material under Pure Shear Cyclic Loading.

Solids Example, Elastic Plastic Kinematic Hardening

The Real-ESSI input files for this example are available [HERE](#). The compressed package of Real-ESSI input files and postprocessing results for this example is available [HERE](#).

Model Description:

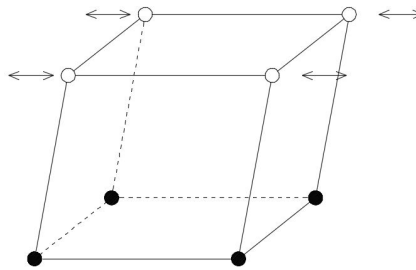


Figure 2.86: Pure Shear Cyclic Loading.

Material Response at Gauss Point:

Inelastic Beam Example, Steel and Reinforced Concrete

The Real-ESSI input files for this example are available [HERE](#). The compressed package of Real-ESSI input files and postprocessing results for this example is available [HERE](#).

The Elastic-Plastic beam is represented by the fiber section. This example is under the load of normal loading.

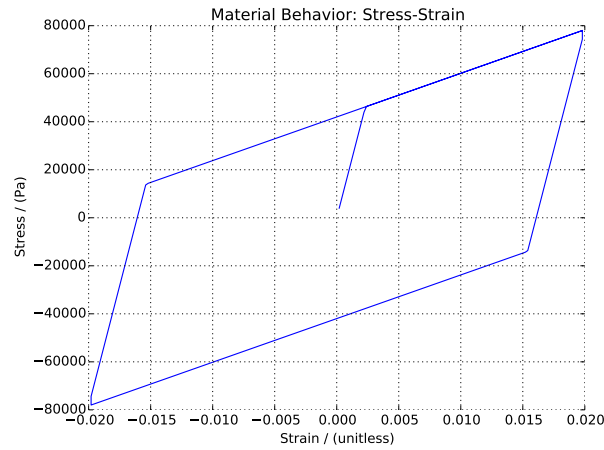


Figure 2.87: Displacement-Control of Kinematic Hardening Material under Pure Shear Cyclic Loading.

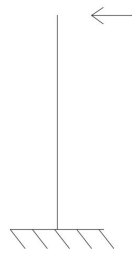


Figure 2.88: Bending on the Fiber Beam with Elastic-Plastic Section

The fiber represents the rebar. The section of all fibers represents the cross section properties of the inelastic beam.

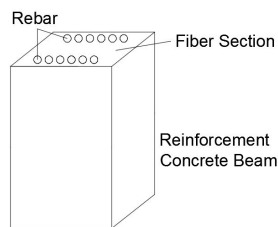


Figure 2.89: Diagram of the Fiber Beam with Elastic-Plastic Section.

2.13.3 Statics, Solution Algorithms

Statics, Solution Algorithm: No Convergence Check

The Real-ESSI input files for this example are available [HERE](#). The compressed package of Real-ESSI input files and postprocessing results for this example is available [HERE](#).

When no convergence check is used, the stress-strain curves drift away a little. The stress-strain curve did not close, as shown in Figure 2.57.

Model Description:

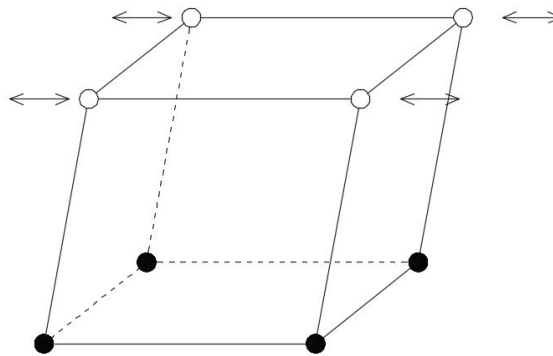


Figure 2.90: Pure Shear Cyclic Loading.

Material Response at Gauss Point:

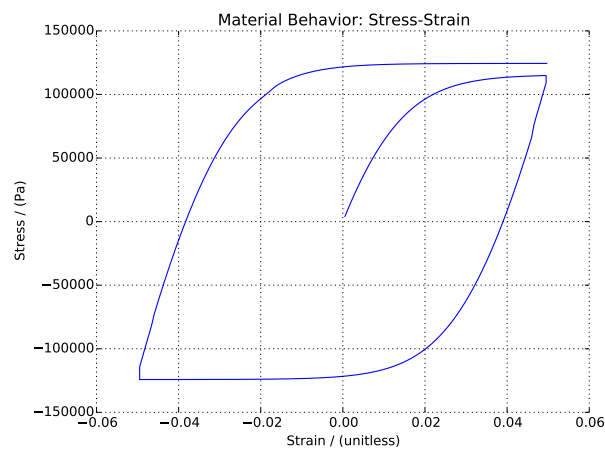


Figure 2.91: Results of No-Convergence-Check Pure Shear Cyclic Loading.

Statics, Solution Algorithm: Newton Algorithm

The Real-ESSI input files for this example are available [HERE](#). The compressed package of Real-ESSI input files and postprocessing results for this example is available [HERE](#).

Model Description:

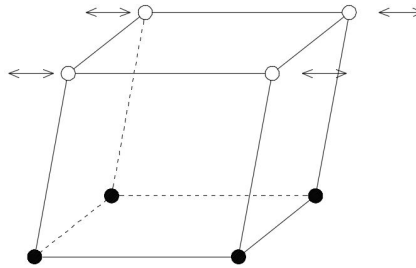


Figure 2.92: Pure Shear Cyclic Loading.

Material Response at Gauss Point:

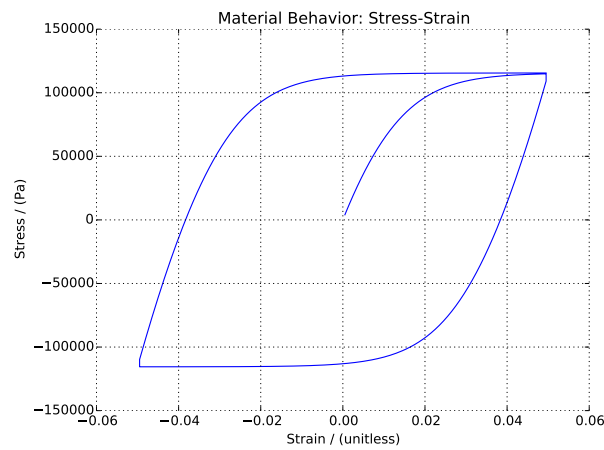


Figure 2.93: Results of Convergence Check with Newton-Raphson Iteration under Pure Shear Cyclic Loading.

Statics, Solution Algorithm: Newton Algorithm with Line Search

The Real-ESSI input files for this example are available [HERE](#). The compressed package of Real-ESSI input files and postprocessing results for this example is available [HERE](#).

Model Description:

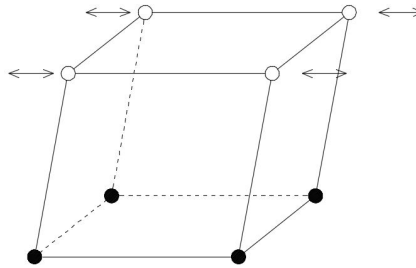


Figure 2.94: Pure Shear Cyclic Loading.

Material Response at Gauss Point:

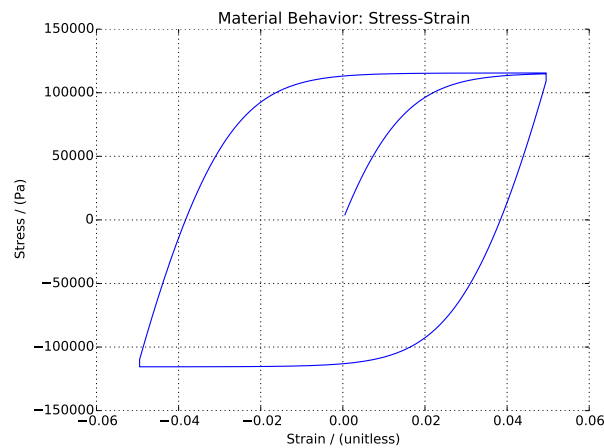


Figure 2.95: Results of Convergence Check with Newton-Raphson Iterations and Line Search under Pure Shear Cyclic Loading.

2.13.4 Statics, Solution Advancement Control, Iterations: Convergence Criteria

Statics, Solution Advancement Control, Convergence Criteria: Unbalanced Force

The Real-ESSI input files for this example are available [HERE](#). The compressed package of Real-ESSI input files and postprocessing results for this example is available [HERE](#).

Model Description:

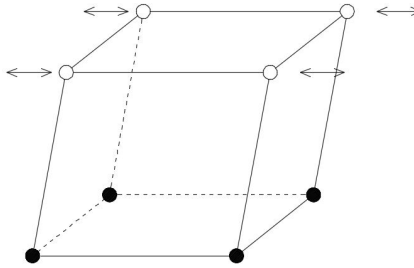


Figure 2.96: Pure Shear Cyclic Loading.

Material Response at Gauss Point:

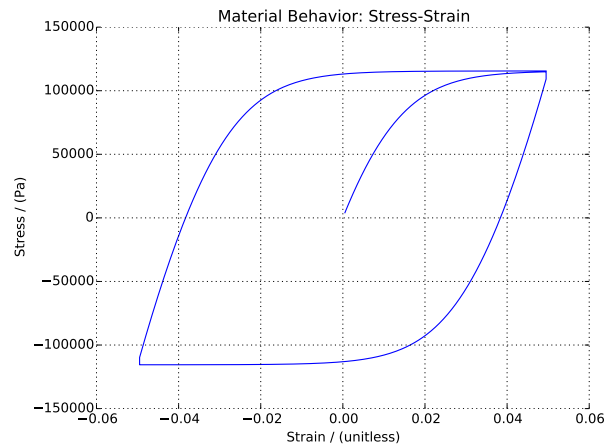


Figure 2.97: Results of Convergence Check with Unbalanced Force Criteria under Pure Shear Cyclic Loading.

Statics, Solution Advancement Control, Convergence Criteria: Displacement Increment

The Real-ESSI input files for this example are available [HERE](#). The compressed package of Real-ESSI input files and postprocessing results for this example is available [HERE](#).

Model Description:

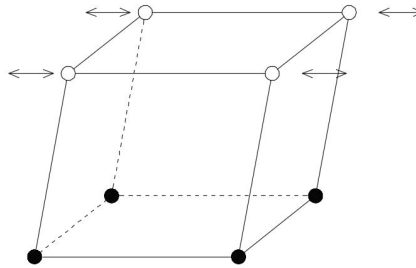


Figure 2.98: Pure Shear Cyclic Loading.

Material Response at Gauss Point:

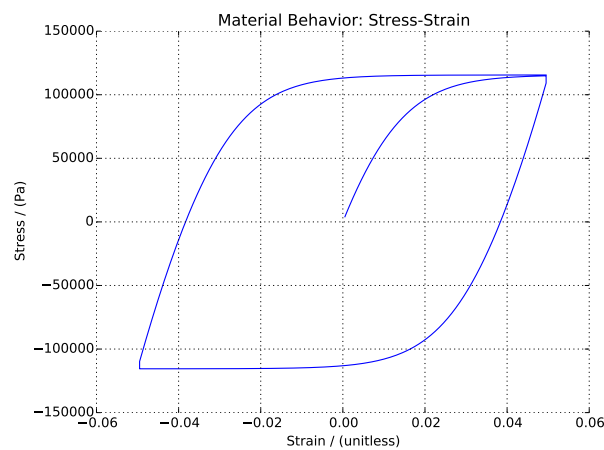


Figure 2.99: Results of Convergence Check with Displacement Increment under Pure Shear Cyclic Loading.

2.13.5 Statics, Solution Advancement Control, Different Convergence Tolerances (Examples in preparation)

2.14 Statics, Small Practical Examples

2.14.1 Statics, Elastic Beam Element for a Simple Frame Structure

The Real-ESSI input files for this example are available [HERE](#). The compressed package of Real-ESSI input files and postprocessing results for this example is available [HERE](#).

Problem Description

- Dimensions: width=6m, height=6m, force=100N
- Element dimensions: length=6m, cross section width=1m, cross section height=1m, mass density $\rho = 0.0\text{kN/m}^3$, Young's modulus $E = 1E8 \text{ Pa}$, Poisson's ratio $\nu = 0.0$.

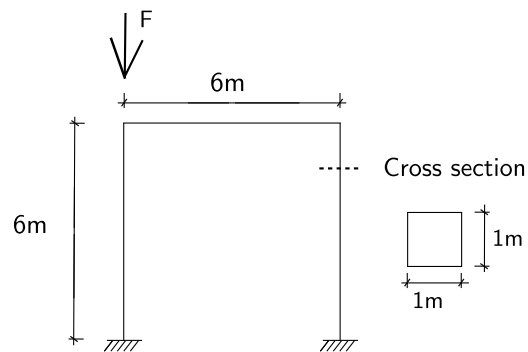


Figure 2.100: Elastic frame with *beam_elastic* elements.

2.14.2 Statics, 4NodeANDES Square Plate, Four Edges Clamped

The Real-ESSI input files for this example are available [HERE](#). The compressed package of Real-ESSI input files and postprocessing results for this example is available [HERE](#).

Problem description

Length=20m, Width=20m, Height=1m, Force=100N, $E=1E8Pa$, $\nu = 0.3$.

The four edges are **clamped**.

The load is a self weight.

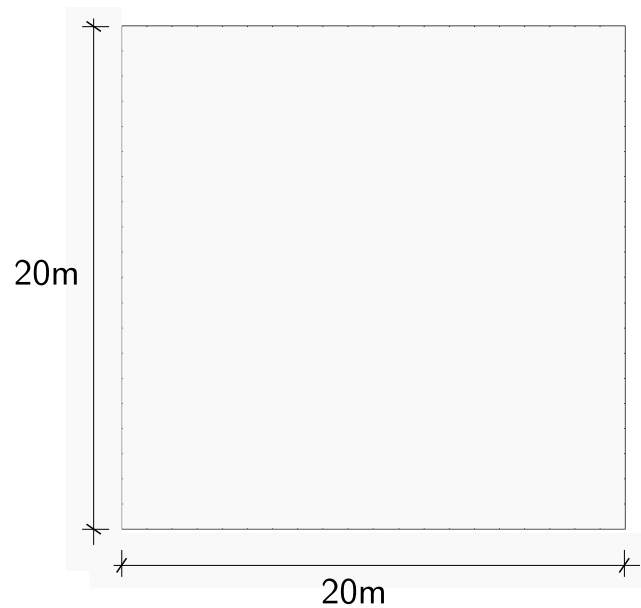


Figure 2.101: Square plate with four edges clamped.

Numerical model

The element side length is 1 meter.

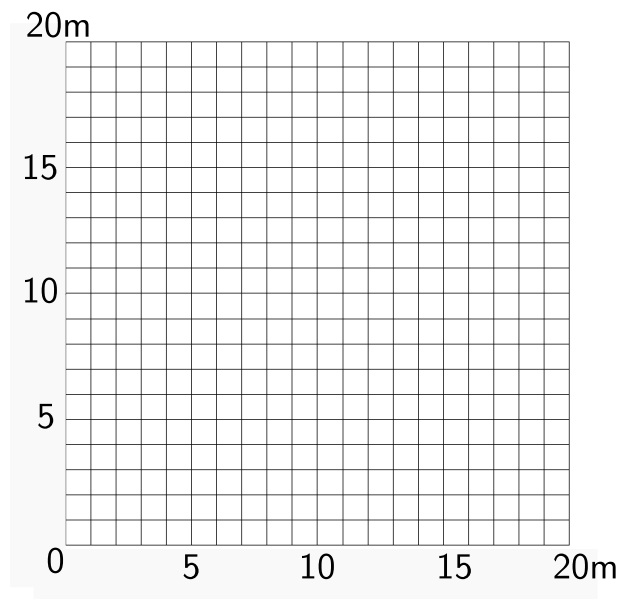


Figure 2.102: 4NodeANDES edge clamped square plate with element side length 1m.

2.14.3 Statics, Six Solid Blocks Example With Interface/Contact

The Real-ESSI input files for this example are available [HERE](#). The compressed package of Real-ESSI input files and postprocessing results for this example is available [HERE](#).

This is a 3-D solid block example with initial normal and then tangential load on different surfaces as shown below.

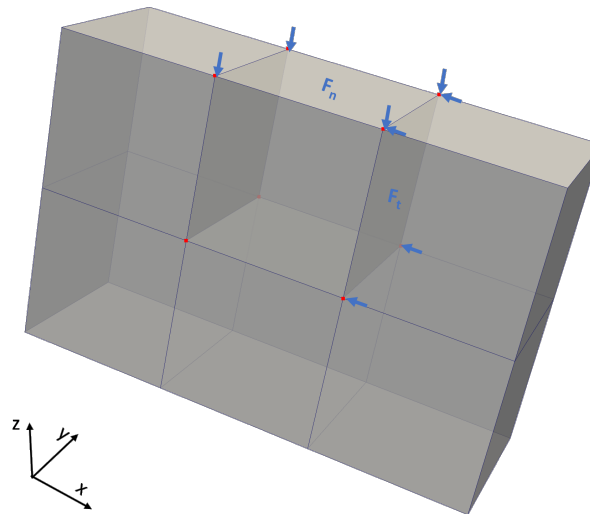


Figure 2.103: Illustration of Six Solid Blocks Example with Interface/Contact with first normal and then tangential loading stages.

The generalized displacement field of the two loading stages **normal loading** and **tangential loading** is shown below..

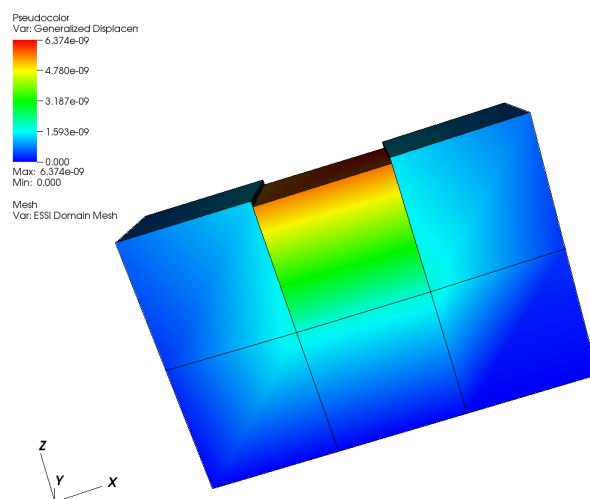


Figure 2.104: Generalized displacement magnitude visualization of normal loading.

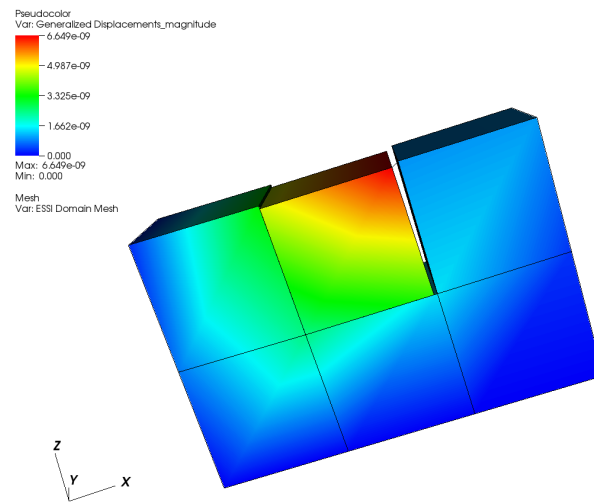


Figure 2.105: Generalized displacement magnitude visualization of tangential loading.

Chapter 3

Dynamic Examples

(2016-2017-2018-2019-2021-)

(In collaboration with Prof. José Abell, Dr. Yuan Feng, Mr. Sumeet Kumar Sinha, Dr. Hexiang Wang, and Dr. Han Yang)

3.1 Chapter Summary and Highlights

In this Chapter dynamic/transient modeling and simulation of solids and structures is illustrated through a number of examples.

All the examples described here, and many more, organized in sub-directories, for constitutive behavior, static and dynamic behavior can be directly downloaded from a repository at: http://sokocalo.engr.ucdavis.edu/~jeremic/lecture_notes_online_material/Real-ESSI_Examples/education_examples. These examples can then be tried, analyzed using Real-ESSI Simulator that is available on Amazon Web Services (AWS) computers around the world. Login to AWS market place and search for Real-ESSI...

3.2 Dynamic Solution Advancement (in Time)

3.2.1 Dynamics: Newmark Method

Newmark Model Description

The Real-ESSI input files for this example are available [HERE](#). The compressed package of Real-ESSI input files and postprocessing results for this example is available [HERE](#).

Firstly, the model is given an initial displacement at one side. Second, the model starts free vibration.

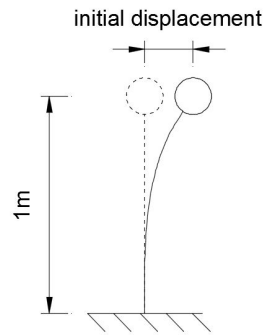


Figure 3.1: Problem Description for Newmark Method

Newmark Results

With damping, the displacement peak is smaller and smaller. The displacement at the top is

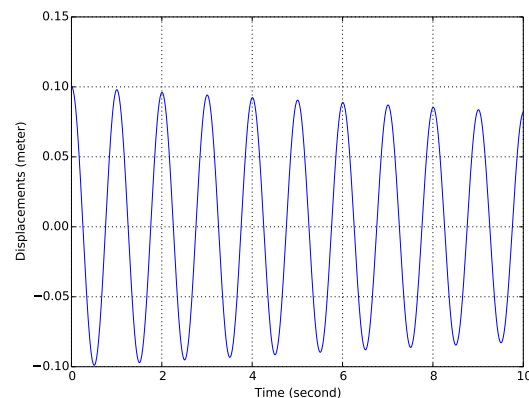


Figure 3.2: Results for Newmark Method

3.2.2 Dynamics: Hilber-Hughes-Taylor (α) Method

HHT Model Description

The Real-ESSI input files for this example are available [HERE](#). The compressed package of Real-ESSI input files and postprocessing results for this example is available [HERE](#).

Firstly, the model is given an initial displacement at one side. Second, the model starts free vibration.

HHT Results

With NO damping, the displacement peak keeps the same. The displacement at the top is

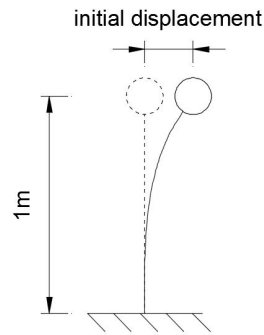


Figure 3.3: Problem Description for HHT Method

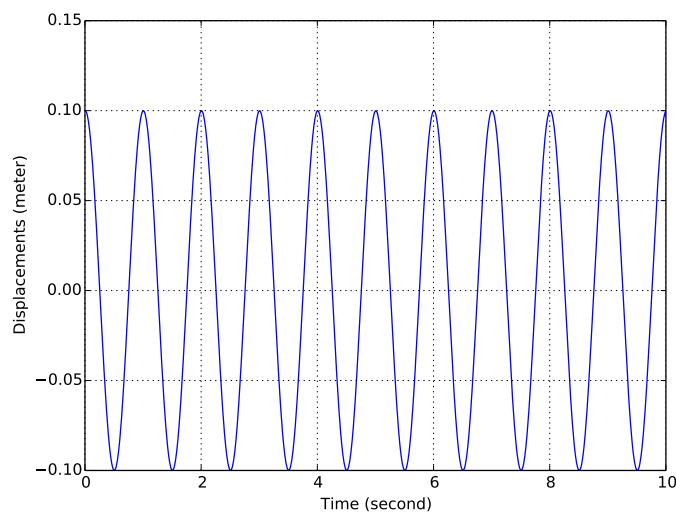


Figure 3.4: Results for HHT Method

3.3 Dynamics: Solution Advancement: Time Step Size

3.3.1 Dynamics: Solution Advancement: Equal Time Step

Model Description

The Real-ESSI input files for this example are available [HERE](#). The compressed package of Real-ESSI input files and postprocessing results for this example is available [HERE](#).

The model is given an earthquake input motion at the bottom with equal time step. After the wave propagation, the motion at the top is recorded.

Results

The input motion is on the left, while the output motion is on the right.

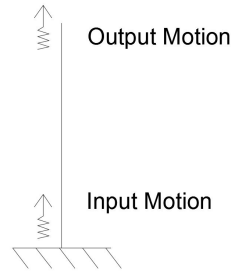


Figure 3.5: Problem Description for Solution Advancement

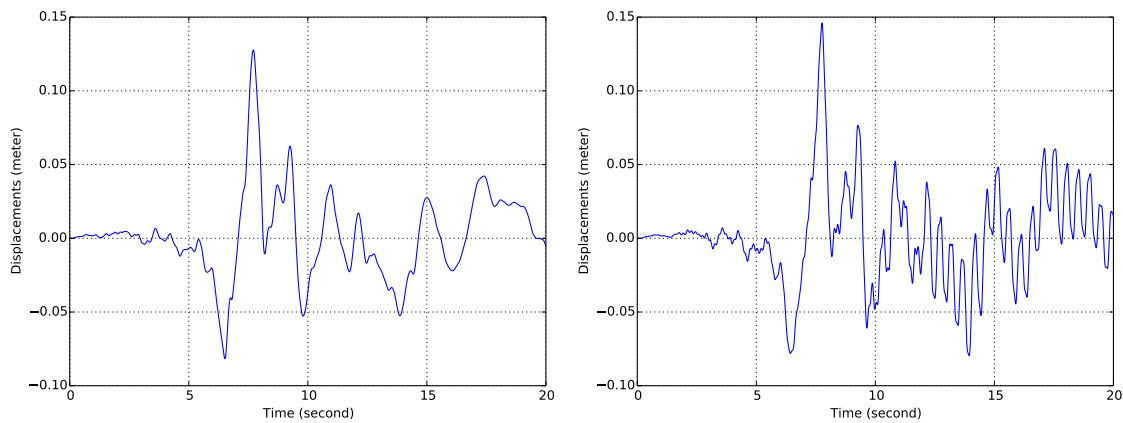


Figure 3.6: Input Motion (Left) And Output Motion (Right)

3.3.2 Dynamics Solution Advancement: Variable Time Step

Model Description

The Real-ESSI input files for this example are available [HERE](#). The compressed package of Real-ESSI input files and postprocessing results for this example is available [HERE](#).

The model is given an earthquake input motion at the bottom with variable time step. After the wave propagation, the motion at the top is recorded.

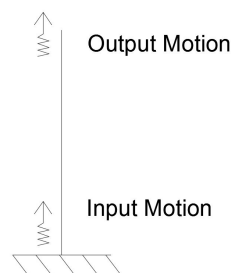


Figure 3.7: Problem Description for Newmark Method

Results

The input motion is on the left, while the output motion is on the right. The input motion is in variable time step. As shown in Fig 3.8, from time 10-11 second, the input motion is a straight line (a big time step) without the small time steps.

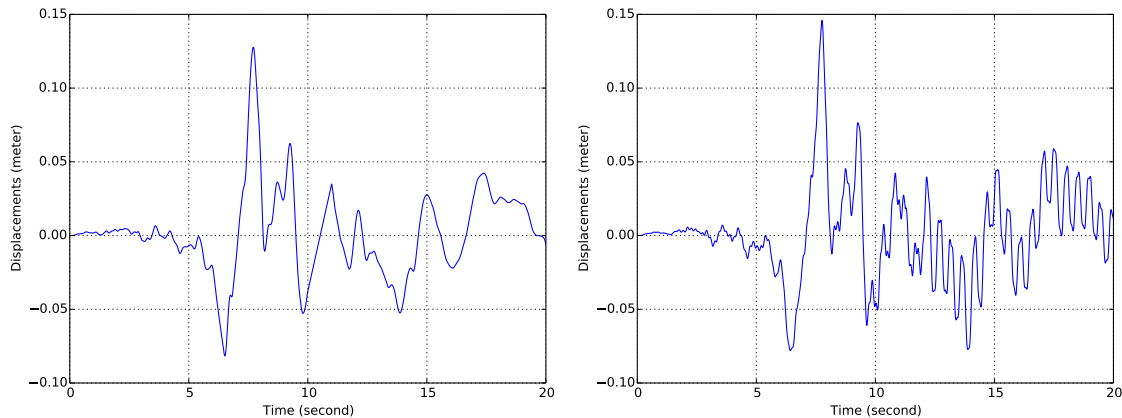


Figure 3.8: Input Motion (Left) And Output Motion (Right)

3.4 Dynamics: Energy Dissipation, Damping

3.4.1 Dynamics: Energy Dissipation: Viscous Damping

Dynamics: Energy Dissipation, Viscous Damping: Rayleigh Damping

Model Description The Real-ESSI input files for this example are available [HERE](#). The compressed package of Real-ESSI input files and postprocessing results for this example is available [HERE](#).

Firstly, the model is given an initial displacement at the top from 0 to 1 second. Second, after the time 1 second, the model starts free vibration.

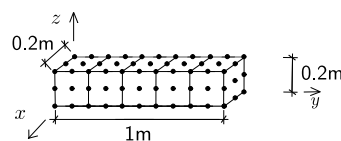


Figure 3.9: Problem Description for Newmark Method

Results This model employs Rayleigh damping. The displacement at the top is

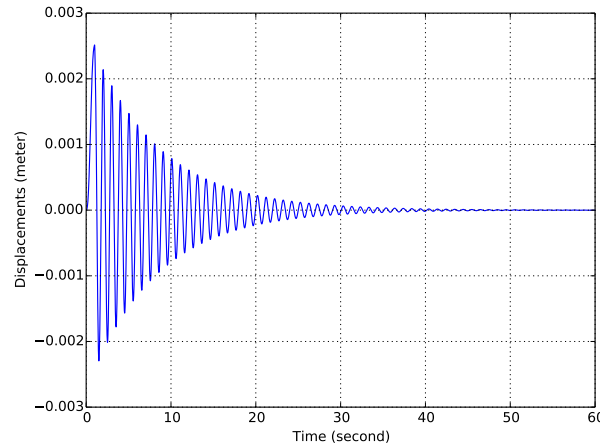


Figure 3.10: Results for Newmark Method

Dynamics: Energy Dissipation, Viscous Damping: Caughey Damping

Model Description The Real-ESSI input files for this example are available [HERE](#). The compressed package of Real-ESSI input files and postprocessing results for this example is available [HERE](#).

Firstly, the model is given an initial displacement at the top from 0 to 1 second. Second, after the time 1 second, the model starts free vibration.

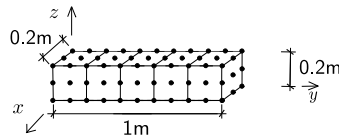


Figure 3.11: Problem Description for Newmark Method

Results This model employs Caughey damping. The displacement at the top is

3.4.2 Dynamics: Energy Dissipation: Material (Elastic-Plastic, Hysteretic) Damping

Dynamics: Energy Dissipation, Material Damping: Elastic Perfectly Plastic Models

Model Description The Real-ESSI input files for this example are available [HERE](#). The compressed package of Real-ESSI input files and postprocessing results for this example is available [HERE](#).

The model is a one-element solid brick example with perfectly plastic materials.

Results The Hysteretic loop at the Gauss point is

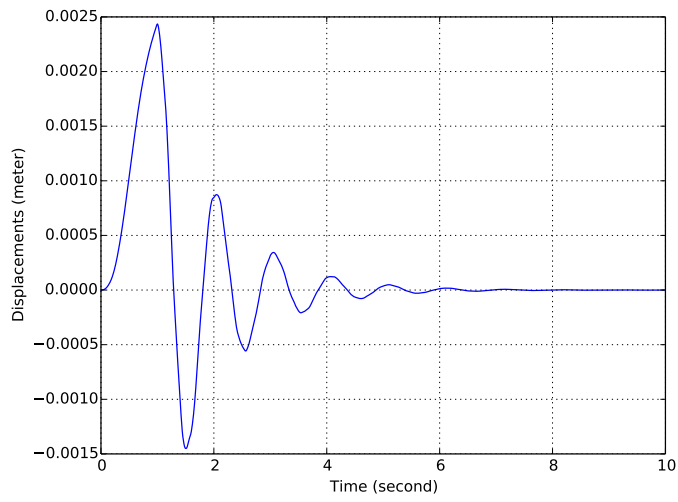


Figure 3.12: Results for Newmark Method

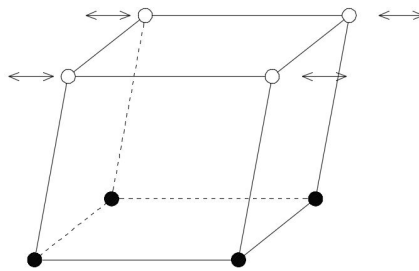


Figure 3.13: Problem Description for Newmark Method

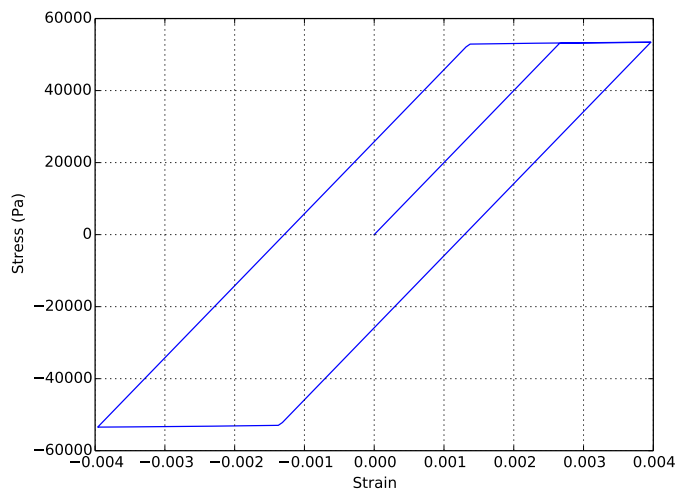


Figure 3.14: Results for Newmark Method

Dynamics: Energy Dissipation, Material/Hysteretic Damping: Elastic Plastic Isotropic Hardening Models

Model Description The Real-ESSI input files for this example are available [HERE](#). The compressed package of Real-ESSI input files and postprocessing results for this example is available [HERE](#).

The model is a one-element solid brick example with isotropic hardening materials.

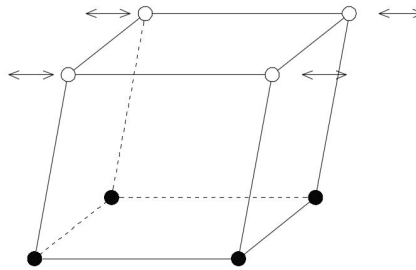


Figure 3.15: Problem Description for Newmark Method

Results The Hysteretic loop at the Gauss point is

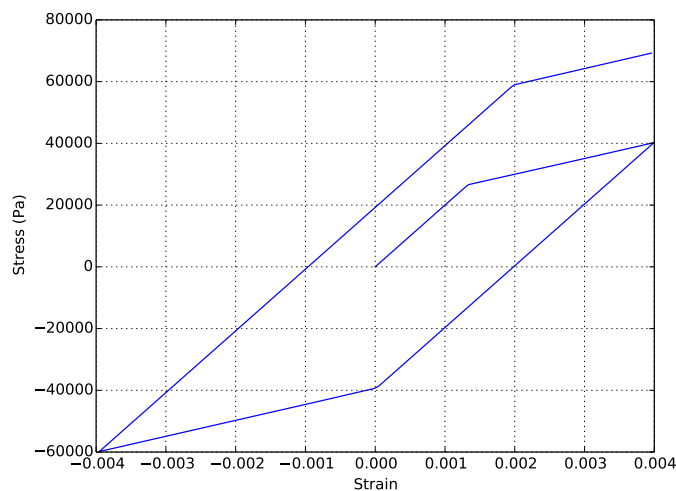


Figure 3.16: Results for Newmark Method

Dynamics: Energy Dissipation, Material/Hysteretic Damping: Elastic Plastic Kinematic Hardening Models

Model Description The Real-ESSI input files for this example are available [HERE](#). The compressed package of Real-ESSI input files and postprocessing results for this example is available [HERE](#).

The model is a one-element solid brick example with kinematic hardening materials.

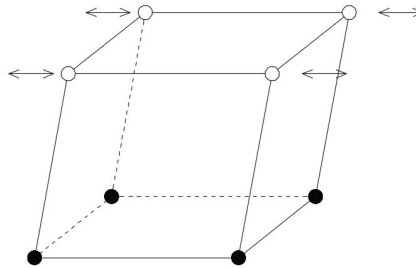


Figure 3.17: Problem Description for Newmark Method

Results The Hysteretic loop at the Gauss point is

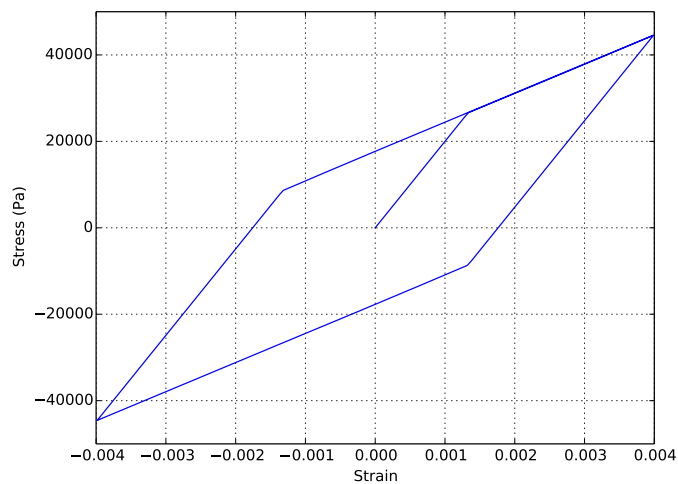


Figure 3.18: Results for Newmark Method

Dynamics: Energy Dissipation, Material/Hysteretic Damping: Elastic Plastic Armstrong-Frederick Models

Model Description The Real-ESSI input files for this example are available [HERE](#). The compressed package of Real-ESSI input files and postprocessing results for this example is available [HERE](#).

The model is a one-element solid brick example with materials with nonlinear hardening Armstrong-Frederick.

Results The Hysteretic loop at the Gauss point is

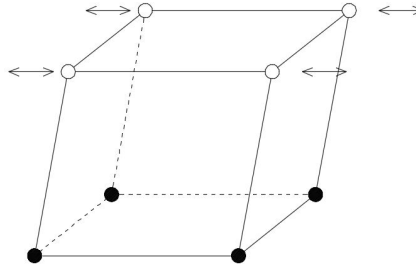


Figure 3.19: Problem Description for Newmark Method

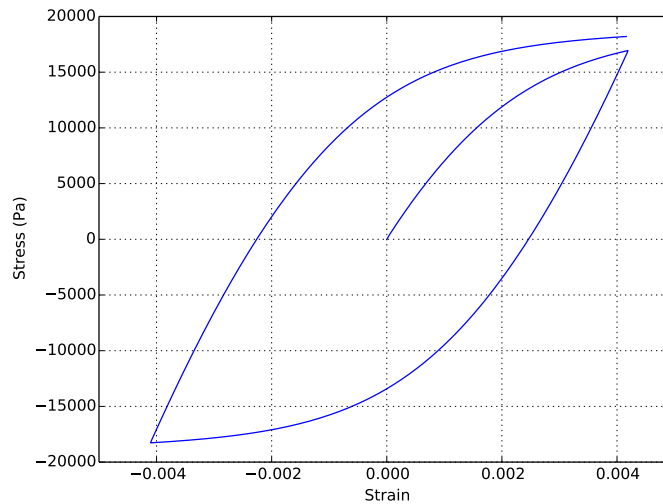


Figure 3.20: Results for Material Armstrong-Frederick

3.4.3 Dynamics: Energy Dissipation: Numerical Damping

Energy Dissipation, Numerical Damping: Newmark Method

Model Description The Real-ESSI input files for this example are available [HERE](#). The compressed package of Real-ESSI input files and postprocessing results for this example is available [HERE](#).

Firstly, the model is given an initial displacement in the first loading stage. In the second loading stage, the model starts free vibration.

Results This model employs Newmark numerical damping. The displacement at the top in the second loading stage is

Dynamics: Energy Dissipation, Numerical Damping: Hilber-Hughes-Taylor (α) Method

Model Description The Real-ESSI input files for this example are available [HERE](#). The compressed package of Real-ESSI input files and postprocessing results for this example is available [HERE](#).

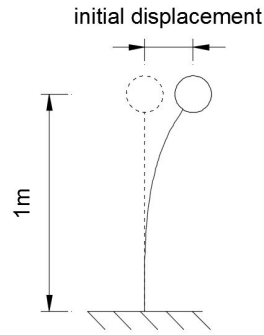


Figure 3.21: Problem Description for Newmark Method

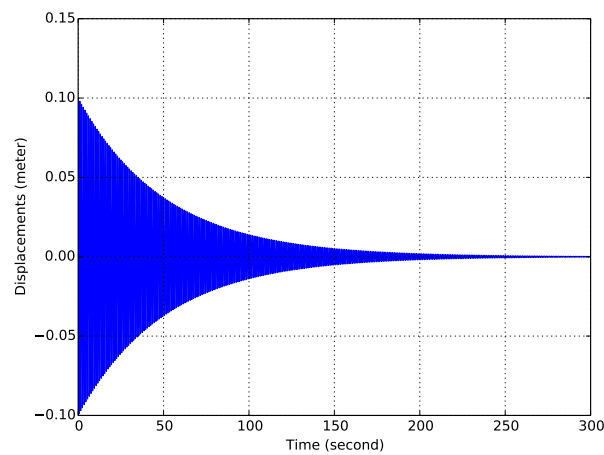


Figure 3.22: Results for Newmark Method

Firstly, the model is given an initial displacement in the first loading stage. In the second loading stage, the model starts free vibration.

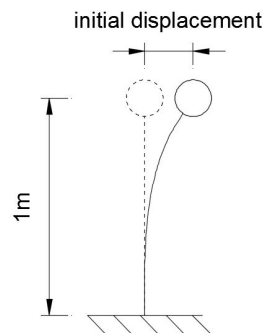


Figure 3.23: Problem Description

Results This model employs HHT numerical damping. The displacement at the top in the second loading stage is

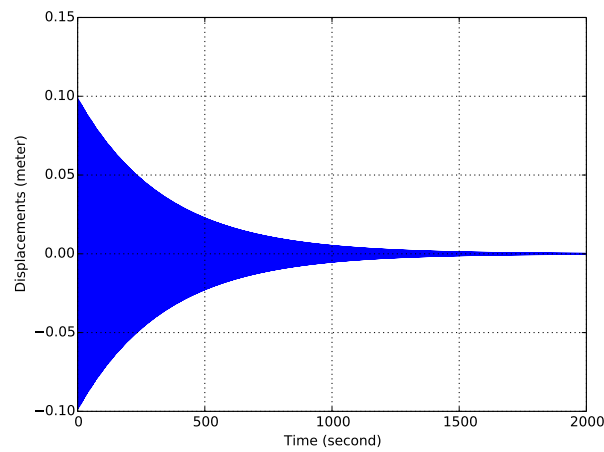


Figure 3.24: Results for HHT Method

3.5 Dynamics: Elastic Solid Dynamic Examples

3.5.1 Model Description

The Real-ESSI input files for this example are available [HERE](#). The compressed package of Real-ESSI input files and postprocessing results for this example is available [HERE](#).

Firstly, the model is given an initial displacement at the top from 0 to 1 second. Second, after the time 1 second, the model starts free vibration.

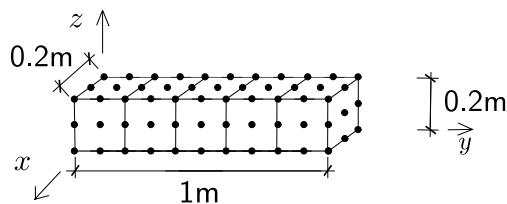


Figure 3.25: Problem Description for Newmark Method

3.5.2 Results

This model employs Caughey damping. The displacement at the top is

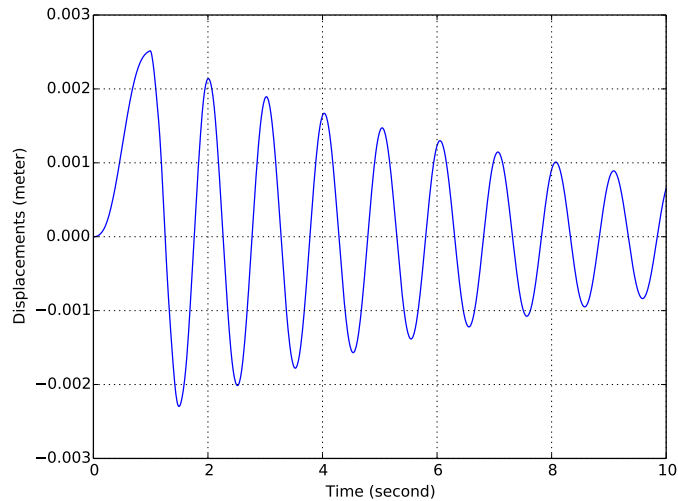


Figure 3.26: Results for Newmark Method

3.6 Dynamics: Elastic Structural Dynamic Examples

3.6.1 Model Description

The Real-ESSI input files for this example are available [HERE](#). The compressed package of Real-ESSI input files and postprocessing results for this example is available [HERE](#).

Firstly, the model is given an initial displacement in the first loading stage. In the second loading stage, the model starts free vibration.

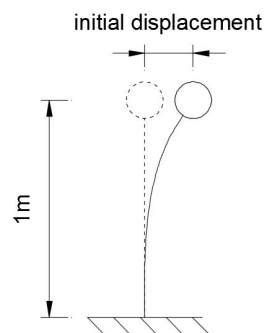


Figure 3.27: Problem Description for Newmark Method

3.6.2 Results

With NO damping, the displacement peak keeps the same. The displacement at the top is

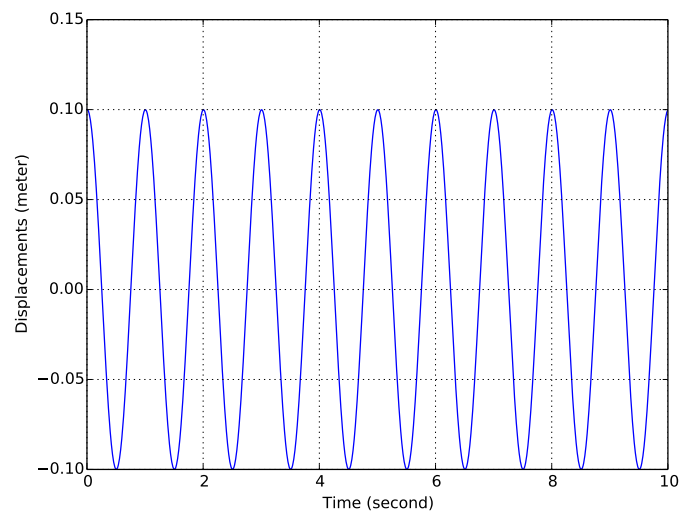


Figure 3.28: Results for Newmark Method

3.7 Dynamics: Interface/Contact Elements

3.7.1 Dynamics: Hard Interface/Contact: One Bar Normal Interface/Contact Dynamics

Model Description

This is an example of a ball, bouncing on a solid flat surface. There is only normal contact/interface between the ball and the floor. An upward force is first applied to the concentrated mass lifting it up by $0.1m$ and then the force is removed, resulting in free vibration of the ball. An illustrative diagram of the problem is shown below.

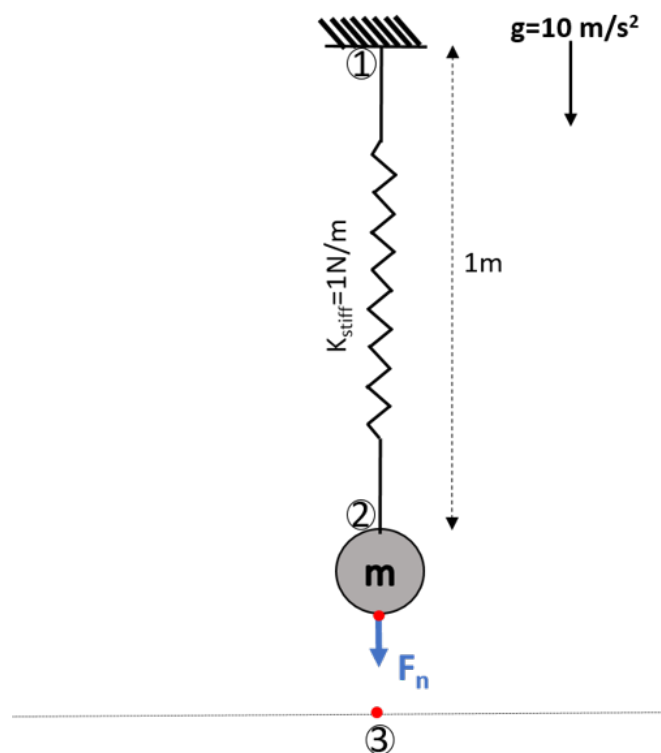


Figure 3.29: Illustration of one bar normal contact/interface dynamics.

The same example can be modeled with different contact/interface and simulation parameters as shown below. For all the different cases shown below, no numerical damping is applied. Only the contact parameters are changed to expose their functionality. The response of node 2 is plotted for all the cases.

Dynamics: No Viscous Damping

The Real-ESSI input files for this example are available [HERE](#). The compressed package of Real-ESSI input files and postprocessing results for this example is available [HERE](#).

Results Here, no viscous damping between the contact/interface pair nodes is applied. The displacement output of *Node 2* is shown below.

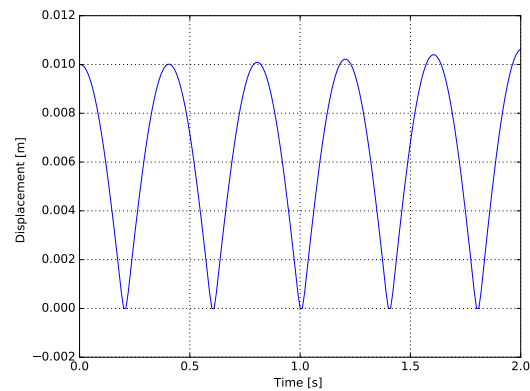


Figure 3.30: Displacement of Node 2

Dynamics: Normal Viscous Damping Between Interface/Contact Node Pairs

The Real-ESSI input files for this example are available [HERE](#). The compressed package of Real-ESSI input files and postprocessing results for this example is available [HERE](#).

Results Viscous damping between the contact/interface pair nodes is applied in normal contact/interface direction. The displacement output of *Node 2* is shown below.

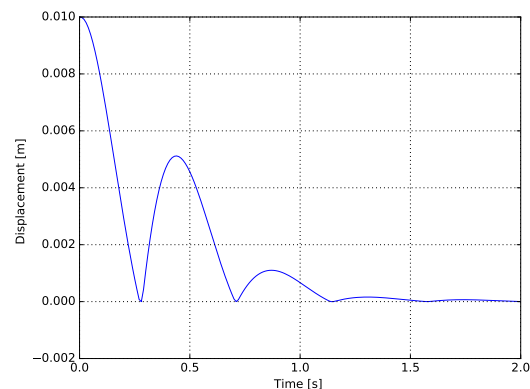


Figure 3.31: Displacement of Node 2

Dynamics: Explicit Simulation

The Real-ESSI input files for this example are available [HERE](#). The compressed package of Real-ESSI input files and postprocessing results for this example is available [HERE](#).

Results With no viscous damping, the analysis is run explicitly without any convergence check. The displacement output of *Node 2* is shown below.

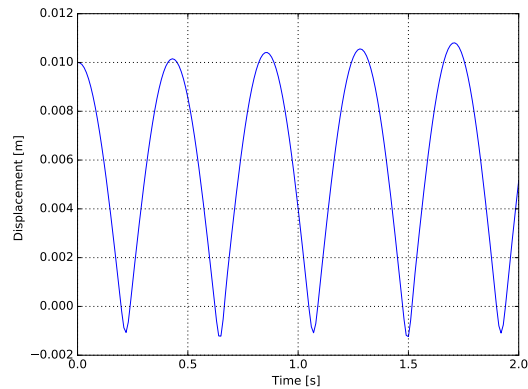


Figure 3.32: Displacement of Node 2

3.7.2 Dynamics: Hard Interface/Contact: Frictional Single Degree of Freedom Problem

Model Description This is an example of a block on a rough surface under gravity. It has been attached to a spring at one end. At the other end a tangential load is applied greater than the coulomb friction and is then removed. The block oscillates back and forth with continuously losing energy because of frictional force and then stops, with some permanent deformation. This kind of damping is called frictional damping which is linear as compared to exponential in case of viscous damping. An illustrative diagram of the problem is shown below.

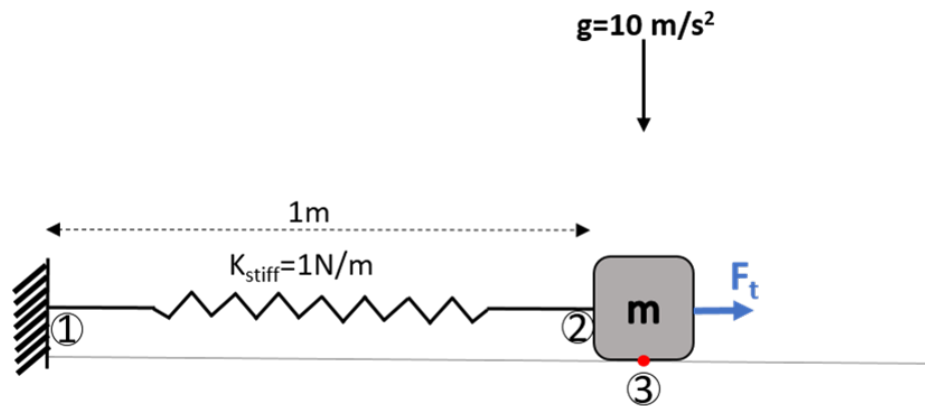


Figure 3.33: Illustration of frictional single degree of freedom problem

The same example can be modeled with different contact/interface and simulation parameters as shown below. For all the different cases shown below, no numerical damping is applied. Only the contact/interface parameters are changed to expose their functionality. The response of node 2 is plotted for all the cases.

Dynamics: No Viscous Damping

The Real-ESSI input files for this example are available [HERE](#). The compressed package of Real-ESSI input files and postprocessing results for this example is available [HERE](#).

Results In this examples, no viscous damping between the contact/interface pair nodes is applied. The displacement output of *Node 2* is shown below.

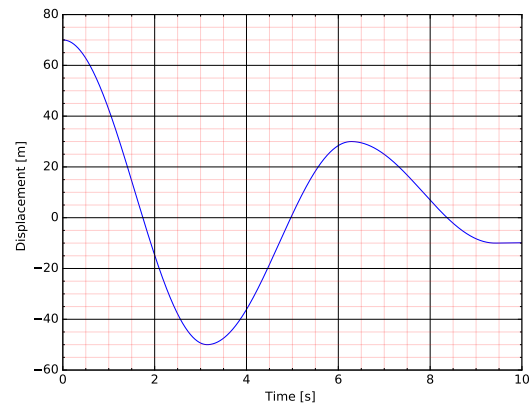


Figure 3.34: Displacement of Node 2

Dynamics: Tangential Viscous Damping Between Interface/Contact Node Pairs

The Real-ESSI input files for this example are available [HERE](#). The compressed package of Real-ESSI input files and postprocessing results for this example is available [HERE](#).

Results Viscous damping between the contact/interface pair nodes is applied in tangential contact/interface direction. The displacement output of *Node 2* is shown below.

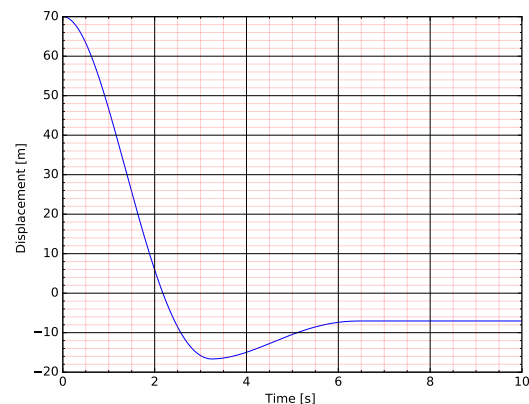


Figure 3.35: Displacement of Node 2

Dynamics: Explicit Simulation

The Real-ESSI input files for this example are available [HERE](#). The compressed package of Real-ESSI input files and postprocessing results for this example is available [HERE](#).

Results With no viscous damping, the analysis is run explicitly without any convergence check. The displacement output of *Node 2* is shown below.

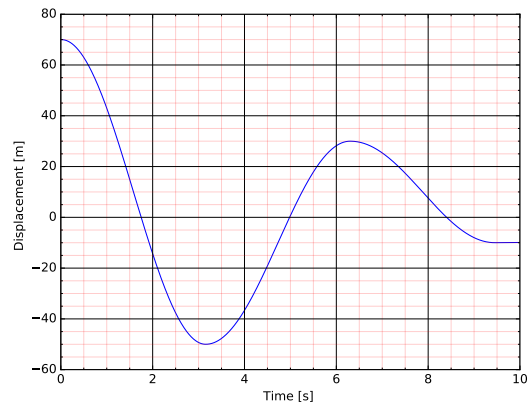


Figure 3.36: Displacement of Node 2

3.7.3 Dynamics: Soft Interface/Contact: One Bar Normal Interface/Contact Dynamics

Model Description This is an example of a ball, bouncing on a solid flat surface. There is only normal contact/interface between the ball and the floor. An upward force is first applied to the concentrated mass lifting it up by $0.1m$ and then the force is removed, resulting in free vibration of the ball. An illustrative diagram of the problem is shown below.

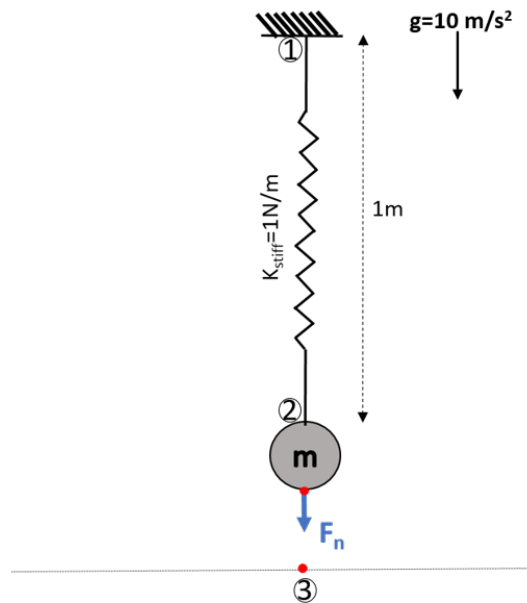


Figure 3.37: Illustration of one bar normal contact/interface dynamics

The same example can be modeled with different contact/interface and simulation parameters as shown below. For all the different cases shown below, no numerical damping is applied. Only the contact/interface parameters are changed to expose their functionality. The response of node 2 is plotted for all the cases.

Dynamics: No Viscous Damping

The Real-ESSI input files for this example are available [HERE](#). The compressed package of Real-ESSI input files and postprocessing results for this example is available [HERE](#).

Results In this example, no viscous damping between the contact/interface pair nodes is applied. The displacement output of *Node 2* is shown below.

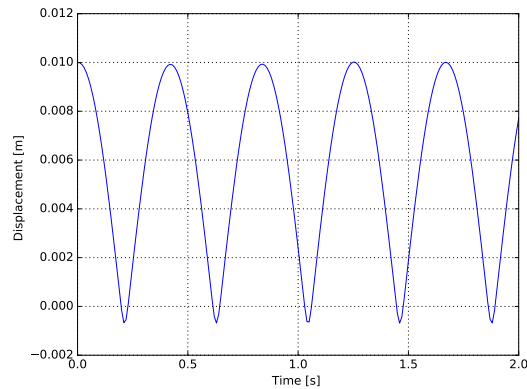


Figure 3.38: Displacement of Node 2

Dynamics: With Normal Viscous Damping Between Interface/Contact Node Pairs

The Real-ESSI input files for this example are available [HERE](#). The compressed package of Real-ESSI input files and postprocessing results for this example is available [HERE](#).

Results Viscous damping between the contact/interface pair nodes is applied in normal contact/interface direction. The displacement output of *Node 2* is shown below.

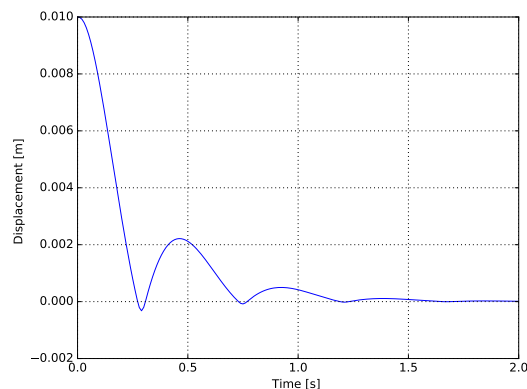


Figure 3.39: Displacement of Node 2

Dynamics: Explicit Simulation

The Real-ESSI input files for this example are available [HERE](#). The compressed package of Real-ESSI input files and postprocessing results for this example is available [HERE](#).

Results With no viscous damping, the analysis is run explicitly without any convergence check. The displacement output of *Node 2* is shown below.

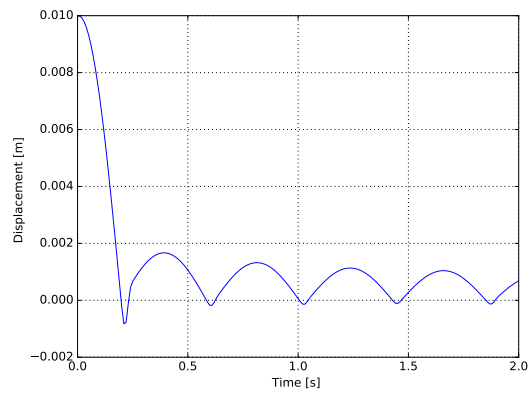


Figure 3.40: Displacement of Node 2

3.7.4 Dynamics: Soft Interface/Contact: Frictional Single Degree of Freedom Problem

Model Description This is an example of a block on a rough surface under gravity. It has been attached to a spring at one end. At the other end a tangential load is applied greater than the coulomb friction and is then removed. The block oscillates back and forth with continuously losing energy because of frictional force and then stops, with some permanent deformation. This kind of damping is called frictional damping which is linear as compared to exponential in case of viscous damping. An illustrative diagram of the problem is shown below.

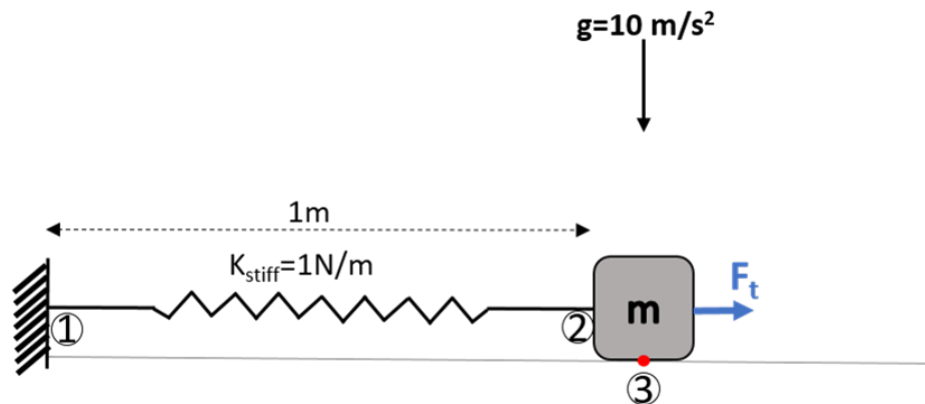


Figure 3.41: Illustration of frictional single degree of freedom problem

The same example can be modeled with different contact/interface and simulation parameters as shown below. For all the different cases shown below, no numerical damping is applied. Only the contact/interface parameters are changed to expose their functionality. The response of node 2 is plotted for all the cases.

Dynamics: No Viscous Damping

The Real-ESSI input files for this example are available [HERE](#). The compressed package of Real-ESSI input files and postprocessing results for this example is available [HERE](#).

Results In this example, no viscous damping between the contact/interface pair nodes is applied. The displacement output of *Node 2* is shown below.

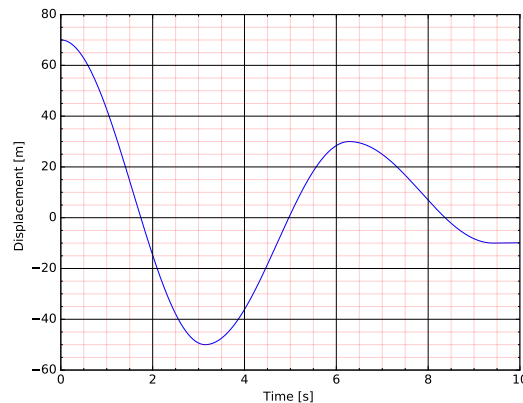


Figure 3.42: Displacement of Node 2

Dynamics: Tangential Viscous Damping Between Interface/Contact Node Pairs

The Real-ESSI input files for this example are available [HERE](#). The compressed package of Real-ESSI input files and postprocessing results for this example is available [HERE](#).

Results Viscous damping between the contact/interface pair nodes is applied in tangential contact/interface direction. The displacement output of *Node 2* is shown below.

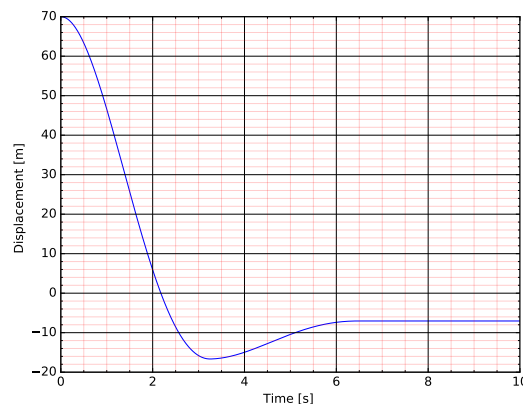


Figure 3.43: Displacement of Node 2

Dynamics: Explicit Simulation

The Real-ESSI input files for this example are available [HERE](#). The compressed package of Real-ESSI input files and postprocessing results for this example is available [HERE](#).

Results With no viscous damping, the analysis is run explicitly without any convergence check. The displacement output of *Node 2* is shown below.

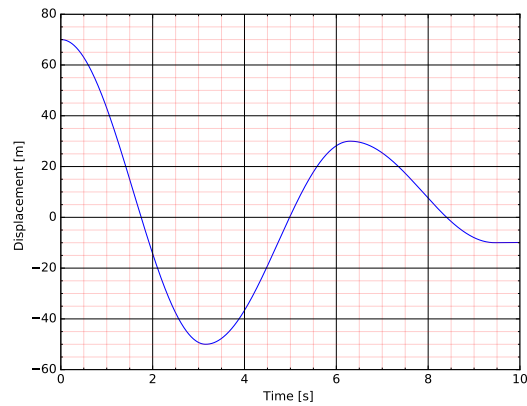


Figure 3.44: Displacement of Node 2

3.7.5 Dynamics: Split Beam

Model Description

In this example, a normal beam is split into two halves along its depth. A uniform surface load of 50 Pa is applied to the top half of the beam, pulling it away from its lower part. Then, the load is removed, to allow free vibration between the split beams. An illustrative diagram of the problem is shown below.

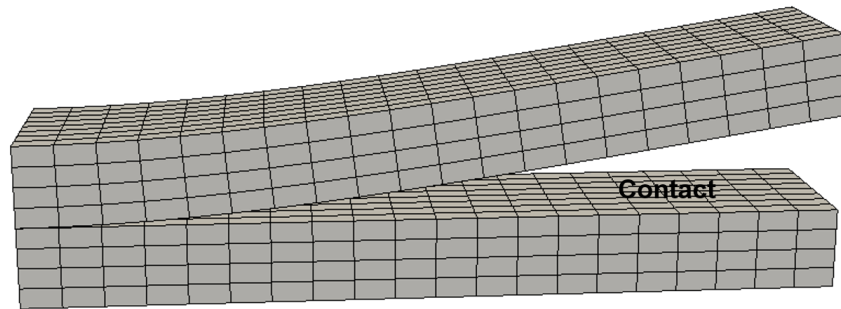


Figure 3.45: Illustration of Split Beam Analysis

The same example was modelled with soft and hard contact/interface. Numerical as well as viscous damping between contact/interface pair nodes was applied. The displacement response of the extreme right mid node of top half beam is plotted.

Dynamics: Split Beam With Hard Interface/Contact

The Real-ESSI input files for this example are available [HERE](#). The compressed package of Real-ESSI input files and postprocessing results for this example is available [HERE](#).

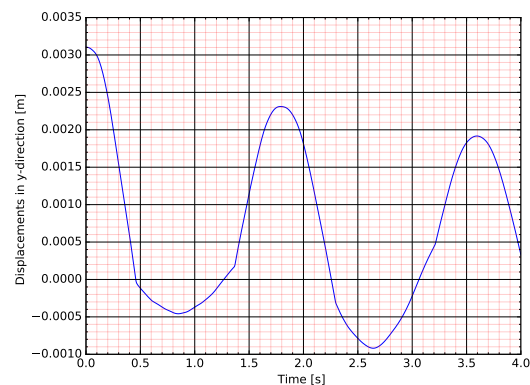


Figure 3.46: Displacement response of extreme mid node of top half beam

Dynamics: Split Beam With Soft Interface/Contact

The Real-ESSI input files for this example are available [HERE](#). The compressed package of Real-ESSI input files and postprocessing results for this example is available [HERE](#).

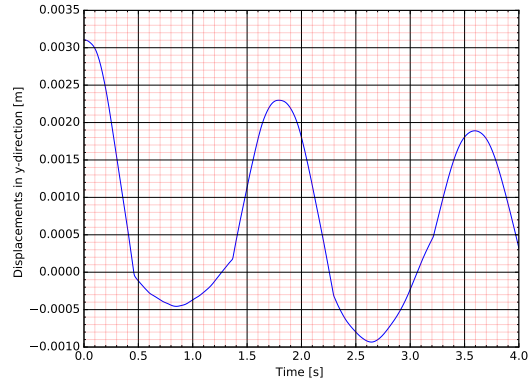


Figure 3.47: Displacement response of extreme mid node of top half beam

3.7.6 Dynamics: Block on Soil ESSI

Model Description The Real-ESSI input files for this example are available [HERE](#). The compressed package of Real-ESSI input files and postprocessing results for this example is available [HERE](#).

A solid block is placed in the soil. There is contact/interface between the interface of solid and the soil. First, self-weight and then a uniform acceleration in x-direction is applied to the whole model. This analysis would provide relative displacement, velocity and acceleration response for the given shaking. An illustrative diagram of the problem is shown below.

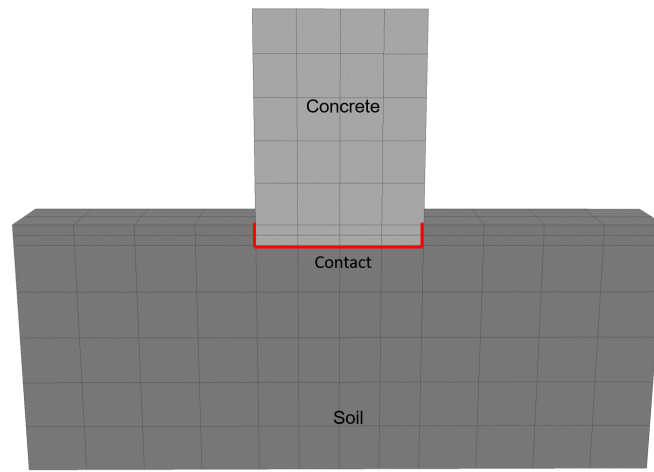


Figure 3.48: Illustration of frictional single degree of freedom problem

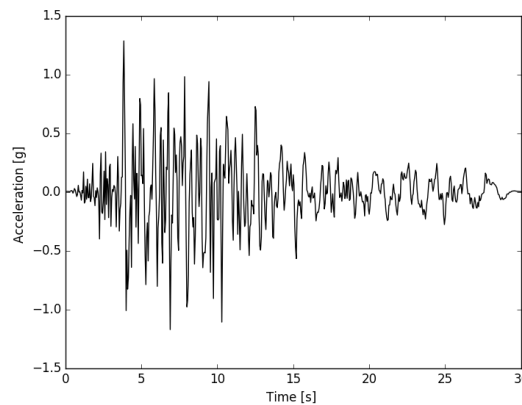


Figure 3.49: Applied Motion

Results Displacement response of the top of the solid block is shown below. Numerical Damping, Raleigh damping and viscous damping between contact/interface node pairs are applied.

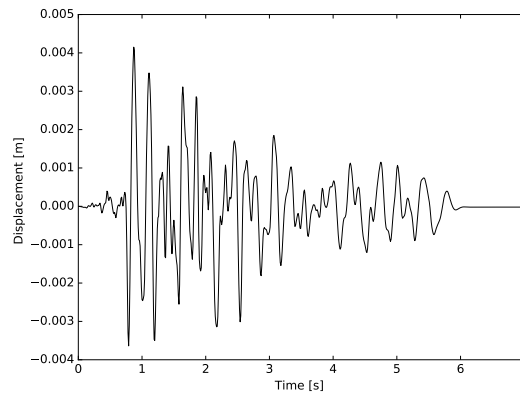


Figure 3.50: Displacement response at the top of the block

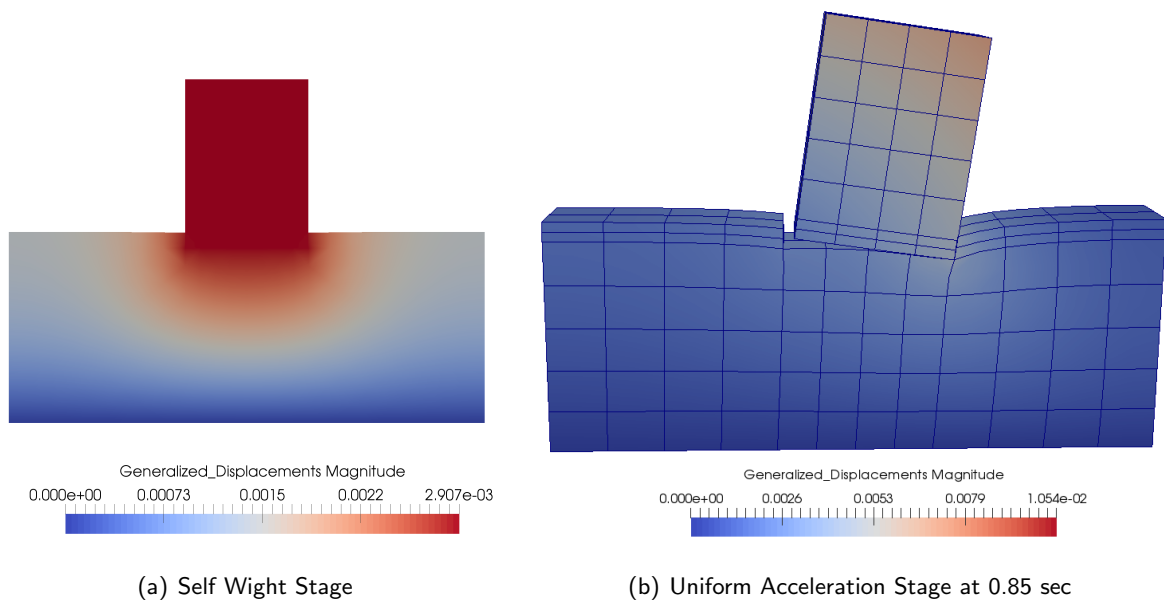


Figure 3.51: Simulation results visualization

3.8 Dynamics: Inelastic Solid Examples

The Real-ESSI input files for this example are available [HERE](#). The compressed package of Real-ESSI input files and postprocessing results for this example is available [HERE](#).

Firstly, the model is given an initial displacement at the top from 0 to 1 second. Second, after the time 1 second, the model starts free vibration.

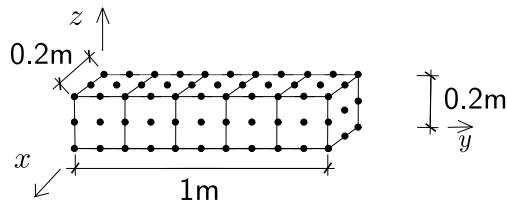


Figure 3.52: Problem Description for Newmark Method

Results This model has material damping. The displacement at the top is

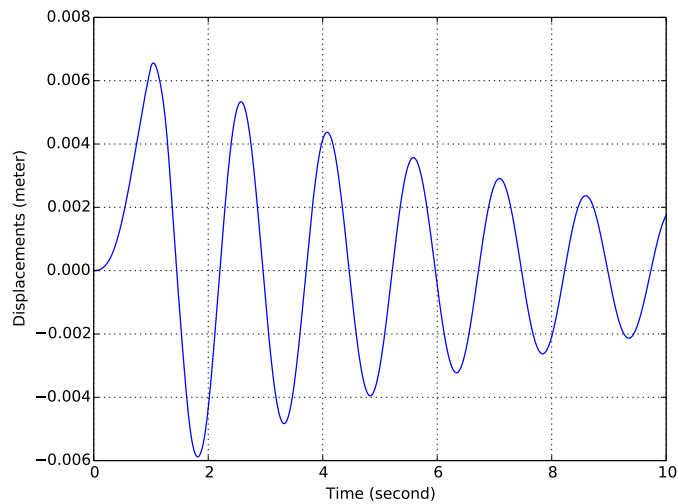


Figure 3.53: Results for Newmark Method

3.9 Dynamics: Inelastic Structural Examples

The Real-ESSI input files for this example are available [HERE](#). The compressed package of Real-ESSI input files and postprocessing results for this example is available [HERE](#).

The column beam is represented by the fiber section. This example is under the dynamic load of ground motion.

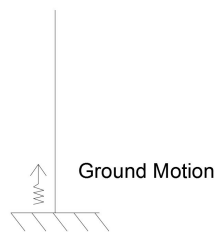


Figure 3.54: Ground motion on the Fiber Beam with Column Section

The fiber represents the rebar. The section of all fibers represents the cross section properties of the inelastic beam.

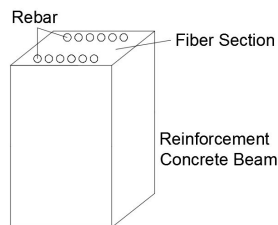


Figure 3.55: Diagram of the Fiber Beam with Column Section

3.10 Dynamics: Domain Reduction Method (DRM)

3.10.1 Dynamics: DRM One Dimensional (1D) Model

The Real-ESSI input files with 8NodeBrick for this example are available

[HERE](#).

The same model for this example with 27NodeBrick is available

[HERE](#).

A simple 1D DRM model is shown in Fig.(3.56). The "DRM element", "Exterior node" and "Boundary node" are required to be designated in the DRM HDF5 input. The format and script for the HDF5 input is available in DSL/input manual.

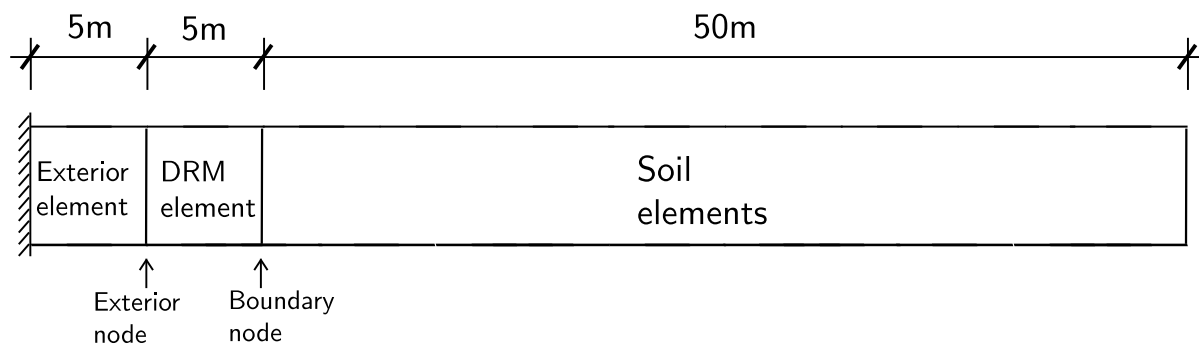


Figure 3.56: 1D DRM model.

Numerical model

Long 1D DRM model 1000:1 The Real-ESSI input files for this example are available

[HERE](#).

The results can also be seen from this

[ANIMATION](#).

To show the wave propagation explicitly, a long 1D model (1000:1) similar to the 1D DRM model above was made in this section.

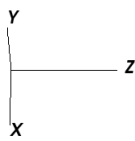
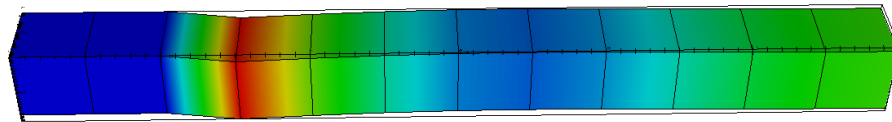
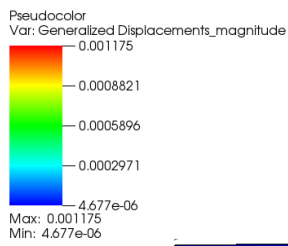
The model description is same to Fig.(3.56) except this model use far more soil elements.

The general view is shown in Fig.(3.58) below.

There is still now outgoing waves at the exterior layers, which is shown in Fig(3.59).

DB: DRM_1D.h5.feiooutput
Time:2.87

Mesh
Var: ESSI Domain Mesh



user: yuan
Sat Nov 7 11:34:02 2015

Figure 3.57: 1D DRM model.

DB: DRM_1D.h5.feiooutput
Time: 7.97

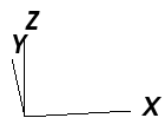
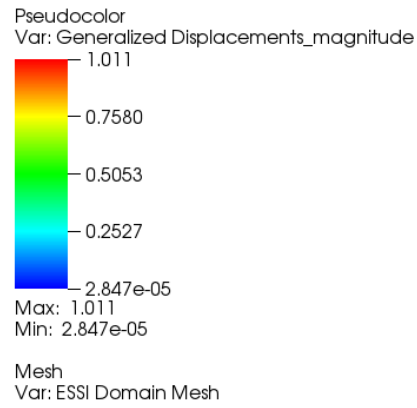


Figure 3.58: Long 1D DRM model

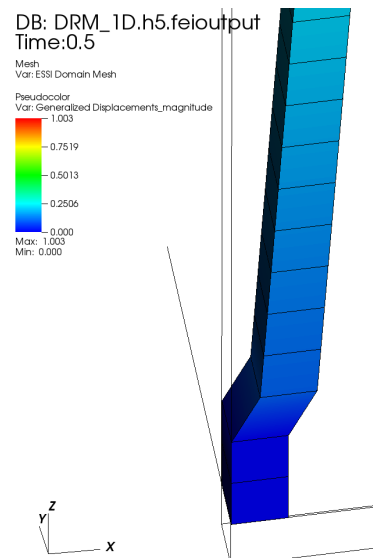


Figure 3.59: Long 1D DRM model: exterior layer

3.10.2 Dynamics: Three Dimensional (3D) DRM Model

The Real-ESSI input files with 8NodeBrick for this example are available

[HERE](#).

The same model for this example with 27NodeBrick is available

[HERE](#).

As shown in Fig.(3.60), the DRM layer is used to add the earthquake motion.

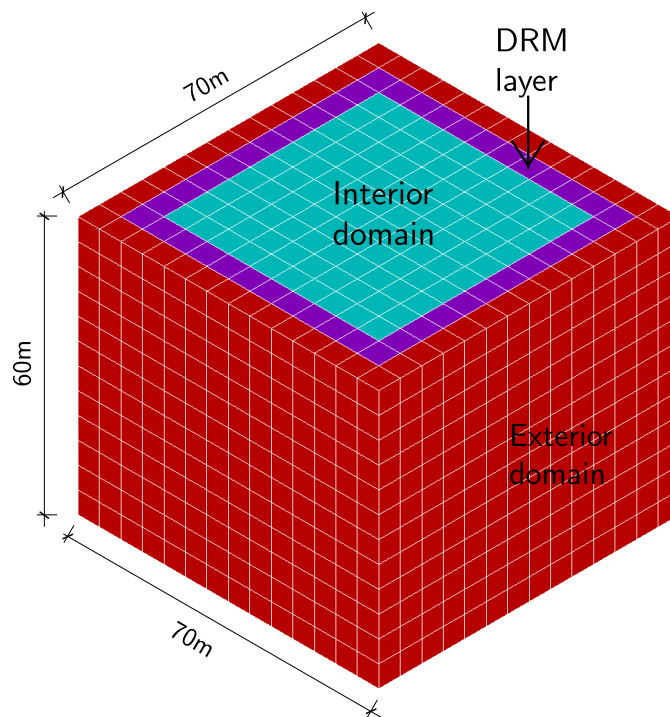


Figure 3.60: The diagram for 3D Domain Reduction Method example.

Numerical result

DB: DRM_3D.h5.feiooutput
Time:0.81

Mesh
Var: ESSI Domain Mesh

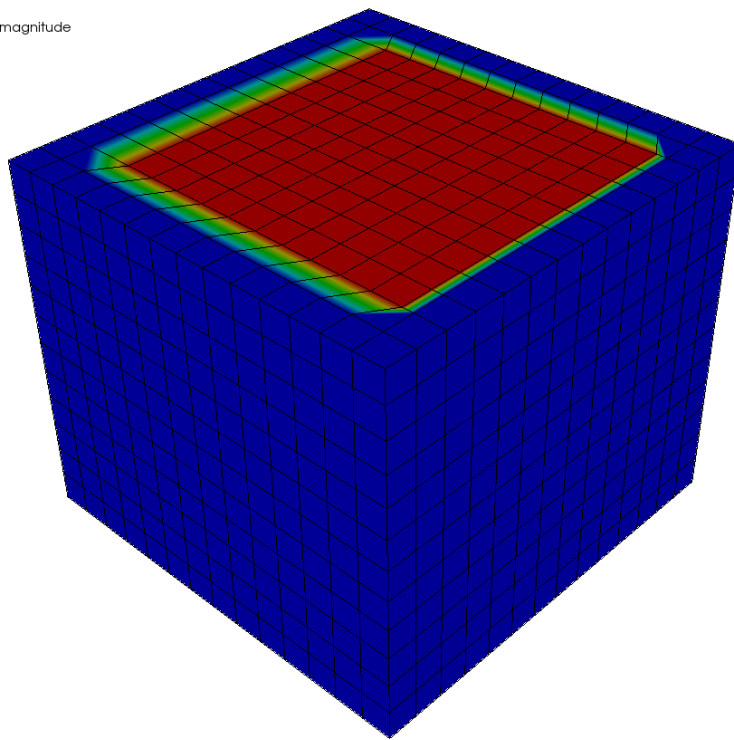
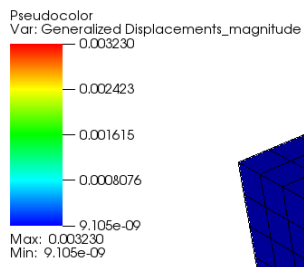


Figure 3.61: Diagram for the 3D DRM model.

3.10.3 Dynamics: DRM Model with Structure

Problem description The Real-ESSI input files for this example are available [HERE](#).

The compressed package of Real-ESSI input files and postprocessing results for this example is available [HERE](#).

As shown in Fig.(3.62), the structure is placed in the middle. Five different materials are assigned to structure, contact/interface zones, soil, DRM layer, and damping layers, respectively.

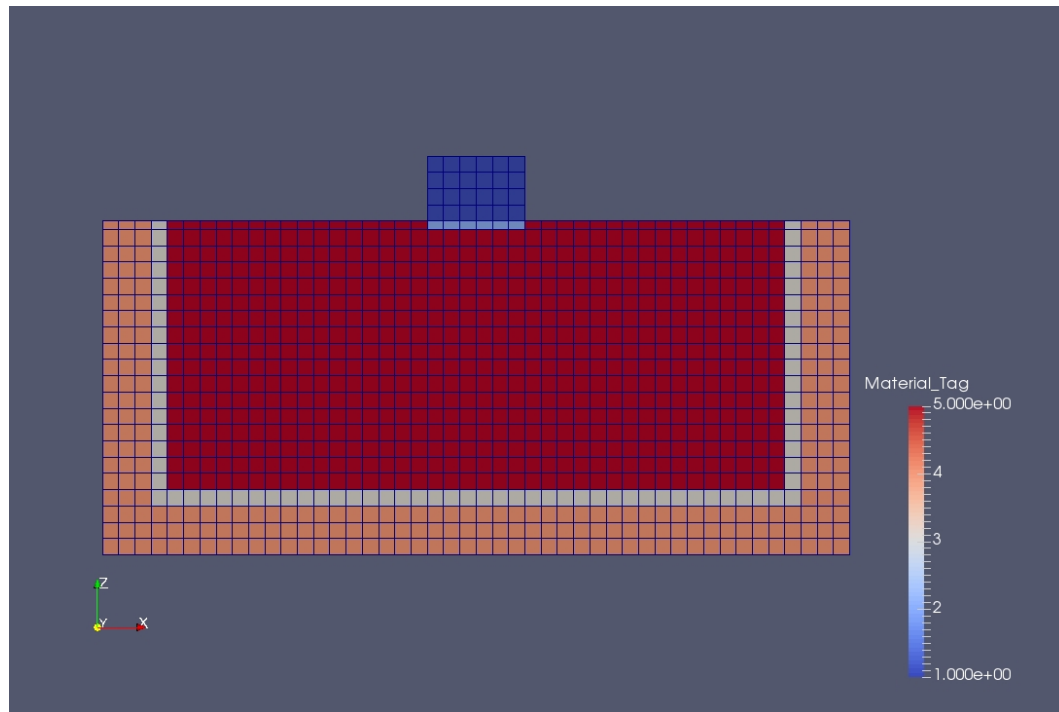


Figure 3.62: A Domain Reduction Method example with a Simple Structure.

3.11 Dynamics: Eigen Analysis

The Real-ESSI input files for this example are available [HERE](#). The compressed package of Real-ESSI input files and postprocessing results for this example is available [HERE](#).

Model is a brick beam with distributed mass.

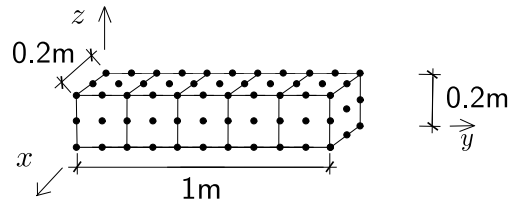


Figure 3.63: Problem Description for Newmark Method

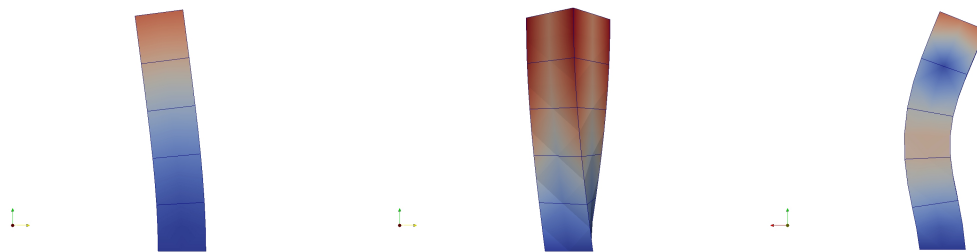


Figure 3.64: Solid Brick Cantilever Eigen Mode 1, 3, 4(From left to Right)

Results

3.12 Dynamics: Fully Coupled u-p-U and u-p Elements

The Real-ESSI input files for coupled example are available [HERE](#).

3.13 Dynamics: Partially Saturated / Unsaturated u-p-U Element (example in development)

3.14 Dynamics: Coupled Interface/Contact Element (example in development)

3.15 Dynamics: Buoyant Forces (example in development)

3.16 Chapter Summary and Highlights

In this Chapter stochastic/probabilistic modeling and simulation is illustrated through a number of examples. These examples can then be analyzed using Real-ESSI Simulator that is available for Linux, Windows (through ESL) or MacOS, and on Amazon Web Services (AWS) computers. Please refer to the Real-ESSI web site real-essi.us, for more information on how to install Real-ESSI on your computer (Linux, Windows, MacOS...).

Chapter 4

Stochastic Examples

(2018-2019-2020-2021-)

(In collaboration with Dr. Hexiang Wang)

4.1 Probabilistic Constitutive Modeling

4.1.1 Probabilistic Constitutive Modeling: Linear Elastic

The model description:

The Real-ESSI input files for this example are available in a zip archive [HERE](#).

A stochastic uniaxial elastic material with lognormal distributed random elastic modulus, mean 155 MPa and coefficient of variation 30%.

Results:

The probabilistic stress strain response of the stochastic uniaxial elastic material is shown in Figure [4.1](#).

4.1.2 Probabilistic Constitutive Modeling: Elasto-Plastic

The model description:

The Real-ESSI input files for this example are available in a zip archive [HERE](#).

A stochastic uniaxial elastoplastic material with vanishing elastic region and nonlinear Armstrong-Frederick kinematic hardening rule is modeled. The model parameters are: Armstrong-Frederick parameter H_a follows

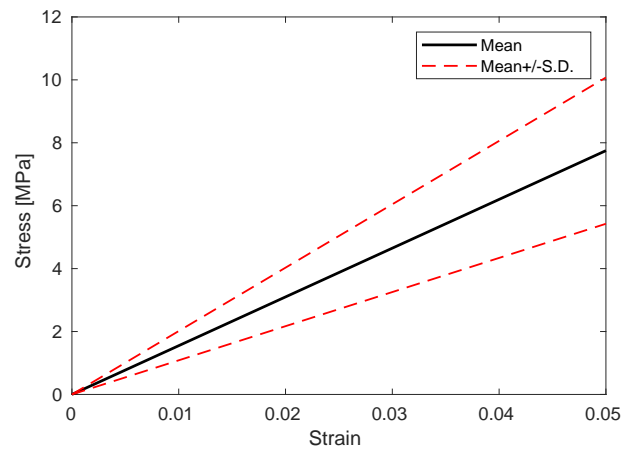


Figure 4.1: Constitutive behavior of stochastic uniaxial elastic material.

lognormal distribution with marginal mean 12 MPa and coefficient of variation 20%. Armstrong-Frederick parameter C_r follows lognormal distribution with marginal mean 200 and coefficient of variation (CV) 20%.

Results:

The probabilistic stress strain response of the stochastic uniaxial elastic material is shown in Figure 4.2.

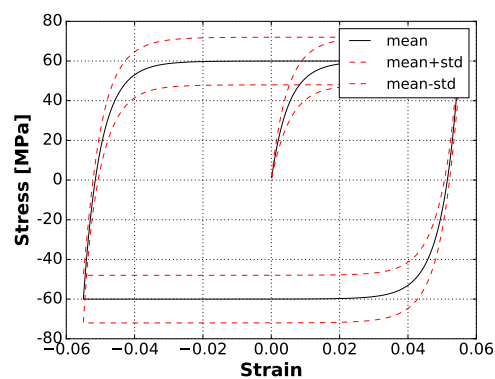


Figure 4.2: Constitutive behavior of stochastic uniaxial elastoplastic material.

4.2 Probabilistic Characterization of Seismic Motions

The model description:

The Real-ESSI input files for this example are available in a zip archive [HERE](#).

For stochastic analysis with uncertain seismic excitations, it is important to characterize input uncertain motions as a non-stationary random process. The random process can be quantified through marginal mean, marginal standard deviation and correlation structure, and can be represented as Hermite polynomial chaos (PC). This example presents such a random process of seismic motions with marginal mean, marginal standard deviation and correlation structure defined through plain text files. It is noted that this random process is used as input bedrock excitations in the subsequent stochastic wave propagation analysis.

Results:

It is important to check that the statistics synthesized from PC representation matches well with the input. Figures 4.3 and 4.2 compare the marginal statistics and correlation structure synthesized from PC representation with the target input.

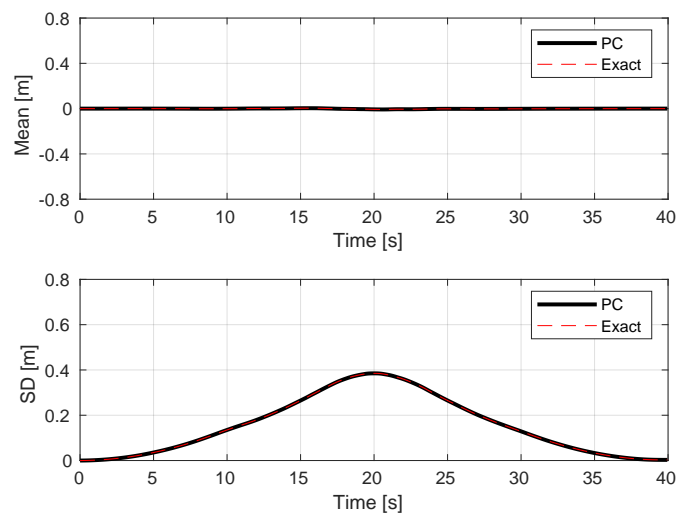


Figure 4.3: Verification of marginal statistics of random process motions.

4.3 1D Stochastic Seismic Wave Propagation

4.3.1 1D Stochastic Seismic Wave Propagation: Linear Elastic

The model description:

The Real-ESSI input files for this example are available in a zip archive [HERE](#).

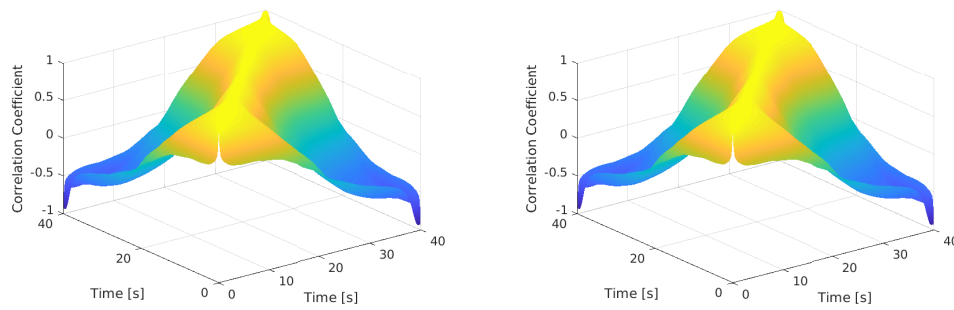


Figure 4.4: Input correlation structure (Left) and PC-synthesized correlation structure (Right).

Presented is 1D stochastic seismic wave propagation through uncertain linear elastic, layered ground. The uncertain motions characterized in section 4.2 is adopted as bedrock input. The ground is 10m thick with three layers and discretized with 10 stochastic shear beam elements as shown in Figure 4.5.

- Layer #1: Thickness 3m, uncertain elastic modulus follows lognormal distribution with marginal mean 120 MPa and 20% coefficient of variation.
- Layer #2: Thickness 3m, uncertain elastic modulus follows lognormal distribution with marginal mean 150 MPa and 25% coefficient of variation.
- Layer #3: Thickness 4m, uncertain elastic modulus follows lognormal distribution with marginal mean 180 MPa and 25% coefficient of variation.

The correlation structure of the uncertain elastic modulus random field follows exponential correlation with correlation length as 10m.

Results:

Time evolving marginal mean and marginal standard deviation of surface probabilistic displacement and acceleration response are shown in Figure 4.6 and 4.7.

4.3.2 1D Stochastic Seismic Wave Propagation: Elasto-Plastic

The model description:

The Real-ESSI input files for this example are available in a zip archive [HERE](#).

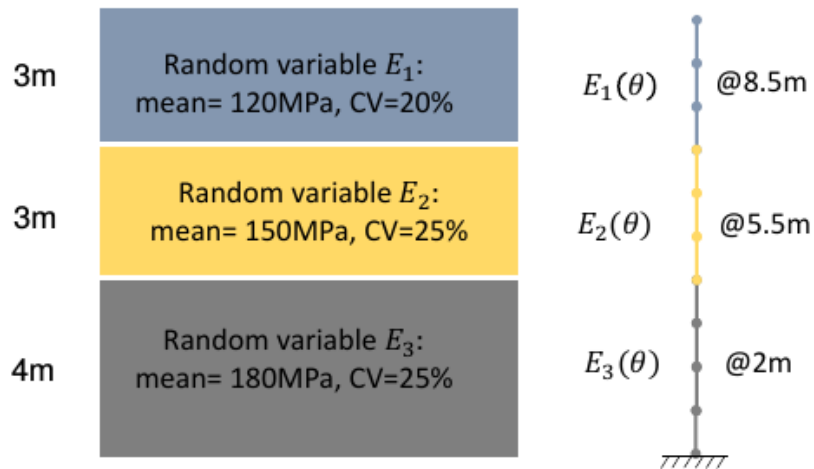


Figure 4.5: 1D layered ground and stochastic shear beam FEM model.

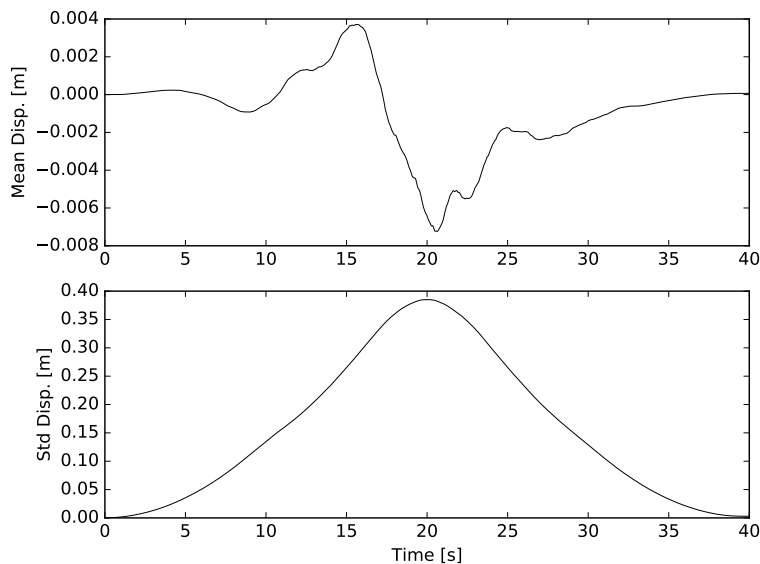


Figure 4.6: Probabilistic displacement response of ground surface.

The model geometry and input seismic excitations are identical to the example in section 4.3.1. The only difference is the constitutive model of soil. In this example, probabilistic elastoplastic soil model with vanishing elastic region and Armstrong-Frederick kinematic hardening is adopted.

Results:

Time evolving marginal mean and marginal standard deviation of surface probabilistic displacement and acceleration response are shown in Figure 4.8 and 4.9.

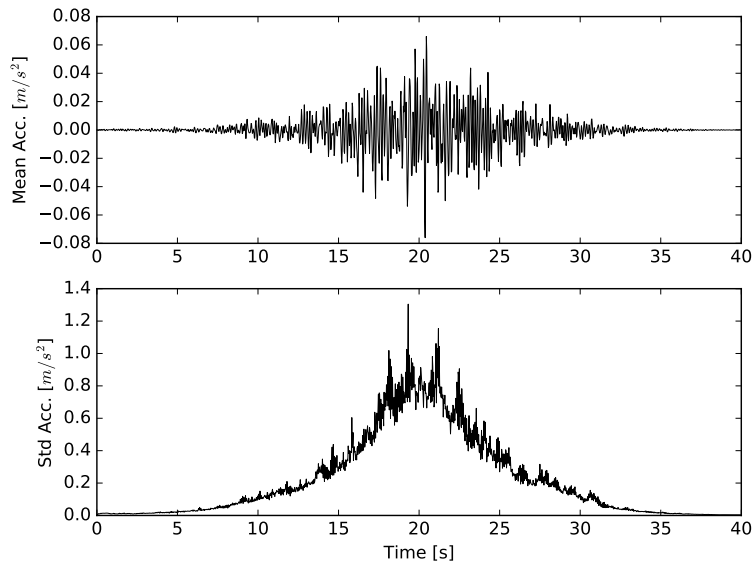


Figure 4.7: Probabilistic acceleration response of ground surface.

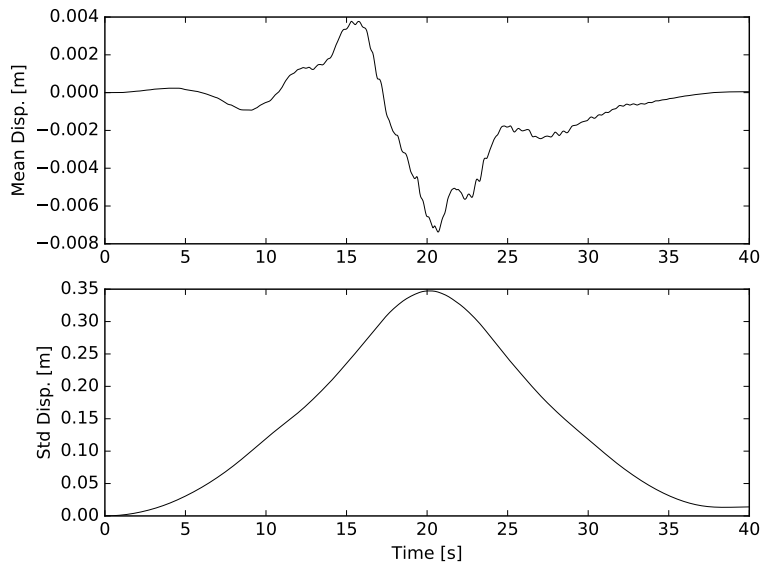


Figure 4.8: Probabilistic displacement response of ground surface.

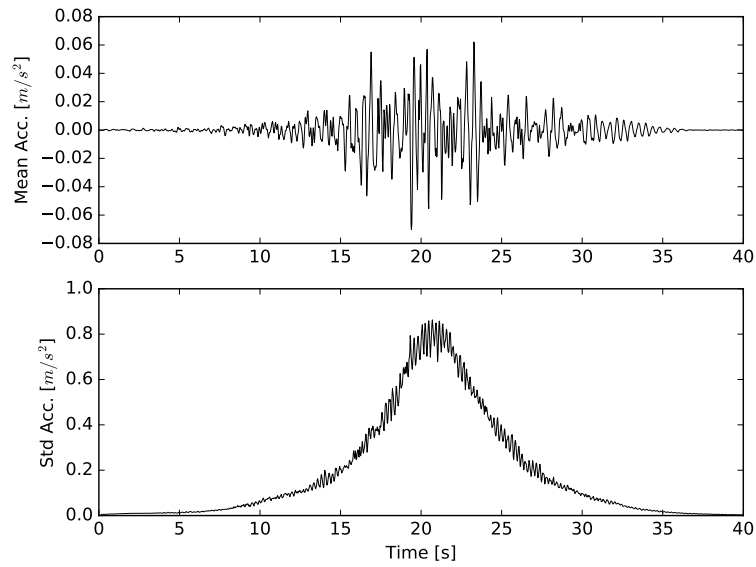


Figure 4.9: Probabilistic acceleration response of ground surface.

4.4 1D Stochastic Seismic Wave Propagation: Sobol Sensitivity Analysis

The Real-ESSI input files for this example are available in a zip archive [HERE](#).

Sobol sensitivity analysis is performed for the stochastic wave propagation example in section 4.3.1. From the sensitivity analysis results for probabilistic response at ground surface, it is shown that for this specific case most of the variance comes from the uncertain input motions.

Chapter 5

Large Scale, Realistic Examples

(2016-2018-)

(In collaboration with Dr. Yuan Feng, Mr. Sumeet Kumar Sinha, Dr. Han Yang, and Dr. Hexiang Wang)

Full scale, realistic examples of statics and dynamics of bridges, dams, buildings and nuclear power plants are presented in part 500 on page 2189 in Jeremić et al. (1989-2025).

Chapter 6

Short Course Examples

(2017-2023-)

(In collaboration with Dr. Yuan Feng and Dr. Han Yang)

6.1 Nonlinear Analysis Steps

6.1.1 Free Field 1C

Elastic Material. The Real-ESSI input files for elastic example are available [HERE](#).

The modeling parameters are listed below:

- Elastic Material Properties
 - Mass Density, ρ , 2000 kg/m^3
 - Shear wave velocity, V_s , 500 m/s
 - Young's modulus, E , 1.1 GPa
 - Poisson's ratio, ν , 0.1

Elastoplastic Material, von Mises with Armstrong-Frederick Kinematic Hardening The Real-ESSI input files for elastoplastic material example are available [HERE](#).

The modeling parameters are listed below

- von-Mises nonlinear hardening material model
 - Mass density, ρ , 2000 kg/m^3
 - Shear wave velocity, V_s , 500 m/s
 - Young's modulus, E , 1.1 GPa
 - Poisson's ratio, ν , 0.1
 - von Mises radius, k , 60 kPa
 - Nonlinear kinematic hardening, H_a , 30 MPa
 - Nonlinear kinematic hardening, C_r , 60
 - Shear strength ($\approx \sqrt{2/3} H_a/C_r$), S_u , 408 kPa
 - Isotropic hardening rate, K_{iso} , 0 Pa

Results of the simulation are shown in Fig. 6.1.

The time series of simulation results is shown in Fig. 6.3.

The response spectrum of motion is shown in Fig. 6.4.



Figure 6.1: Simulation model.

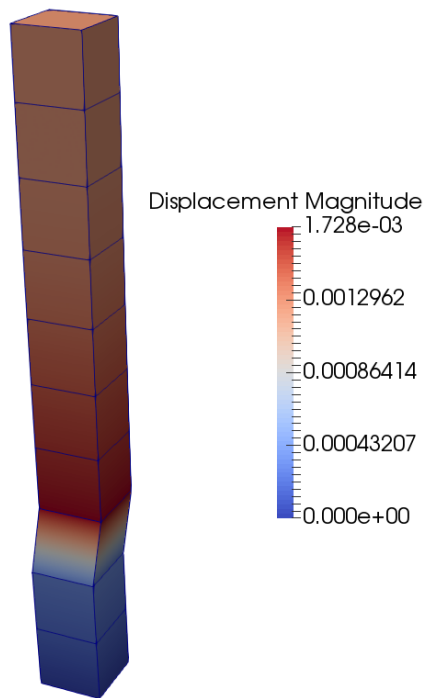


Figure 6.2: Simulation model.

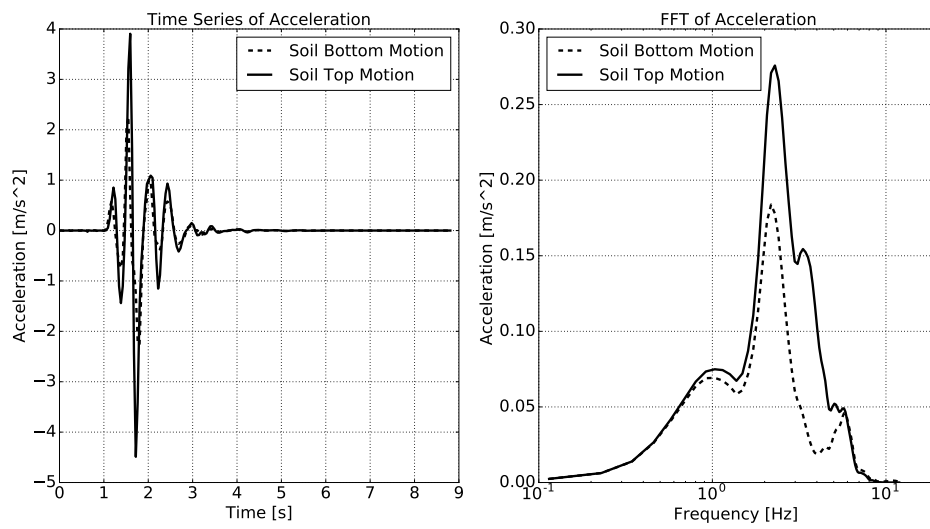


Figure 6.3: Simulation results: acceleration time series.

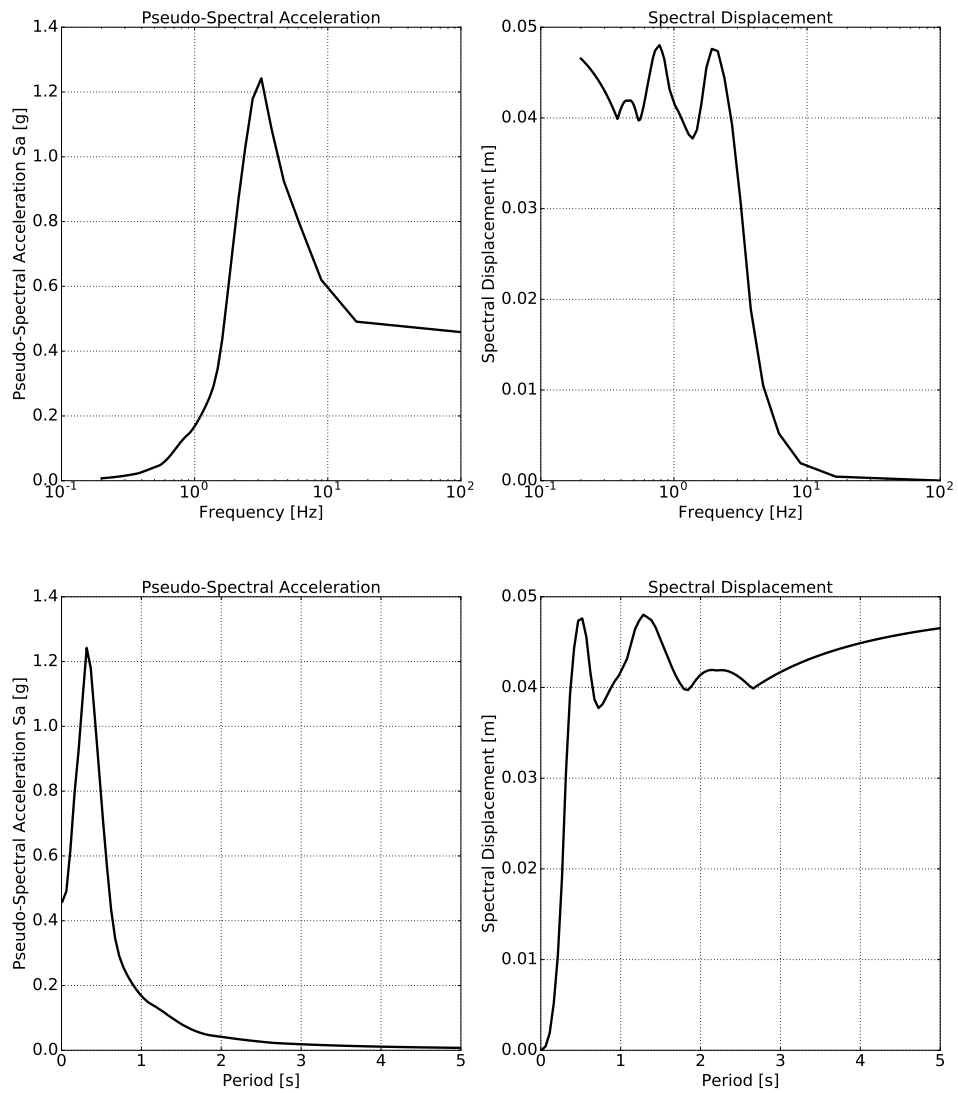


Figure 6.4: Simulation results: response spectrum at soil top.

6.1.2 Free Field 3C

Elastic Material. The compressed package of input files for this example is [HERE](#).

The Modeling parameters are listed below:

- Elastic Material Properties
 - Mass density, ρ , 2000 kg/m^3
 - Shear wave velocity, V_s , 500 m/s
 - Young's modulus, E , 1.1 GPa
 - Poisson's ratio, ν , 0.1

SIMULATION TIME: With 8 cores on AWS EC2 c4.2xlarge instance, the running time for this example is 5 minutes.

von-Mises Armstrong-Frederick Material. The compressed package of input files is [HERE](#).

The Modeling parameters are listed below:

- von-Mises nonlinear hardening material model
 - Mass density, ρ , 2000 kg/m^3
 - Shear wave velocity, V_s , 500 m/s
 - Young's modulus, E , 1.1 GPa
 - Poisson's ratio, ν , 0.1
 - von Mises radius, k , 60 kPa
 - Nonlinear kinematic hardening, H_a , 30 MPa
 - Nonlinear kinematic hardening, C_r , 60
 - Shear strength ($\approx \sqrt{2/3} H_a/C_r$), S_u , 408 kPa
 - Isotropic hardening rate, K_{iso} , 0 Pa

SIMULATION TIME: With 8 cores on AWS EC2 c4.2xlarge instance, the running time for this example is 17 minutes.

von-Mises G/Gmax Material. The compressed package of input files is [HERE](#).

The Modeling parameters are listed below:

- von-Mises G/Gmax material model

- Mass density, ρ , 2000 kg/m³
- Shear wave velocity, V_s , 500 m/s
- Young's modulus, E , 1.1 GPa
- Poisson's ratio, ν , 0.1
- Total number of shear modulus 9
- G over Gmax, 1,0.995,0.966,0.873,0.787,0.467,0.320,0.109,0.063
- Shear strain gamma, 0,1E-6,1E-5,5E-5,1E-4, 0.0005, 0.001, 0.005, 0.01

SIMULATION TIME: With 8 cores on AWS EC2 c4.2xlarge instance, the running time for this example is 565 minutes.

Drucker-Prager G/Gmax Material. The compressed package of input files is [HERE](#).

The Modeling parameters are listed below:

- Drucker-Prager G/Gmax material model
 - Mass density, ρ , 2000 kg/m³
 - Shear wave velocity, V_s , 500 m/s
 - Young's modulus, E , 1.1 GPa
 - Poisson's ratio, ν , 0.1
 - Initial confining stress, p_0 , 100 kPa
 - Reference pressure, p_{refer} , 100 kPa
 - Pressure exponential, n , 0.5
 - Cohesion, n , 1 kPa
 - Total number of Shear Modulus 9
 - G over Gmax, 1,0.995,0.966,0.873,0.787,0.467,0.320,0.109,0.063
 - Shear strain gamma, 0,1E-6,1E-5,5E-5,1E-4, 0.0005, 0.001, 0.005, 0.01

SIMULATION TIME: With 8 cores on AWS EC2 c4.2xlarge instance, the running time for this example is 565 minutes.

Results are shown in Fig. 6.56.

SIMULATION TIME: With 8 cores on AWS EC2 c4.2xlarge instance, the running time for this example is 871 minutes.

The time series of simulation results is shown in Fig. 6.7.

The response spectrum of motion is shown in Fig. 6.8.

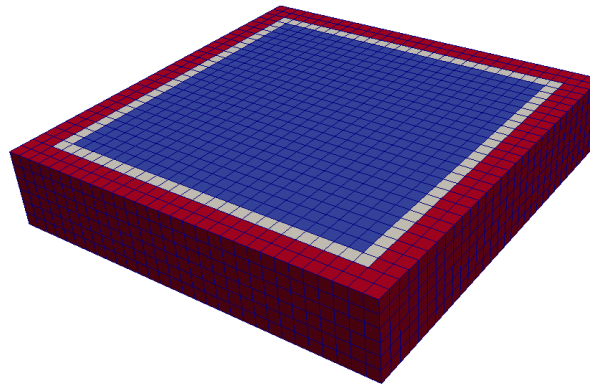


Figure 6.5: Simulation model.

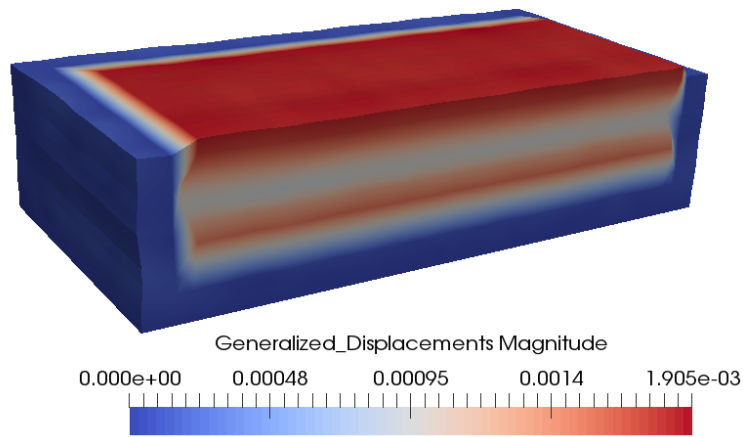


Figure 6.6: Simulation model.

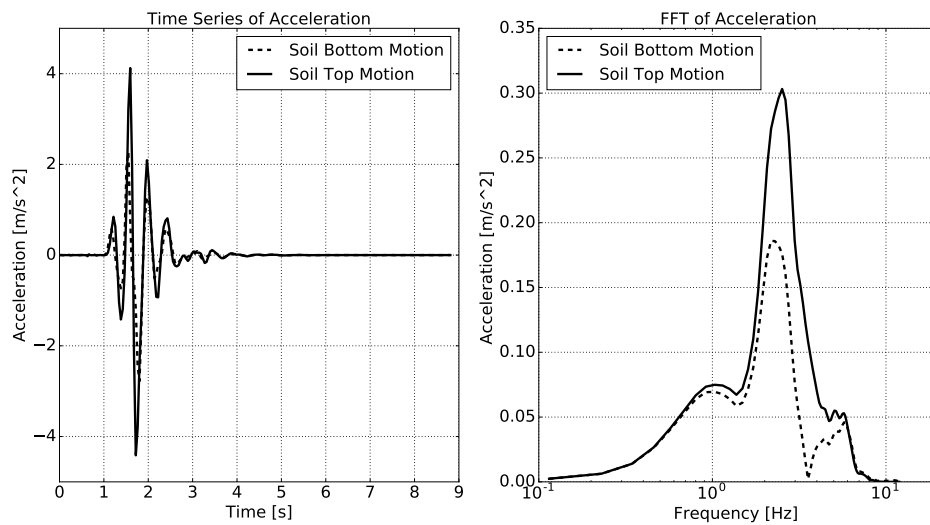


Figure 6.7: Simulation results: acceleration time series.

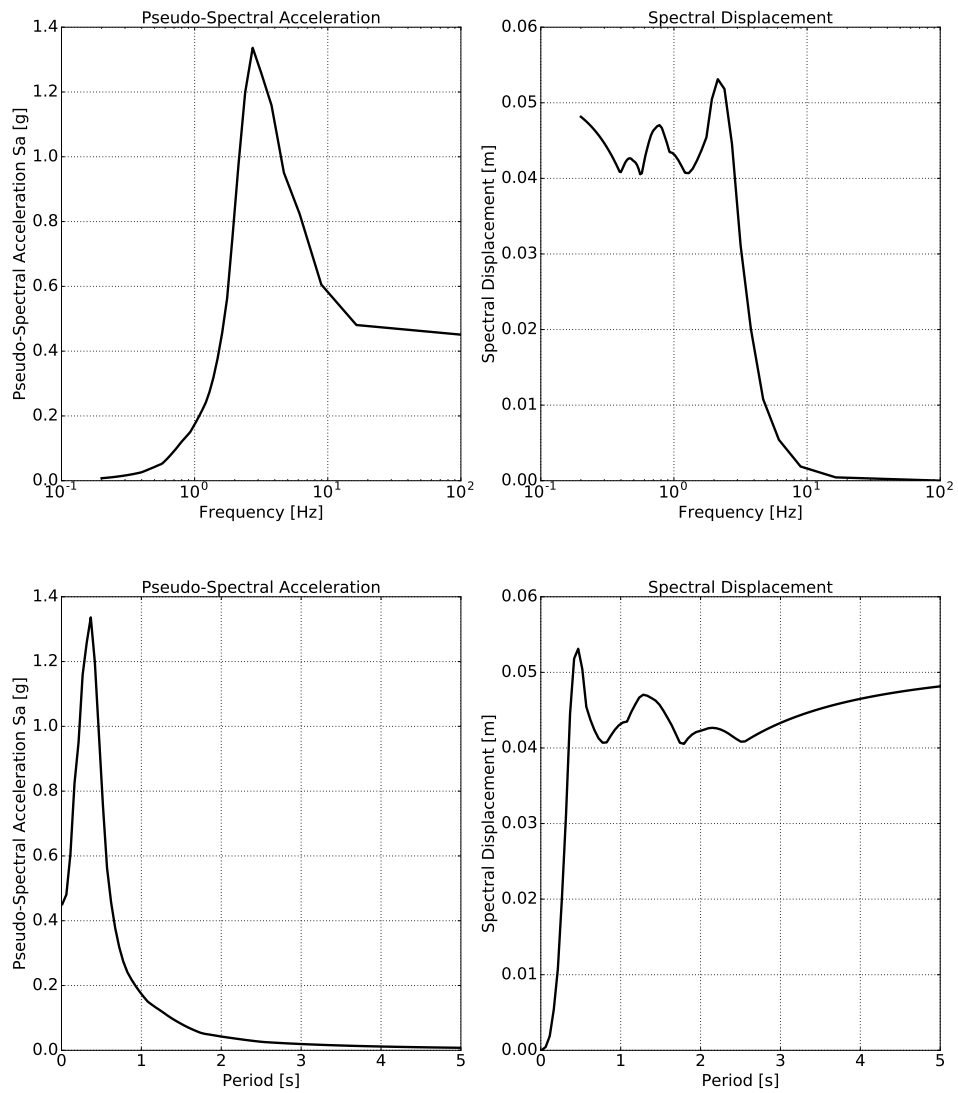


Figure 6.8: Simulation results: response spectrum at soil top.

6.1.3 Soil-Foundation Interaction 3D

Elastic Material. The compressed package of input files is [HERE](#).

The Modeling parameters are listed below:

- Elastic Material Properties
 - Mass density, ρ , 2000 kg/m^3
 - Shear wave velocity, V_s , 500 m/s
 - Young's modulus, E , 1.1 GPa
 - Poisson's ratio, ν , 0.1

SIMULATION TIME: With 8 cores on AWS EC2 c4.2xlarge instance, the running time for this example is 13 minutes.

von-Mises Armstrong-Frederick Material. The compressed package of input files is [HERE](#).

The Modeling parameters are listed below:

- von-Mises nonlinear hardening material model
 - Mass density, ρ , 2000 kg/m^3
 - Shear wave velocity, V_s , 500 m/s
 - Young's modulus, E , 1.1 GPa
 - Poisson's ratio, ν , 0.1
 - von Mises radius, k , 60 kPa
 - Nonlinear kinematic hardening, H_a , 30 MPa
 - Nonlinear kinematic hardening, C_r , 60
 - Shear strength ($\approx \sqrt{2/3} H_a/C_r$), S_u , 408 kPa
 - Isotropic hardening rate, K_{iso} , 0 Pa

SIMULATION TIME: With 8 cores on AWS EC2 c4.2xlarge instance, the running time for this example is 36 minutes.

von-Mises G/Gmax Material. The compressed package of input files is [HERE](#).

The Modeling parameters are listed below:

- von-Mises G/Gmax material model

- Mass density, ρ , 2000 kg/m³
- Shear wave velocity, V_s , 500 m/s
- Young's modulus, E , 1.1 GPa
- Poisson's ratio, ν , 0.1
- Total number of shear modulus 9
- G over Gmax, 1,0.995,0.966,0.873,0.787,0.467,0.320,0.109,0.063
- Shear strain gamma, 0,1E-6,1E-5,5E-5,1E-4, 0.0005, 0.001, 0.005, 0.01

SIMULATION TIME: With 8 cores on AWS EC2 c4.2xlarge instance, the running time for this example is 726 minutes.

Drucker-Prager G/Gmax Material. The compressed package of input files is [HERE](#).

The Modeling parameters are listed below:

- Drucker-Prager G/Gmax material model

- Mass density, ρ , 2000 kg/m³
- Shear wave velocity, V_s , 500 m/s
- Young's modulus, E , 1.1 GPa
- Poisson's ratio, ν , 0.1
- Initial confining stress, p_0 , 100 kPa
- Reference pressure, p_{refer} , 100 kPa
- Pressure exponential, n , 0.5
- Cohesion, n , 1 kPa
- Total number of Shear Modulus 9
- G over Gmax, 1,0.995,0.966,0.873,0.787,0.467,0.320,0.109,0.063
- Shear strain gamma, 0,1E-6,1E-5,5E-5,1E-4, 0.0005, 0.001, 0.005, 0.01

SIMULATION TIME: With 8 cores on AWS EC2 c4.2xlarge instance, the running time for this example is 1252 minutes.

Contact/Interface/Joint Elements. The compressed package of input files is [HERE](#).

The Modeling parameters are listed below:

- Elastic Material Properties

- Mass density, ρ , 2000 kg/m^3
- Shear wave velocity, V_s , 500 m/s
- Young's modulus, E , 1.1 GPa
- Poisson's ratio, ν , 0.1

SIMULATION TIME: With 8 cores on AWS EC2 c4.2xlarge instance, the running time for this example is 24 minutes.

Both Elastoplastic Material and Contact/Interface/Joint Elements. The compressed package of input files is [HERE](#).

SIMULATION TIME: With 8 cores on AWS EC2 c4.2xlarge instance, the running time for this example is 41 minutes.

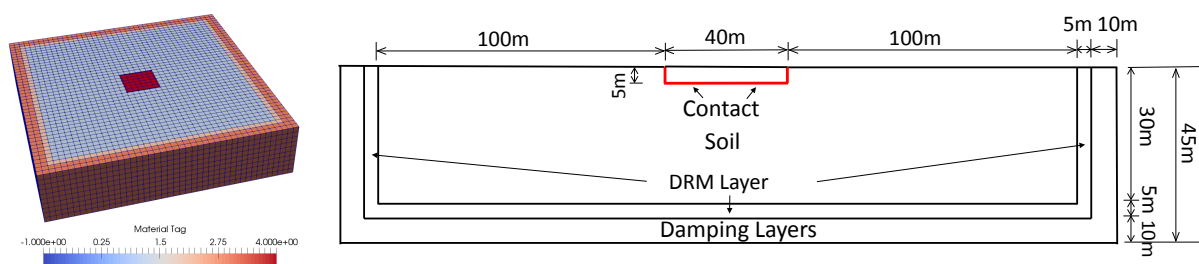


Figure 6.9: Simulation model.

Results of the simulation are shown in Fig. 6.12.

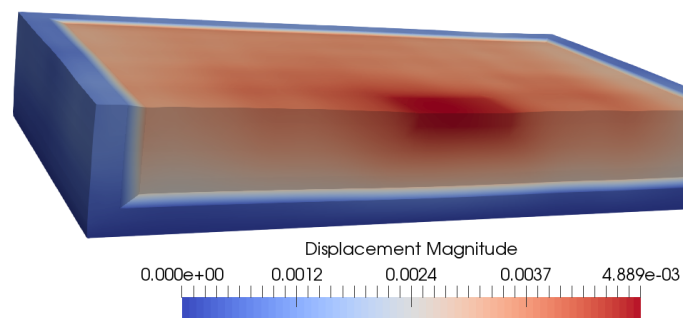


Figure 6.10: Soil foundation interaction results.

6.1.4 Soil-Structure Interaction 3D

Elastic Material. The compressed package of input files is [HERE](#).

The Modeling parameters are listed below:

- Elastic Material Properties
 - Mass density, ρ , 2000 kg/m^3
 - Shear wave velocity, V_s , 500 m/s
 - Young's modulus, E , 1.1 GPa
 - Poisson's ratio, ν , 0.1

SIMULATION TIME: With 8 cores on AWS EC2 c4.2xlarge instance, the running time for this example is 10 minutes.

von-Mises Armstrong-Frederick Material. The compressed package of input files is [HERE](#).

The Modeling parameters are listed below:

- von-Mises nonlinear hardening material model
 - Mass density, ρ , 2000 kg/m^3
 - Shear wave velocity, V_s , 500 m/s
 - Young's modulus, E , 1.1 GPa
 - Poisson's ratio, ν , 0.1
 - von Mises radius, k , 60 kPa
 - Nonlinear kinematic hardening, H_a , 30 MPa
 - Nonlinear kinematic hardening, C_r , 60
 - Shear strength ($\approx \sqrt{2/3} H_a/C_r$), S_u , 408 kPa
 - Isotropic hardening rate, K_{iso} , 0 Pa

SIMULATION TIME: With 8 cores on AWS EC2 c4.2xlarge instance, the running time for this example is 46 minutes.

von-Mises G/Gmax Material. The compressed package of input files is [HERE](#).

The Modeling parameters are listed below:

- von-Mises G/Gmax material model

- Mass density, ρ , 2000 kg/m^3
- Shear wave velocity, V_s , 500 m/s
- Young's modulus, E , 1.1 GPa
- Poisson's ratio, ν , 0.1
- Total number of shear modulus 9
- G over Gmax, 1,0.995,0.966,0.873,0.787,0.467,0.320,0.109,0.063
- Shear strain gamma, 0,1E-6,1E-5,5E-5,1E-4, 0.0005, 0.001, 0.005, 0.01

SIMULATION TIME: With 8 cores on AWS EC2 c4.2xlarge instance, the running time for this example is 755 minutes.

Drucker-Prager G/Gmax Material. The compressed package of input files is [HERE](#).

SIMULATION TIME: With 8 cores on AWS EC2 c4.2xlarge instance, the running time for this example is 1178 minutes.

The Modeling parameters are listed below:

- Drucker-Prager G/Gmax material model
 - Mass density, ρ , 2000 kg/m^3
 - Shear wave velocity, V_s , 500 m/s
 - Young's modulus, E , 1.1 GPa
 - Poisson's ratio, ν , 0.1
 - Initial confining stress, p_0 , 100 kPa
 - Reference pressure, p_{refer} , 100 kPa
 - Pressure exponential, n , 0.5
 - Cohesion, n , 1 kPa
 - Total number of Shear Modulus 9
 - G over Gmax, 1,0.995,0.966,0.873,0.787,0.467,0.320,0.109,0.063
 - Shear strain gamma, 0,1E-6,1E-5,5E-5,1E-4, 0.0005, 0.001, 0.005, 0.01

SIMULATION TIME: With 8 cores, the running time for this example is

Contact/Interface/Joint Elements. The compressed package of input files is [HERE](#).

SIMULATION TIME: With 8 cores on AWS EC2 c4.2xlarge instance, the running time for this example is 15 minutes.

Both Elastoplastic Material and Contact/Interface/Joint Elements. The compressed package of input files is [HERE](#).

The thickness of the shell structure is 2 meters.

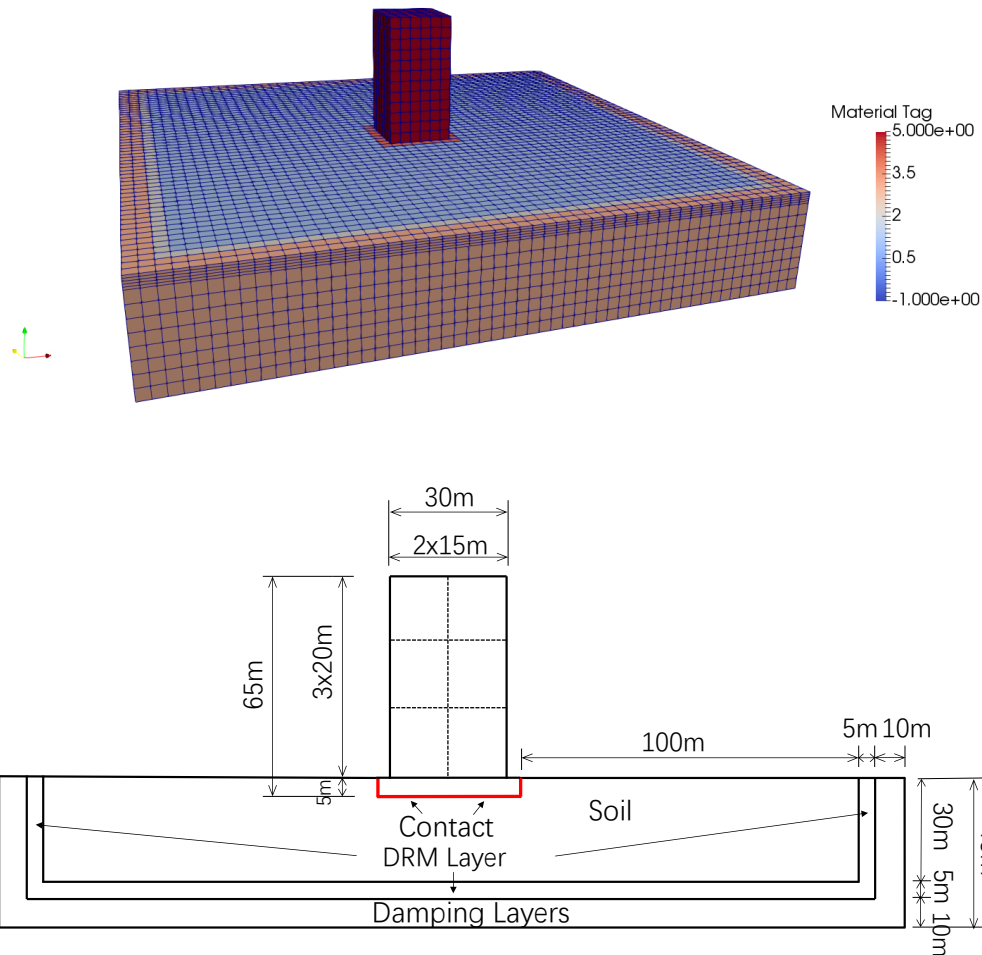


Figure 6.11: Simulation Model.

Results of the simulation are shown in Fig. 6.12.

SIMULATION TIME: With 8 cores on AWS EC2 c4.2xlarge instance, the running time for this example is 47 minutes.

Simulation with 1C motion. The time series of simulation results is shown in Fig. 6.13.

The response spectrum of motion is shown in Fig. 6.14.

Simulation with $3 \times 1C$ motion. The time series of simulation results is shown in Fig. 6.15.

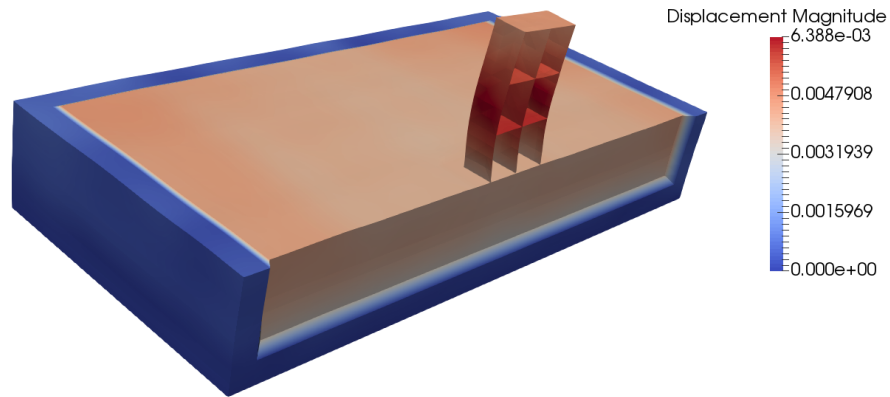


Figure 6.12: Simulation Model.

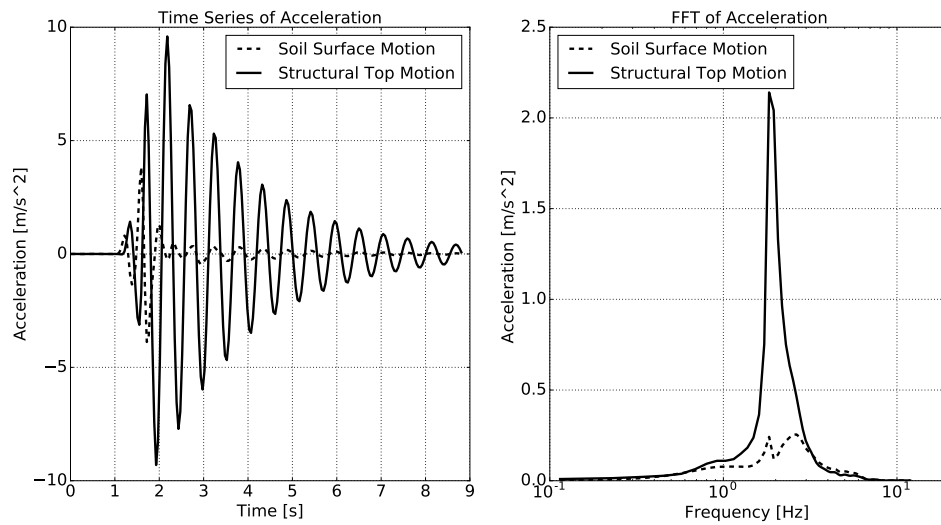


Figure 6.13: Simulation Results: Acceleration Time Series with 1C motion.

The response spectrum of motion is shown in Fig. 6.16.

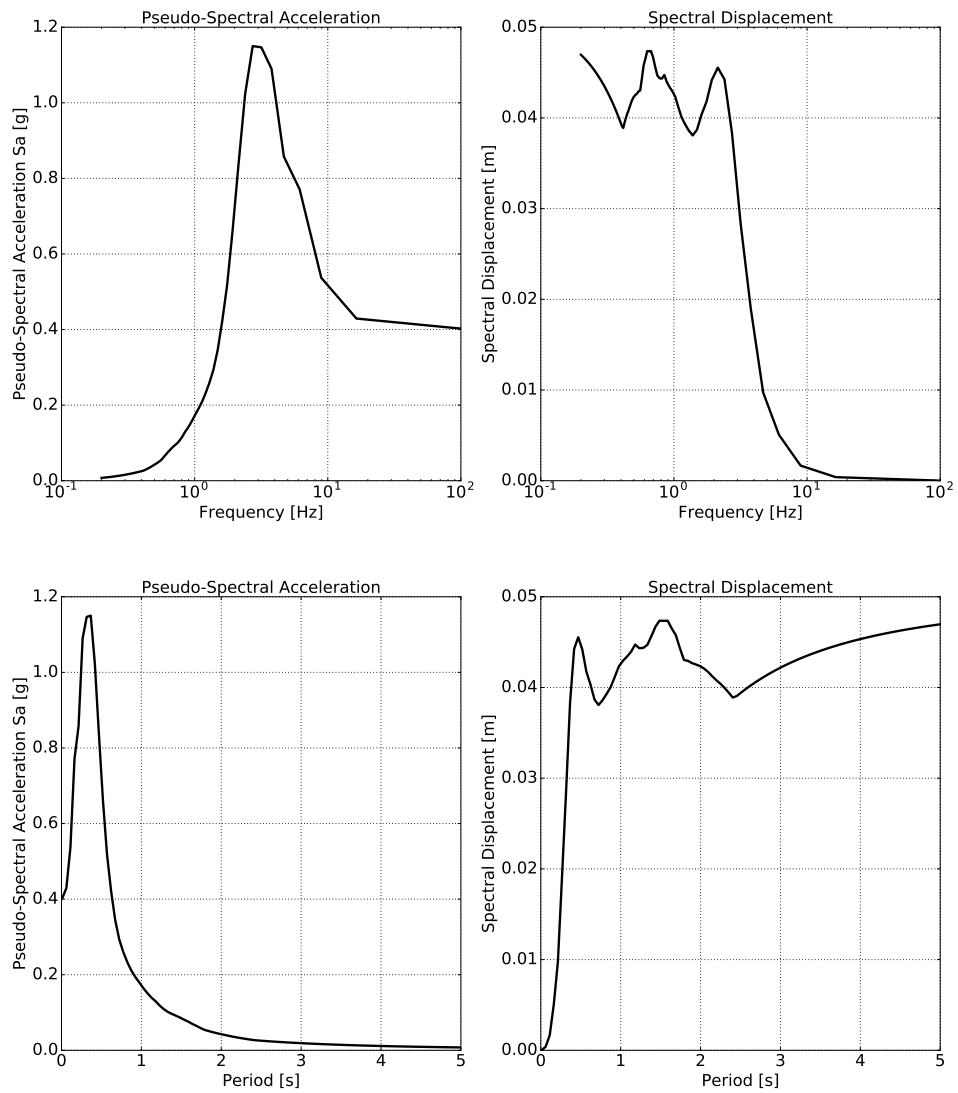


Figure 6.14: Simulation Results: Response Spectrum of Structure Top with 1C motion.

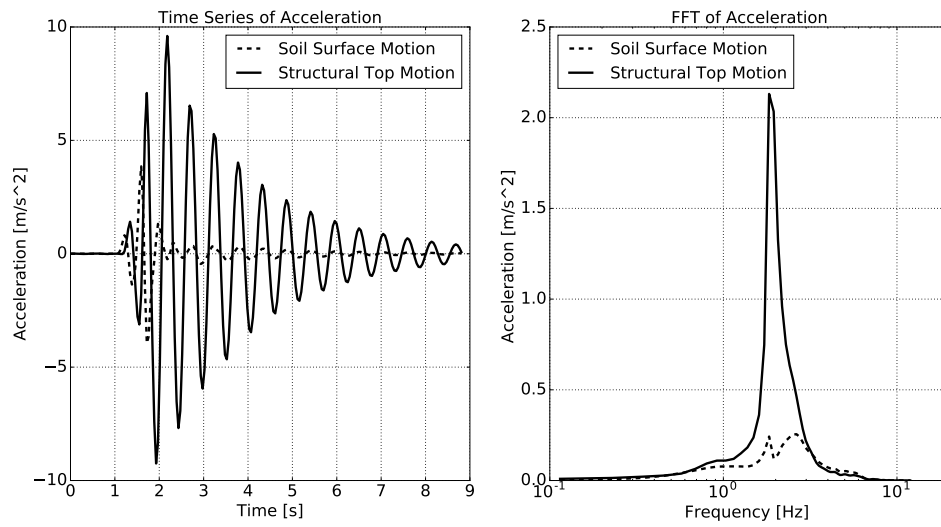


Figure 6.15: Simulation Results: Acceleration Time Series with 3C motion.

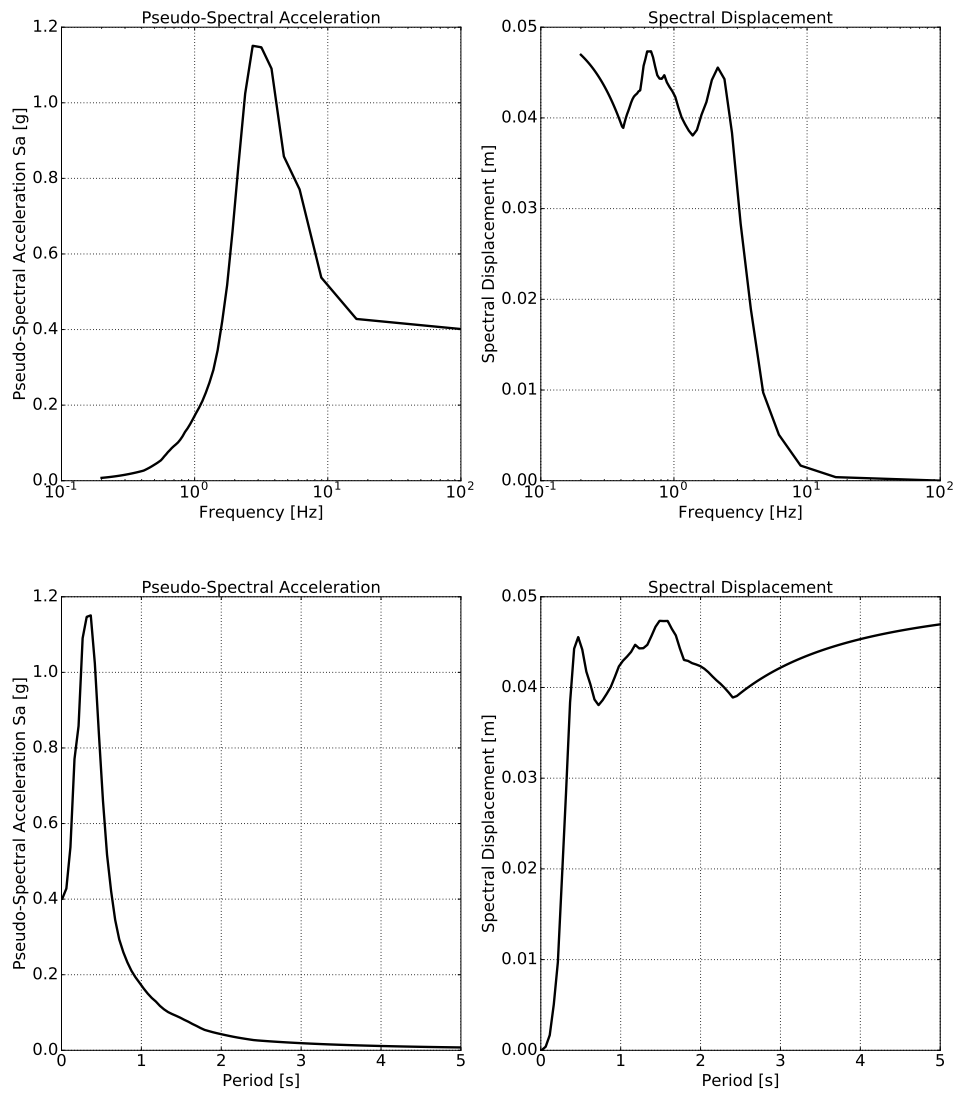


Figure 6.16: Simulation Results: Response Spectrum of Structure Top with 3C motion.

6.1.5 Analysis of a Structure without Soil

Eigen Analysis

Eigen analysis of a fixed base structural model should provide a good check of the structural model, natural (eigen) frequencies, and natural (eigen) modes.

The compressed package of input files is [HERE](#).

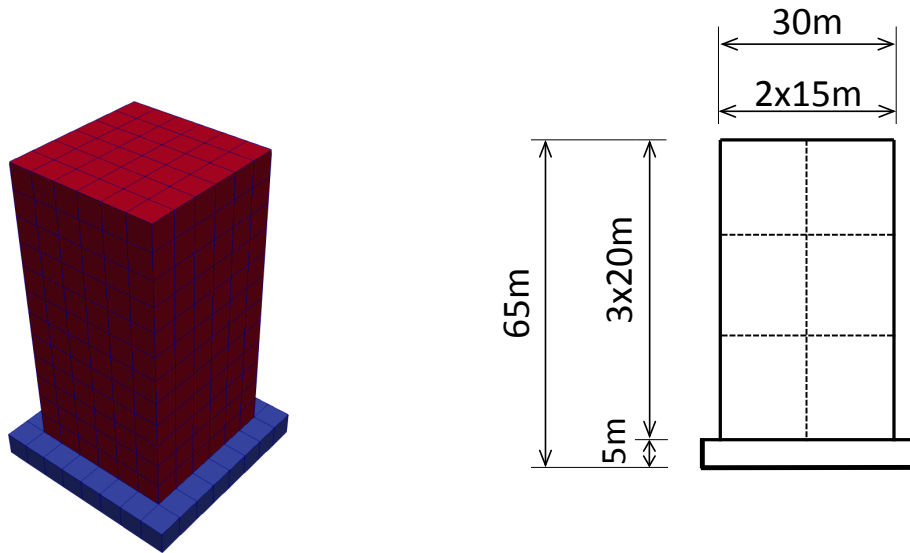


Figure 6.17: Structure on a fixed based simulation model.

For this particular example, eigen modes and frequencies are given in Figures 6.18 and 6.19

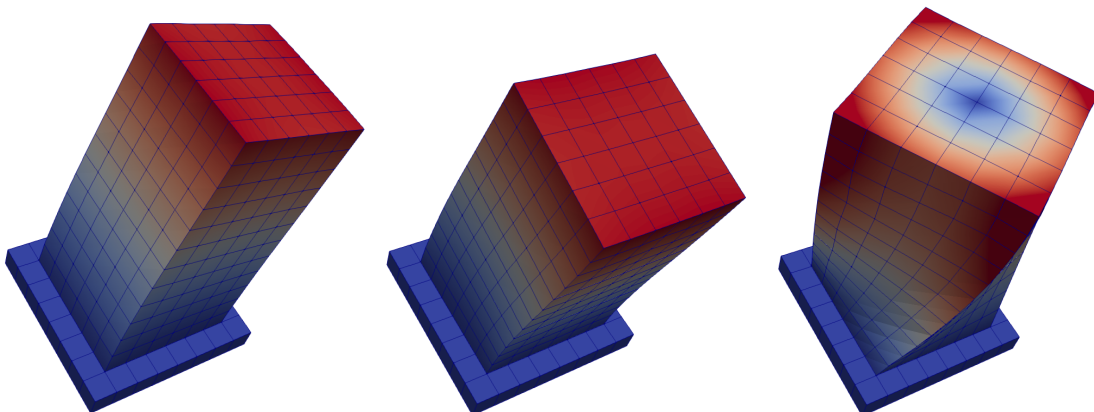


Figure 6.18: Eigen frequencies: $f_1 = 3.47\text{Hz}$ $f_2 = 3.47\text{Hz}$ $f_3 = 6.88\text{Hz}$ (eigen mode 1 to 3 from left to right).

Input files for eigen analysis of the fixed base structure are available at this [LINK](#), and can be directly simulated using Real-ESSI Simulator, <http://real-essi.us/>, that is available on Amazon Web Services,

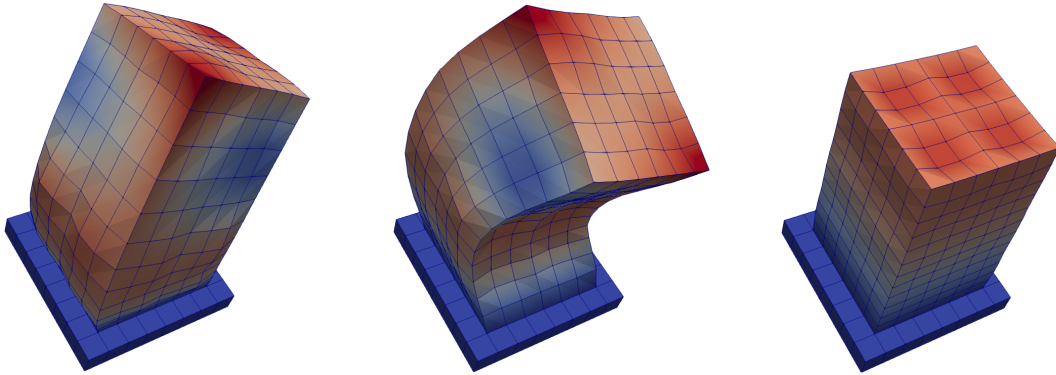


Figure 6.19: Eigen frequencies: $f_4 = 11.50\text{Hz}$ $f_5 = 11.50\text{Hz}$ $f_6 = 12.13\text{Hz}$ (eigen modes 4 to 6 from left to right).

<https://aws.amazon.com/>.

Imposed Motion

The Real-ESSI input files for this example are available [HERE](#). The compressed package of input files is [HERE](#).

In addition to eigen analysis, fixed base structural model is used to test response of a fixed base structure. This is important as it provides an opportunity to compare results between different finite element programs, some of which can only model dynamics of fixed base structures.

The simulation model is shown below.

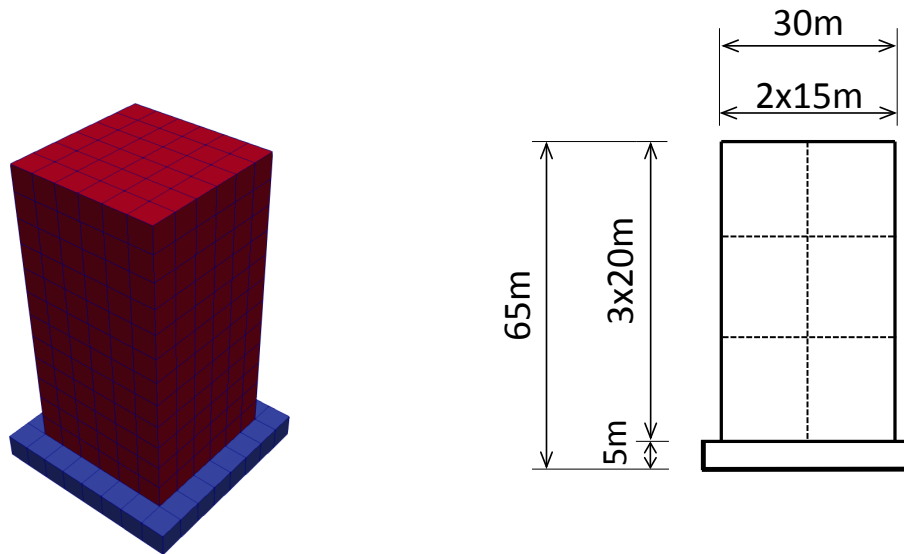


Figure 6.20: Simulation Model.

The simulation results:

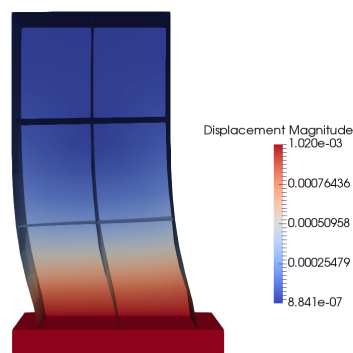


Figure 6.21: Simulation Results.

The time series of simulation results is shown in Fig. 6.22.

The response spectrum of motion is shown in Fig. 6.23.

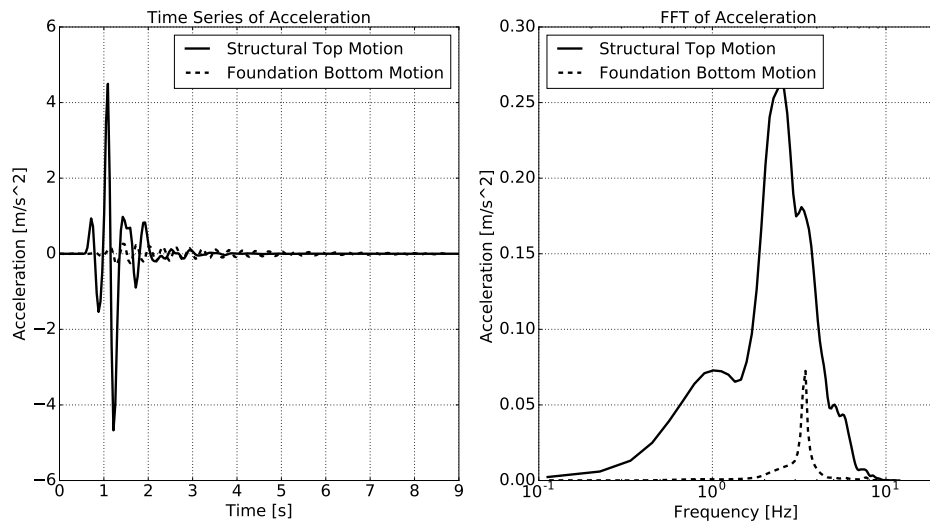


Figure 6.22: Simulation Results: Acceleration Time Series with 1C imposed motion.

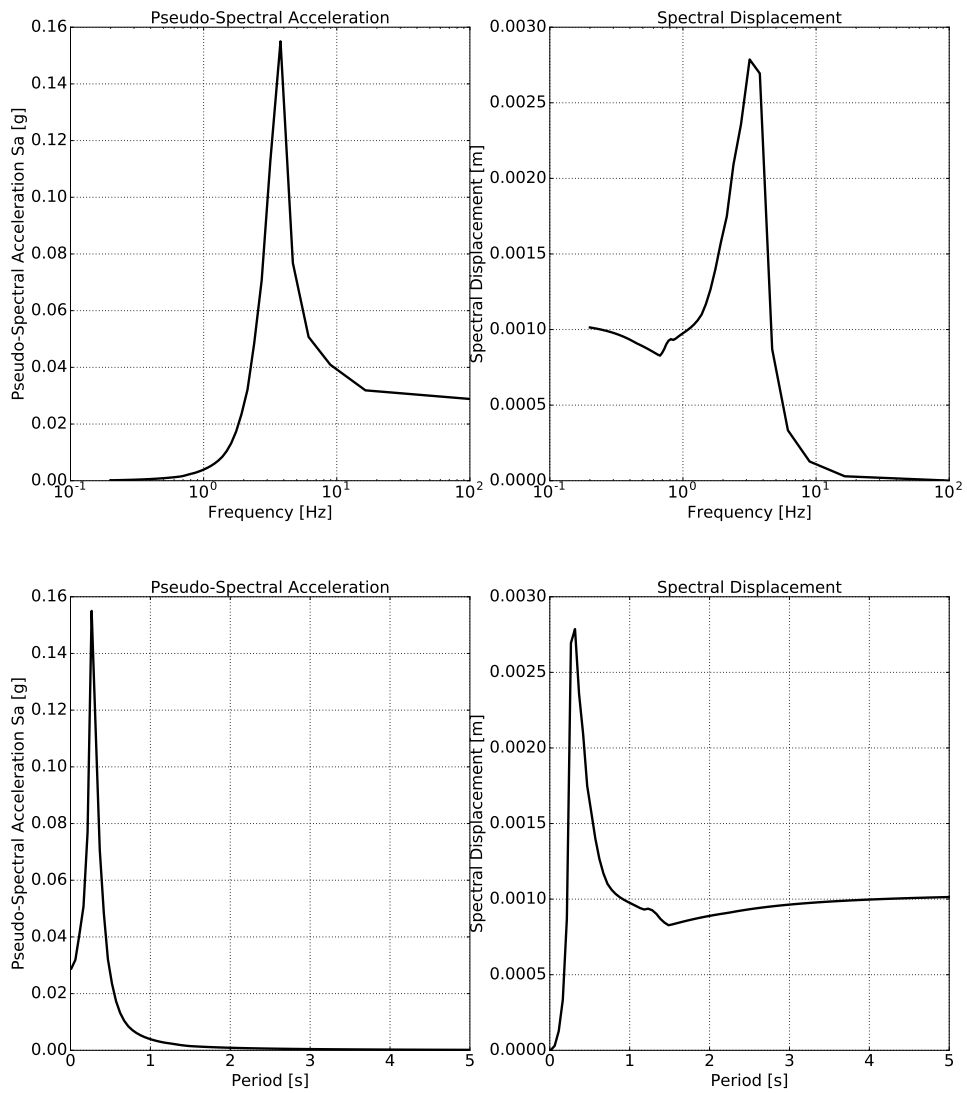


Figure 6.23: Simulation Results: Response Spectrum of Structure Top with 1C imposed motion.

6.2 Day 1: Overview

6.2.1 Nuclear Power Plant with 3C motions from SW4

The Real-ESSI input files for this example are available [HERE](#). The compressed package of Real-ESSI input files for this example is available [HERE](#).

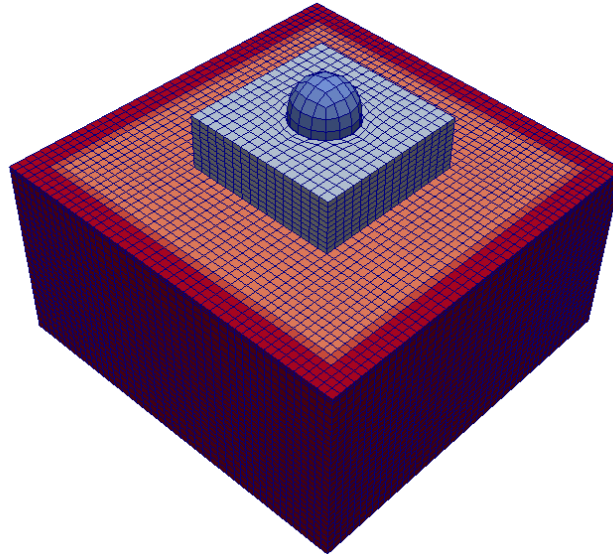


Figure 6.24: Simulation Model.

The Modeling parameters are listed below:

- Soil
 - Unit weight, γ , 21.4 kPa
 - Shear velocity, V_s , 500 m/s
 - Young's modulus, E , 1.3 GPa
 - Poisson's ratio, ν , 0.25
 - Shear strength, S_u , 650 kPa
 - von Mises radius, k , 60 kPa
 - kinematic hardening, H_a , 30 MPa
 - kinematic hardening, C_r , 25

- Structure
 - Unit weight, γ , 24 kPa

- Young's modulus, E , 20 GPa
- Poisson's ratio, ν , 0.21

The input motion at the bottom is a 3C wave from SW4.

SIMULATION TIME: With 32 cores on AWS EC2 c4.8xlarge instance, the running time for this example is 17 hours.

6.2.2 Nuclear Power Plant with 1C motions from Deconvolution

The Real-ESSI input files for this example are available [HERE](#). The compressed package of Real-ESSI input files for this example is available [HERE](#).

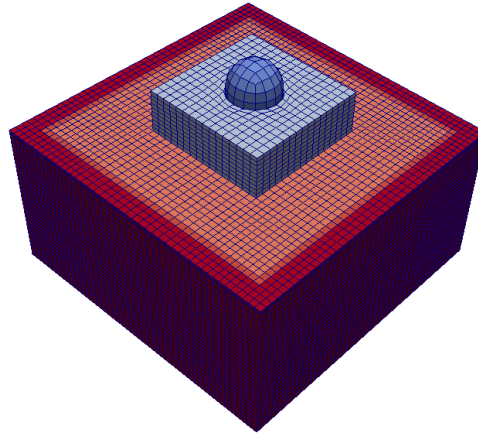


Figure 6.25: Simulation Model.

The input motion at the bottom is the deconvolution of the Northridge earthquake records.

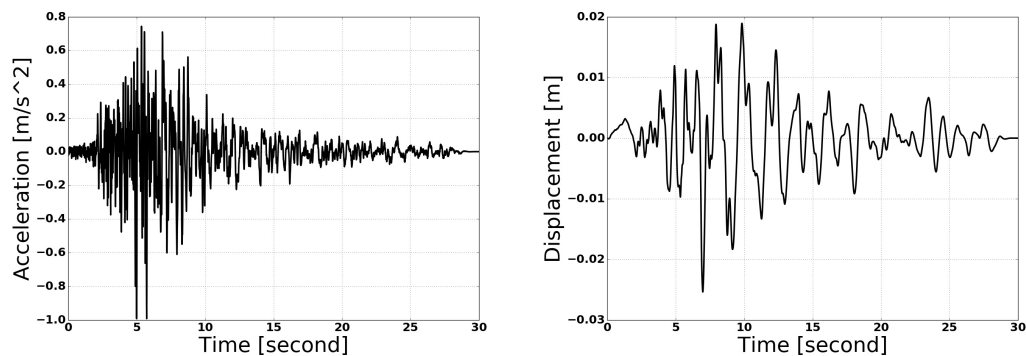


Figure 6.26: Motion Deconvolution.

The Modeling parameters are listed below:

- Soil
 - Unit weight, γ , 21.4 kPa
 - Shear velocity, V_s , 500 m/s
 - Young's modulus, E , 1.3 GPa
 - Poisson's ratio, ν , 0.25
 - Shear strength, S_u , 650 kPa

- von Mises radius, k , 60 kPa
- kinematic hardening, H_a , 30 MPa
- kinematic hardening, C_r , 25
- Structure
 - Unit weight, γ , 24 kPa
 - Young's modulus, E , 20 GPa
 - Poisson's ratio, ν , 0.21

6.2.3 Nuclear Power Plant with 3×1C motions from Deconvolution

The Real-ESSI input files for this example are available [HERE](#). The compressed package of Real-ESSI input files for this example is available [HERE](#).

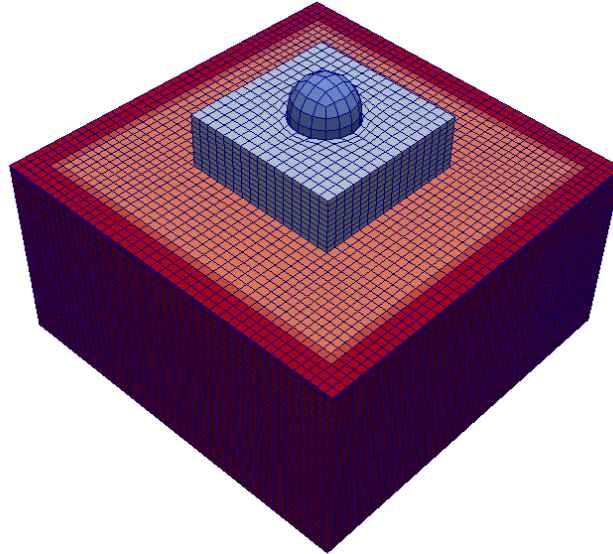


Figure 6.27: Simulation Model.

The input motion at the bottom is the deconvolution of the Northridge earthquake records.

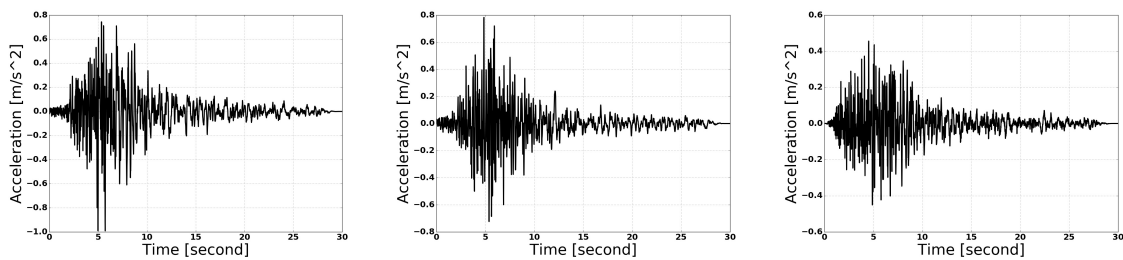


Figure 6.28: Acceleration Deconvolution, from left to right in x, y, z directions respectively. .

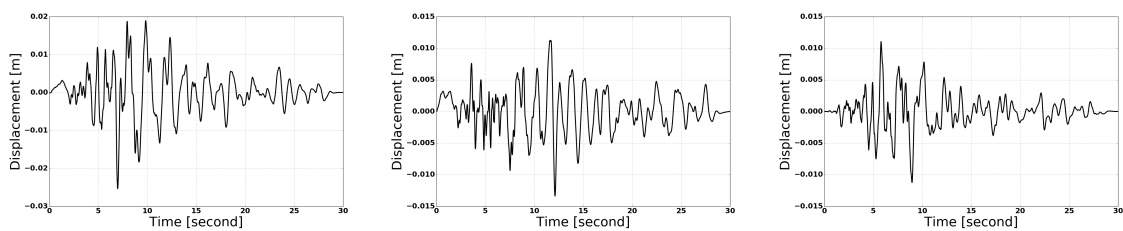


Figure 6.29: Displacement Deconvolution, from left to right in x, y, z directions respectively. .

The Modeling parameters are listed below:

- Soil
 - Unit weight, γ , 21.4 kPa
 - Shear velocity, V_s , 500 m/s
 - Young's modulus, E , 1.3 GPa
 - Poisson's ratio, ν , 0.25
 - Shear strength, S_u , 650 kPa
 - von Mises radius, k , 60 kPa
 - kinematic hardening, H_a , 30 MPa
 - kinematic hardening, C_r , 25

- Structure
 - Unit weight, γ , 24 kPa
 - Young's modulus, E , 20 GPa
 - Poisson's ratio, ν , 0.21

6.2.4 Single Element Models: Illustration of the Elastic-Plastic Behavior

The compressed package of Real-ESSI input files for this example with von-Mises material model are available [HERE](#).

The compressed package of Real-ESSI input files for this example with Drucker-Prager material model are available [HERE](#).

The Modeling parameters are listed below:

- von-Mises linear hardening material model
 - Mass Density, ρ , 0.0 kg/m³
 - Young's modulus, E , 20 MPa
 - Poisson's ratio, ν , 0.0
 - von Mises radius, k , 100 kPa
 - kinematic hardening rate, K_{kine} , 2 MPa
 - isotropic hardening rate, K_{iso} , 0 Pa

- Drucker-Prager nonlinear hardening material model
 - Mass Density, ρ , 0.0 kg/m³
 - Young's modulus, E , 20 MPa
 - Poisson's ratio, ν , 0.0
 - Drucker-Prager, k , 0.179527
 - nonlinear kinematic hardening, H_a , 20 MPa
 - nonlinear kinematic hardening, C_r , 100
 - isotropic hardening rate, K_{iso} , 0 Pa
 - initial confining stress, p_0 , 1 Pa

Inelastic/nonlinear material behavior is shown in Fig. 6.31.

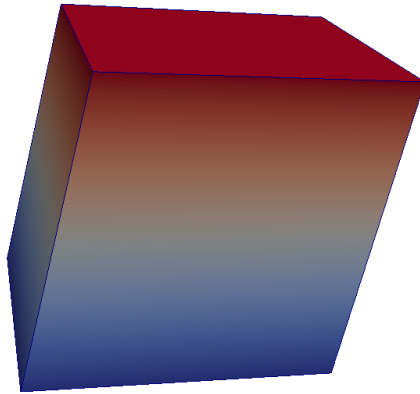


Figure 6.30: Simulation Model of Single Element.

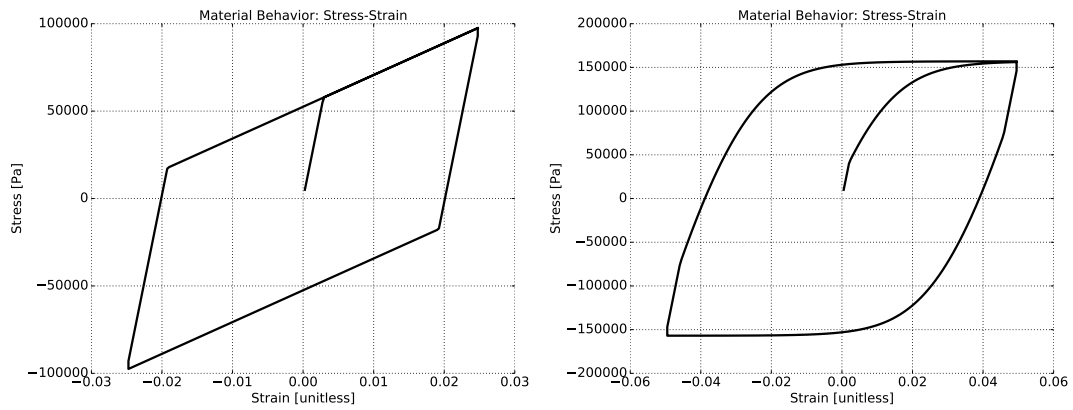


Figure 6.31: Inelastic/Nonlinear material behavior.

6.2.5 Pushover for Nonlinear Frame

The Real-ESSI input files for this example are available [HERE](#). The compressed package of Real-ESSI input files for this example is available [HERE](#).

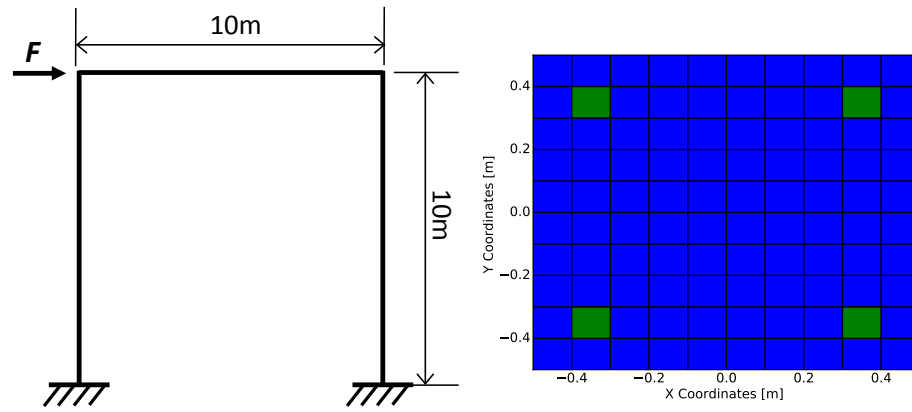


Figure 6.32: Model for pushover simulation and the cross section of fiber beam (concrete and reinforcement).

Results are shown in Fig. 6.33.

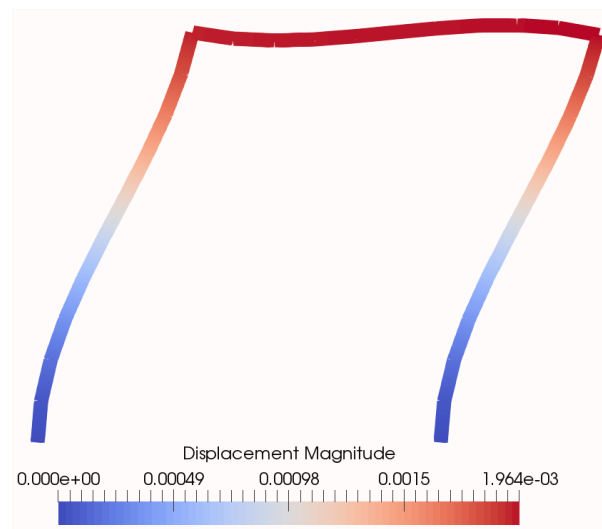


Figure 6.33: Results for fiber beam pushover.

The Modeling parameters are listed below:

- Uniaxial concrete
 - Compressive strength, 24 MPa
 - Strain at compressive strength, 0.001752
 - Crushing strength, 0.0 Pa

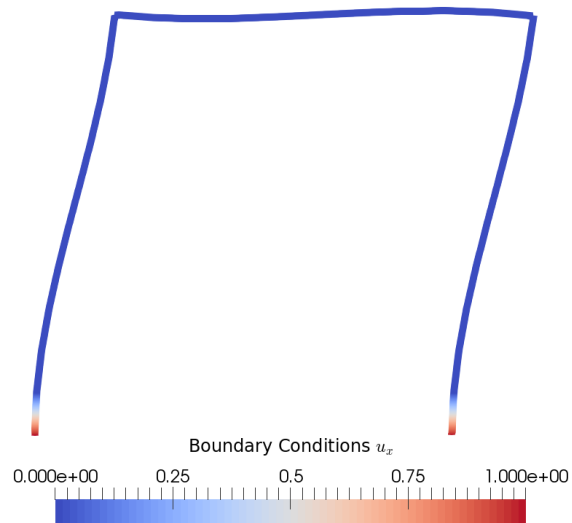


Figure 6.34: Boundary condition u_x for fiber beam pushover.

- Strain at compressive strength, 0.003168
- lambda, 0.5
- Tensile strength, 0 Pa
- Tension softening stiffness, 0 Pa
- Uniaxial steel
 - Yield strength, 413.8 MPa
 - Young's modulus, 200 GPa
 - Strain hardening ratio, 0.01
 - R0, 18.0
 - cR1, 0.925
 - cR2, 0.15
 - a1, 0.0
 - a2, 55.0
 - a3, 0.0
 - a4, 55.0

6.2.6 Pre-Processing examples with Gmsh

Cantilever Example

The Real-ESSI input files for this example are available [HERE](#). The compressed package of Real-ESSI input files for this example is available [HERE](#).

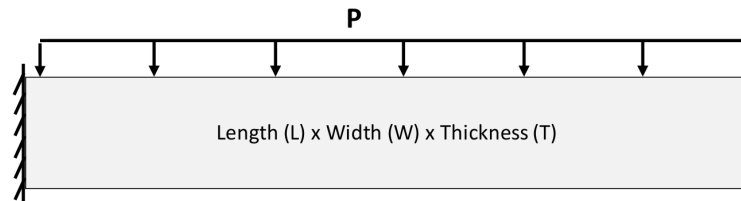


Figure 6.35: Simulation Model Cantilever.

Results are shown in Fig. 6.36.

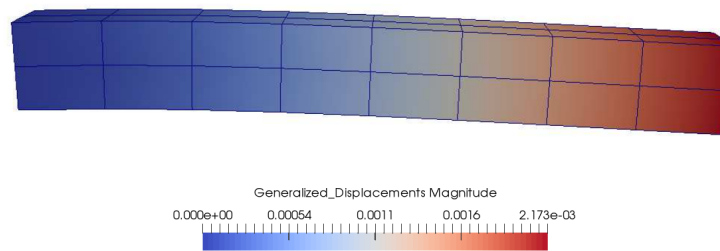


Figure 6.36: Simulation model. cantilever, results.

Brick-shell-beam Example

The Real-ESSI input files for this example are available [HERE](#). The compressed package of Real-ESSI input files for this example is available [HERE](#).

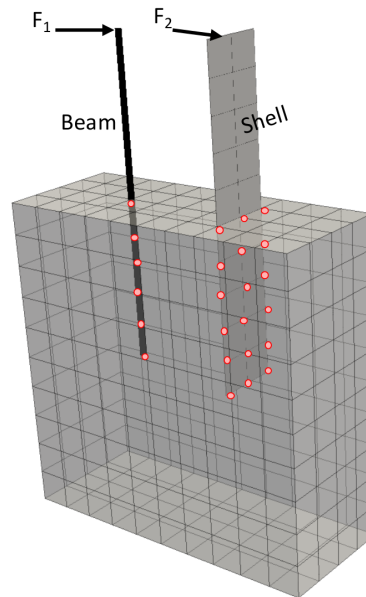


Figure 6.37: Simulation Model Brick-Shell-Beam.

Results are shown in Fig. 6.38.

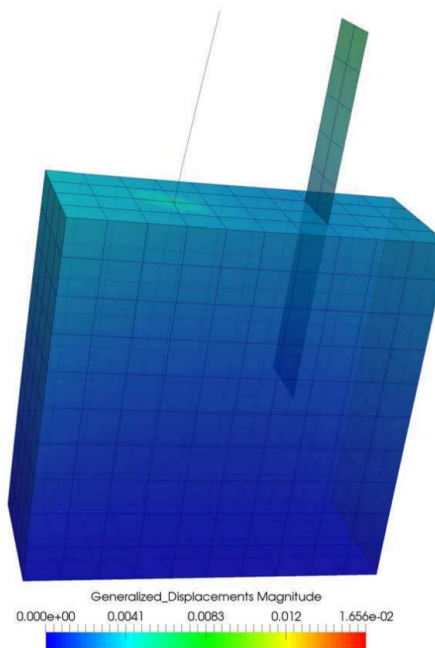


Figure 6.38: Brick-Shell-Beam, Results.

DRM 2D Example

The Real-ESSI input files for this example are available [HERE](#). The compressed package of Real-ESSI input files for this example is available [HERE](#).

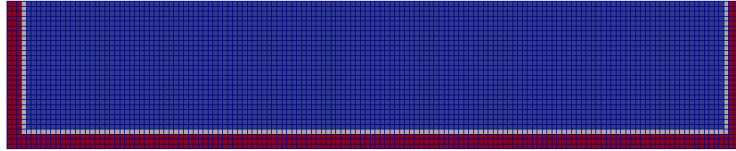


Figure 6.39: Simulation Model DRM 2D.

Results of free field DRM 2D Model under 1C motion are shown in Fig. 6.40.

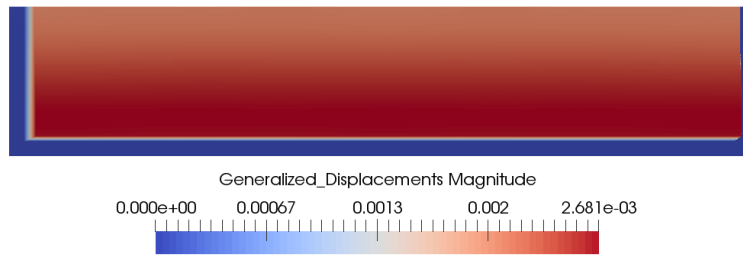


Figure 6.40: Simulation Model DRM 2D.

DRM 3D Example

The Real-ESSI input files for this example are available [HERE](#). The compressed package of Real-ESSI input files for this example is available [HERE](#).

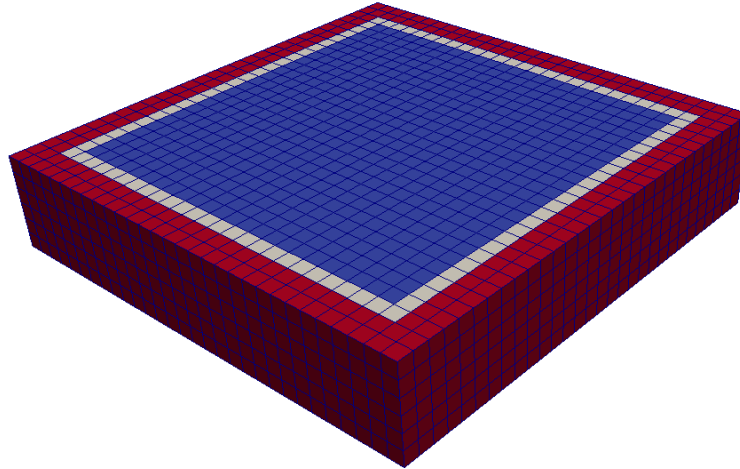


Figure 6.41: Simulation Model DRM 3D.

Results of free field DRM 3D Model under 1C motion are shown in Fig. 6.42.

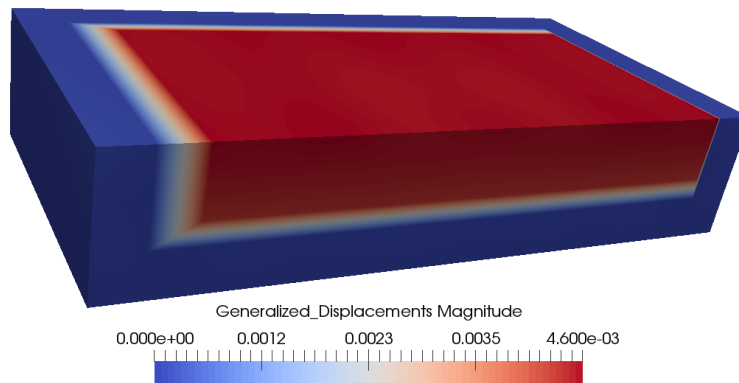


Figure 6.42: Simulation Model DRM 2D.

6.2.7 Post-processing examples with ParaView

Slice Visualization

The Real-ESSI input files for this example are available [HERE](#). The compressed package of Real-ESSI input files for this example is available [HERE](#).

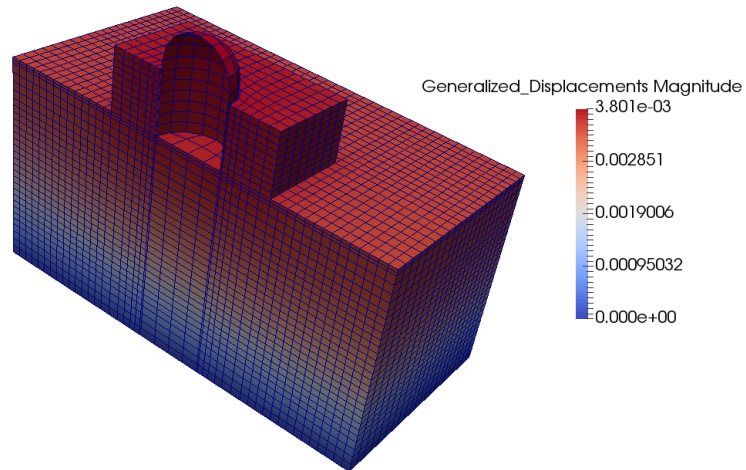


Figure 6.43: Slice Visualization with ParaView.

Stress Visualization

The Real-ESSI input files for this example are available [HERE](#). The compressed package of Real-ESSI input files for this example is available [HERE](#).

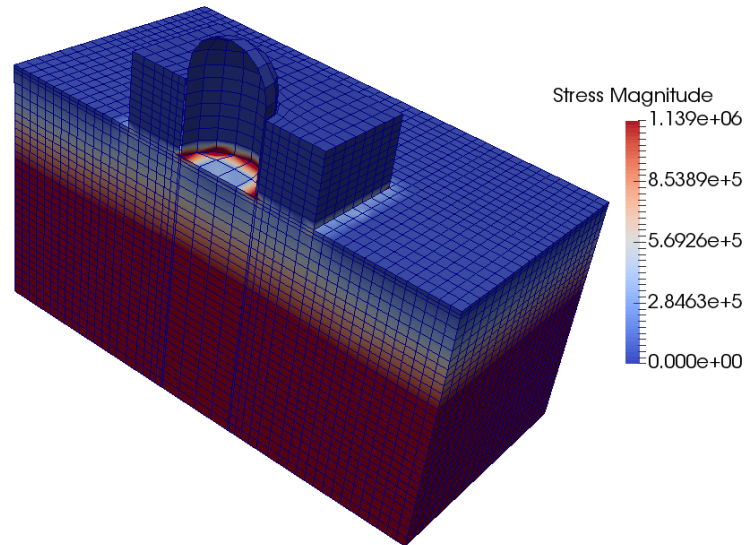


Figure 6.44: Stress Visualization with ParaView.

Pore Pressure Visualization with upU Element

The Real-ESSI input files for this example are available [HERE](#). The compressed package of Real-ESSI input files for this example is available [HERE](#).

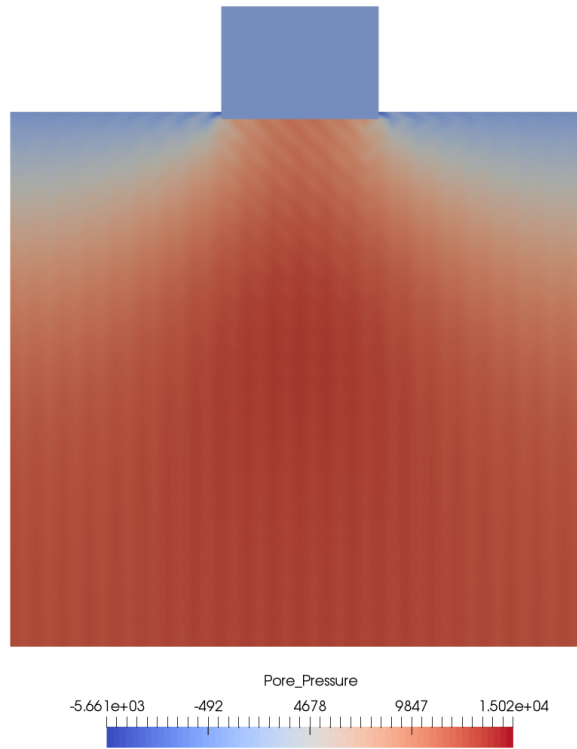


Figure 6.45: Pore Pressure Visualization with Paraview.

Eigen Visualization

The Real-ESSI input files for this example are available [HERE](#). The compressed package of Real-ESSI input files for this example is available [HERE](#).

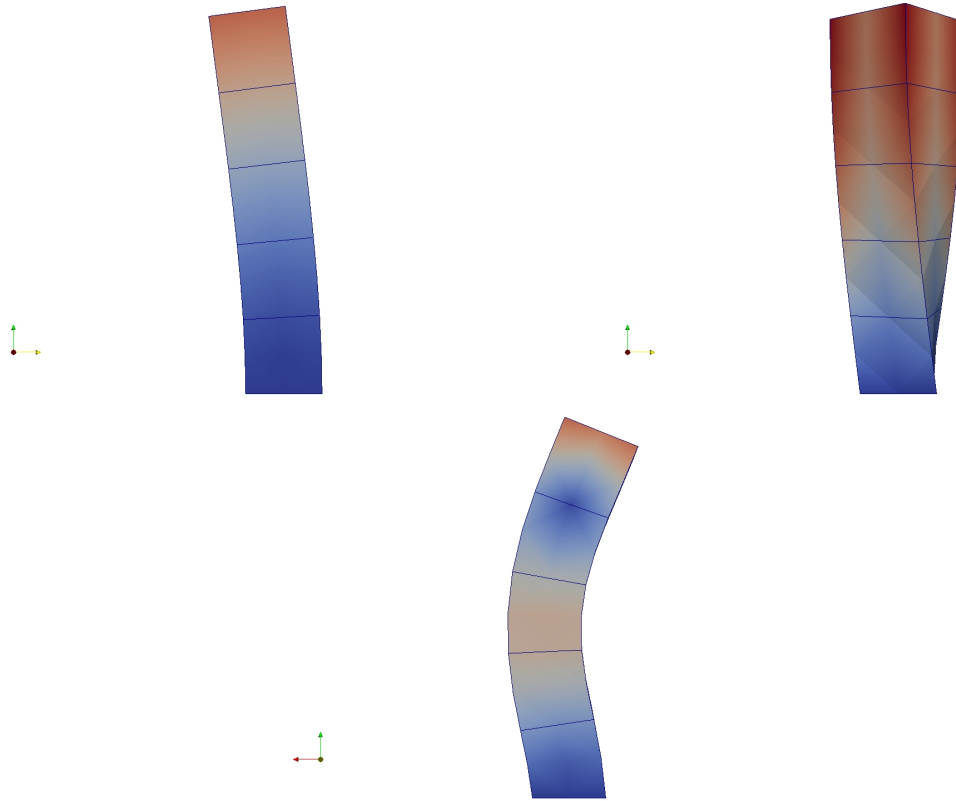


Figure 6.46: Eigen Mode Visualization with Paraview.

6.2.8 Check Model and Visualization of Boundary Conditions

The Real-ESSI input files for this example are available [HERE](#). The compressed package of Real-ESSI input files for this example is available [HERE](#).

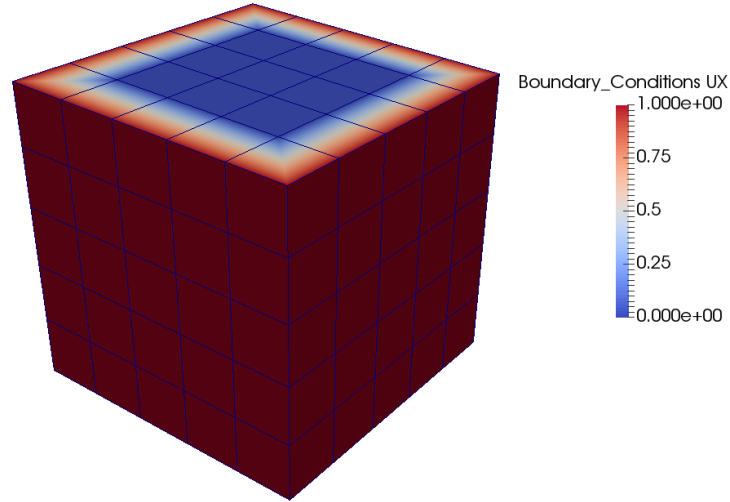


Figure 6.47: Partition Information Visualization with Paraview.

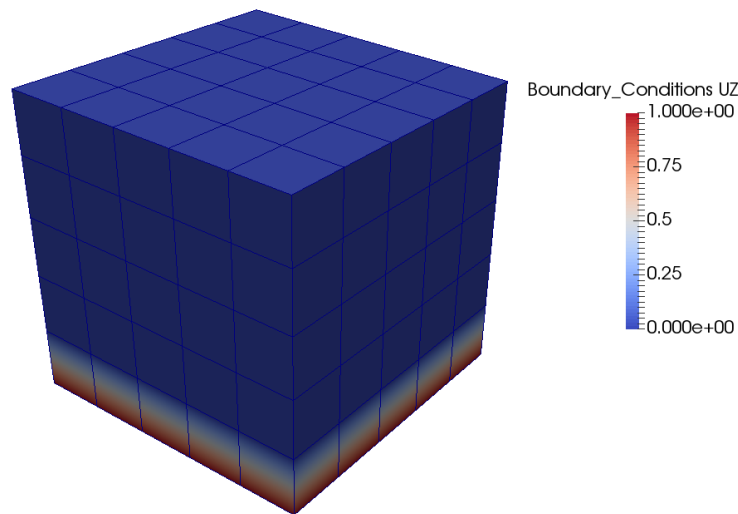


Figure 6.48: Partition Information Visualization with Paraview.

6.2.9 Restart Simulation

Restart in the next stage

The Real-ESSI input files for this example are available [HERE](#). The compressed package of Real-ESSI input files for this example is available [HERE](#).

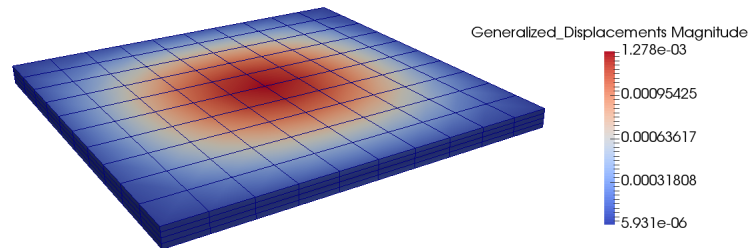


Figure 6.49: Restart Simulation.

This group of examples illustrates the restart functionality between loading stages. There are three test cases in this example. The two loading stages in the first test case is split into two test cases to show the restart feature.

- The first test case run through two loading stages.
- The second test case only run the first loading stage and saves model state at the end.
- The third test case restart the simulation from the saved model state of the second test case. Then, with the restart model state, the test case run the second loading stage only.

Results of the third test case are exactly the same to the first test case.

Restart inside the stage

For the case of lack of convergence, restart with the previous loading stage.

The Real-ESSI input files for this example are available [HERE](#). The compressed package of Real-ESSI input files for this example is available [HERE](#).

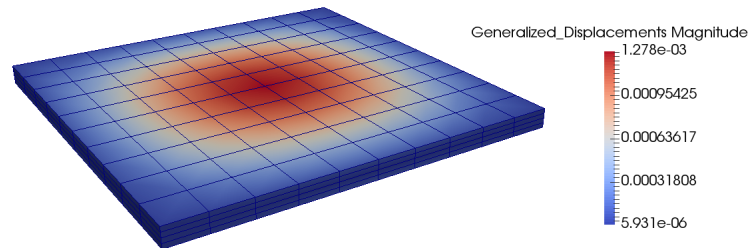


Figure 6.50: Restart Simulation.

This group of examples illustrate the restart functionality inside one loading stage when the simulation cannot converge in the nonlinear analysis. The nonlinear material model, von-Mises Armstrong-Frederick, is used in all test cases.

There are three test cases in this example.

- The first test case run through the whole simulation with a relatively big tolerance of the unbalanced force.
- The second test case failed in the middle of the simulation with a relatively small tolerance of the unbalanced force. When the second test failed, the model reverted to the last commit model state and saved model state.
- The third test case load the saved model state, increased the tolerance of the unbalanced force, and added the remaining load to the model to continue the simulation.

Results of the third test case are exactly the same to the first test case.

Note that in the third test case only the remaining load should be added to the model. Whenever the new loading stage is used, the previous loading are all finished, which means that the static loading becomes constant and the dynamic loading vanishes.

6.3 Day 2: Seismic Motions

6.3.1 Deconvolution and Propagation of 1C Motions, 1D Model

Various deconvolution and propagation 1D models for one component (1C) wave propagation are provided through links below.

Note: Please make sure that the input acceleration record is baseline corrected and the displacement record has no permanent deformation. Otherwise, the unrealistic high frequency components can be brought into the simulation results.

- Deconvolution of Ormsby wavelet, input files are available [HERE](#).
- Deconvolution of Northridge earthquake, input files are available [HERE](#).
- Deconvolution of and DRM propagation of Ormsby wavelet, input files are available [HERE](#).
- Deconvolution of and DRM propagation of Northridge earthquake, input files are available [HERE](#).

6.3.2 Convolution and Propagation of 1C Motions, 1D Model

Various convolution and propagation 1D models for one component (1C) wave propagation are provided through links below:

Note: Please make sure that the input acceleration record is baseline corrected and the displacement record has no permanent deformation. Otherwise, the unrealistic high frequency components can be brought into the simulation results.

- Convolution of Ormsby wavelet, input files are available [HERE](#).
- Convolution of Northridge earthquake, input files are available [HERE](#).
- Convolution of and DRM propagation of Ormsby wavelet, input files are available [HERE](#).
- Convolution of and DRM propagation of Northridge earthquake, input files are available [HERE](#).

6.3.3 Convolution, Deconvolution and Propagation of 1C Motions, 2D Model

Various convolution, deconvolution and propagation 2D models for one component (1C) wave propagation are provided through links below.

Note #1: Please make sure that the input acceleration record is baseline corrected and the displacement record has no permanent deformation. Otherwise, the unrealistic high frequency components can be brought into the simulation results.

Note #2: Please make sure that you develop seismic motions by doing deconvolution and then convolution before analyzing the actual model. File `run.sh` in examples directory has a proper sequence of commands, that is one should first run Real-ESSI on `Deconvolution_DRM_motion.fei` and then, when motions are developed, analyze model.

Examples are available through links below:

- Convolution/Deconvolution of and DRM propagation of Ormsby wavelet, input files are available [HERE](#).
- Convolution/Deconvolution of and DRM propagation of Kobe earthquake records, input files are available [HERE](#).

ESSI 3D building model, deconvolution 1C model, shell model with DRM

The Real-ESSI input files for this example are available [HERE](#). The compressed package of Real-ESSI input files for this example is available [HERE](#).

The Modeling parameters are listed below:

- Elastic Soil Material Properties
 - Mass density, ρ , 2000 kg/m^3
 - Shear Wave Velocity, V_s , 500 m/s
 - Young's modulus, E , 1.1 GPa
 - Poisson's ratio, ν , 0.1

- Elastic Structure Material Properties
 - Mass density, ρ , 2500 kg/m^3
 - Young's modulus, E , 20 GPa
 - Poisson's ratio, ν , 0.1

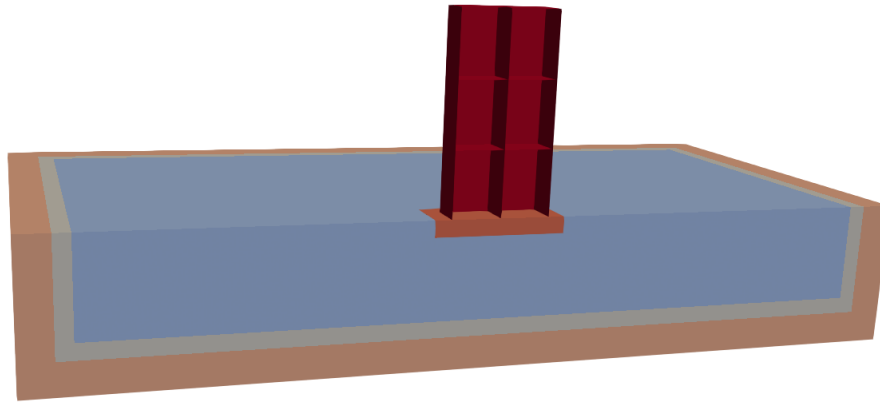


Figure 6.51: Simulation Model.

Results of DRM 3D shell Structure Model under 1C motion are shown in Fig. 6.52.

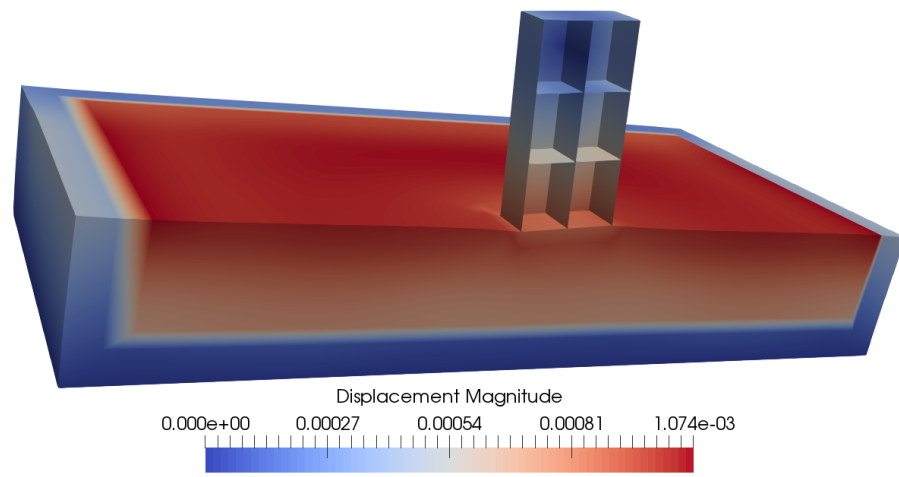


Figure 6.52: Simulation Model.

6.3.4 Deconvolution 3×1C Motions

Free field 1C model, deconvolution 3×1C motion, model with DRM

The Real-ESSI input files for this example are available [HERE](#). The compressed package of Real-ESSI input files for this example is available [HERE](#).

The Modeling parameters are listed below:

- Elastic Material Properties
 - Mass density, ρ , 2000 kg/m^3
 - Shear Wave Velocity, V_s , 500 m/s
 - Young's modulus, E , 1.1 GPa
 - Poisson's ratio, ν , 0.1



Figure 6.53: Simulation Model.

Results of the simulation are shown in Fig. 6.1.

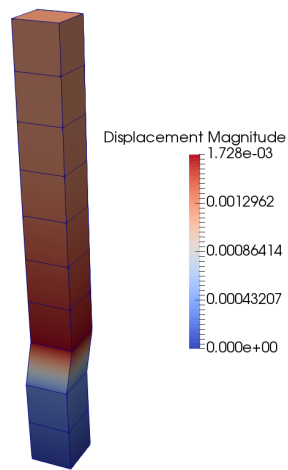


Figure 6.54: Simulation Model.

Free field 3D model, deconvolution $3 \times 1C$ motion, model with DRM

The Real-ESSI input files for this example are available [HERE](#). The compressed package of Real-ESSI input files for this example is available [HERE](#).

The Modeling parameters are listed below:

- Elastic Soil Material Properties
 - Mass density, ρ , 2000 kg/m^3
 - Shear Wave Velocity, V_s , 500 m/s
 - Young's modulus, E , 1.1 GPa
 - Poisson's ratio, ν , 0.1

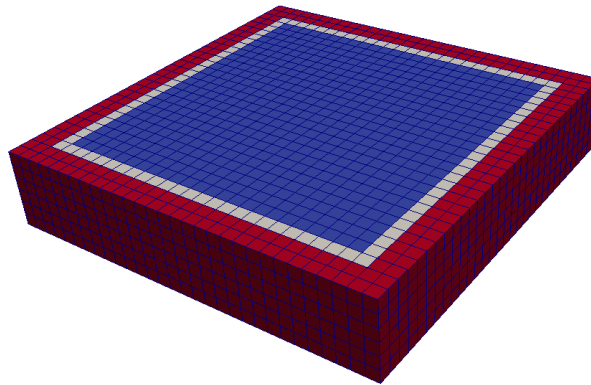


Figure 6.55: Simulation Model.

Results of the simulation are shown in Fig. 6.56.

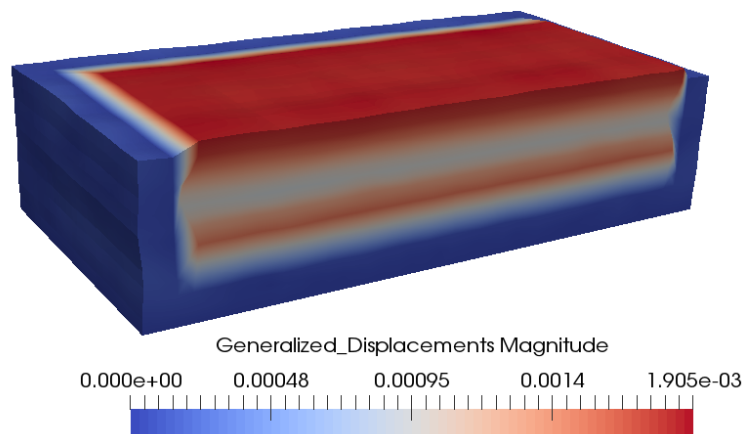


Figure 6.56: Simulation Model.

ESSI 3D building model, deconvolution $3 \times 1C$ motion, shell model with DRM

The Real-ESSI input files for this example are available [HERE](#). The compressed package of Real-ESSI input files for this example is available [HERE](#).

The Modeling parameters are listed below:

- Elastic Soil Material Properties
 - Mass density, ρ , 2000 kg/m^3
 - Shear Wave Velocity, V_s , 500 m/s
 - Young's modulus, E , 1.1 GPa
 - Poisson's ratio, ν , 0.1

- Elastic Structure Material Properties
 - Mass density, ρ , 2500 kg/m^3
 - Young's modulus, E , 20 GPa
 - Poisson's ratio, ν , 0.1

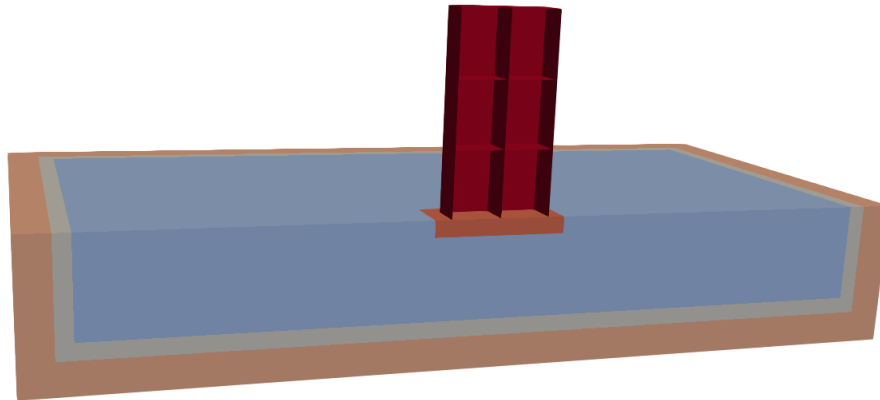


Figure 6.57: Simulation Model.

Results of DRM 3D shell Structure Model under 1C motion are shown in Fig. 6.58.

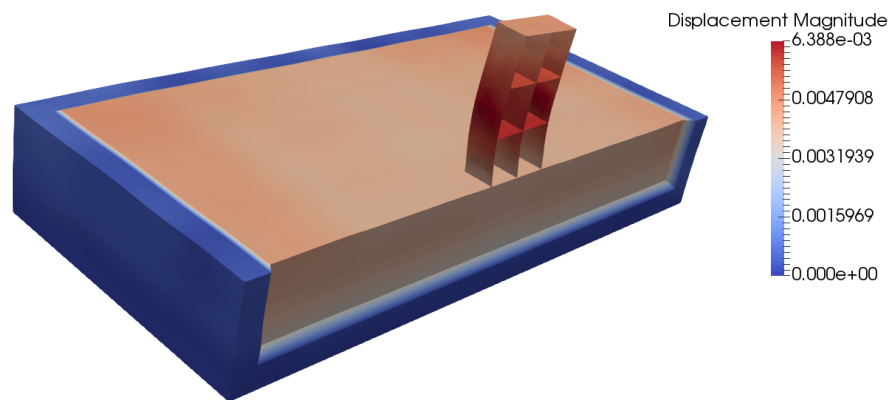


Figure 6.58: Simulation Model.

6.3.5 Mesh Dependence of Wave Propagation Frequencies

The Real-ESSI input files for this example are available [HERE](#). The compressed package of Real-ESSI input files for this example is available [HERE](#).

Show the mesh dependence of high frequency wave with Ormsby wavelet.



Figure 6.59: Simulation Model.

Results of mesh dependence are shown in Fig. 6.60.

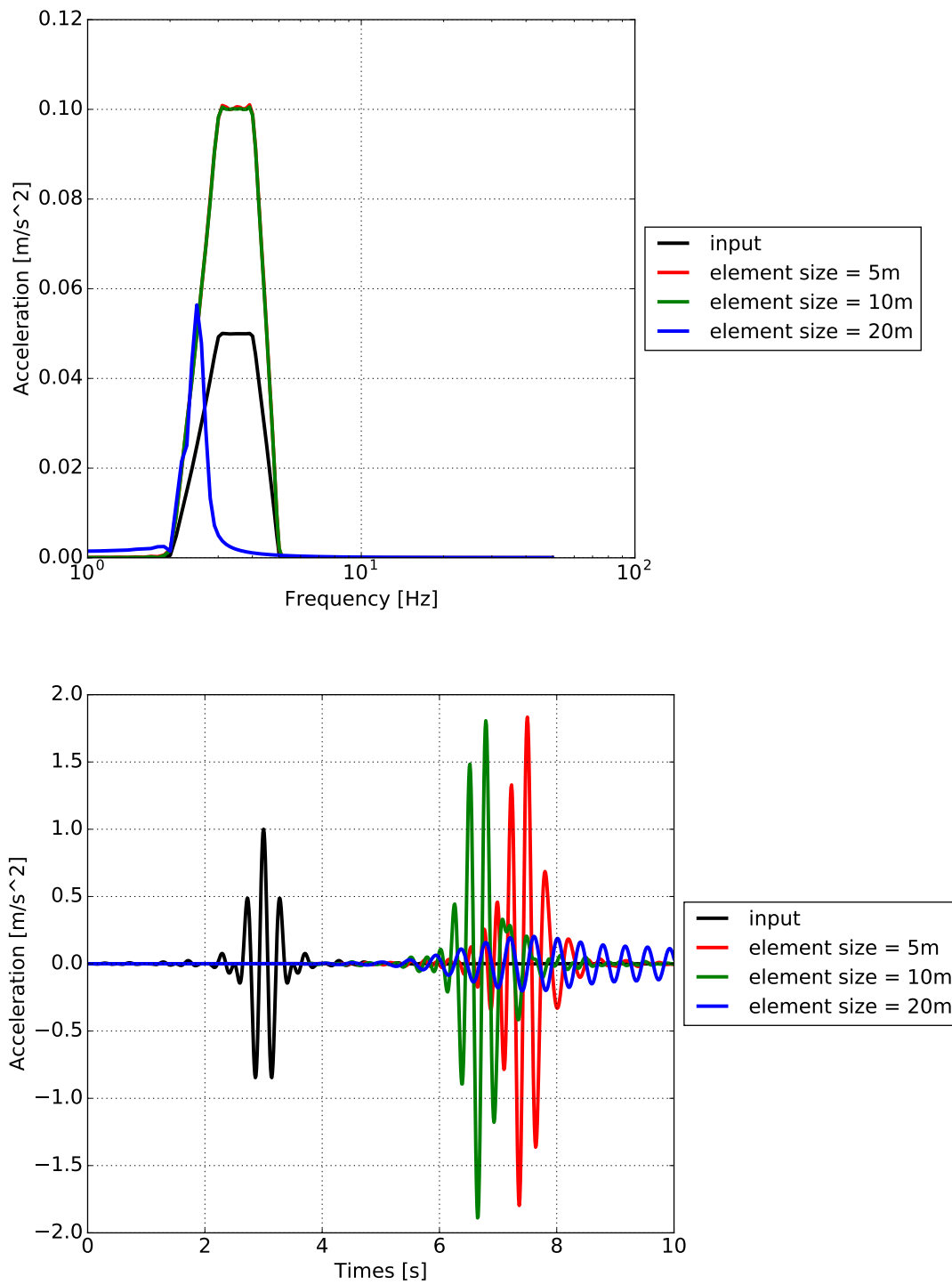


Figure 6.60: Convolution Results and Mesh Dependence.

6.3.6 Application of 3C Motions from SW4

3C Seismic Motion from SW4

A 3C seismic motion field has been developed by using SW4. The characteristic parameters of the seismic motion are given below:

- Geological model: length $3km$, width $3km$, height $1.7km$, grid size $50m$, width of super grid damping layer $30m$.
- Material model: Elastic material, First $1km$: $V_p = 4630.76m/s$, $V_s = 2437.56m/s$, $\rho = 2600kg/m^3$.
 $1km \sim 1.7km$: $V_p = 6000m/s$, $V_s = 3464m/s$, $\rho = 2700kg/m^3$
- Source type: point moment source, moment seismic moment $M_{xy} = 5e^{15}N \cdot m$, moment magnitude 4.5.
- Time function: Gaussian function, with dominant frequency $2.5Hz$ and maximum frequency $6.5Hz$.

The time series displacement and acceleration response at the center of the model is shown below in figure 6.61. And figure 6.62 gives corresponding FFT response.

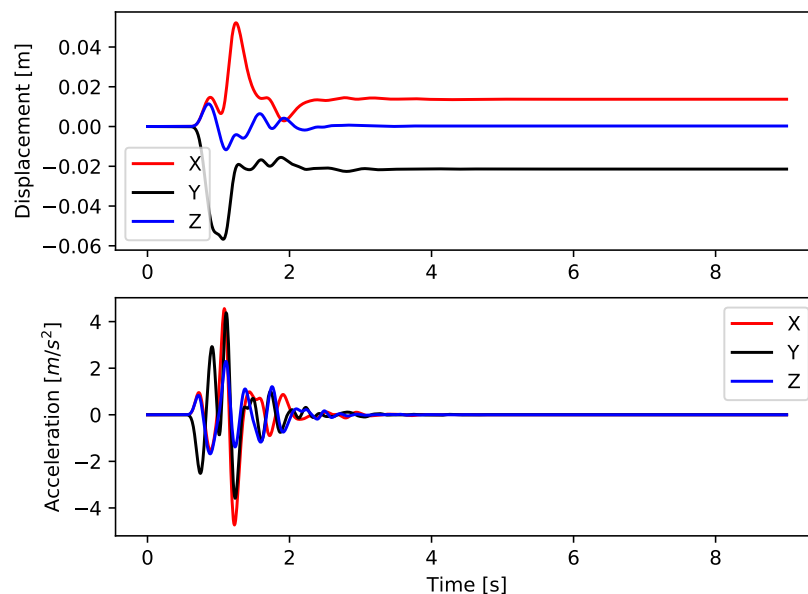


Figure 6.61: Time series response of 3C motion.

During the simulation of SW4, the time series motions at many ESSI nodes (basically are some pre-defined record stations) of an ESSI box ($300m \times 300m \times 100m$) are recorded and written into **SAC** files. Then an

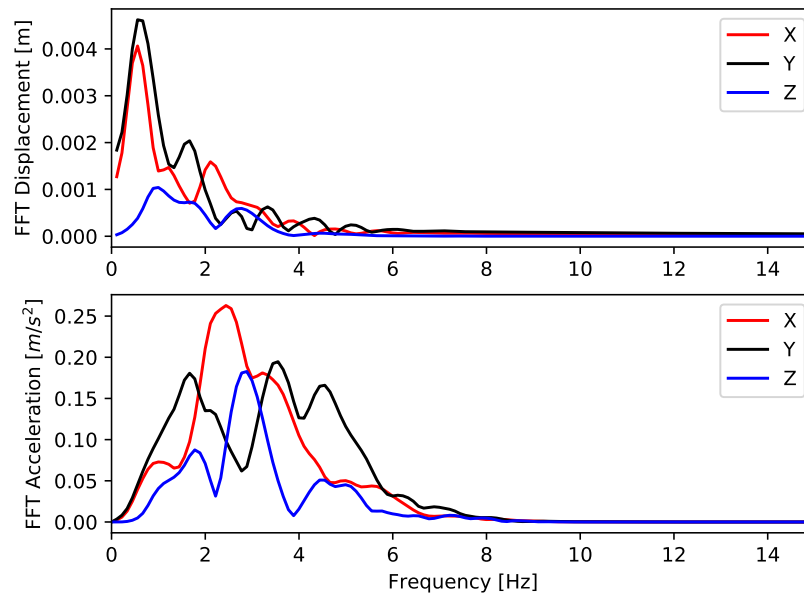


Figure 6.62: FFT response of 3C motion.

transition program SW42ESSI has been developed to interpolate these motions to DRM nodes of localized ESSI model by specifying some geometric translational and rotational transformation, as shown in figure ??.

To launch SW42ESSI, following parameters are needed:

- DRM input: specify the name of DRM input files. This DRM file just contains the geometric information of DRM layer in ESSI model (e.g. DRM node IDs, nodal coordinates, etc).
- SW4 motion directory: specify the output directory of SW4, that contains SAC files.
- origin coordinates of ESSI box (x , y , z): the SW4 coordinates of the origin of ESSI box, i.e. the coordinates of ESSI nodes, whose station ID is (0, 0, 0).
- dimensions of ESSI Box (length, width, height): specify the dimension (length, width and height) of ESSI box.
- spacing of ESSI nodes: specify the grid spacing of ESSI nodes (i.e. motion recording stations)
- interval of time steps for sampling: specify the sampling frequency, if 1 is used here, ESSI simulation time step is the same as the simulation time step of SW4.
- reference point in ESSI model for translational transformation (x , y , z): specify the coordinate of reference point for translational transformation in ESSI model.

- reference point in SW4 model for translational transformation (x, y, z): specify the coordinate of reference point for translational transformation in SW4 model.
- conduct rotational transformation (yes/no): input yes and provide more rotational transformation parameters to enable rotational transformation. If input no, no more parameters are required.
- reference point in SW4 model for rotational transformation (x, y, z): specify the coordinate of reference point for rotational transformation in SW4 model.
- degrees of rotation along three axes (x, y, z): specify the degrees of rotation along three axes. The sign of rotation degrees follows right hand rule.

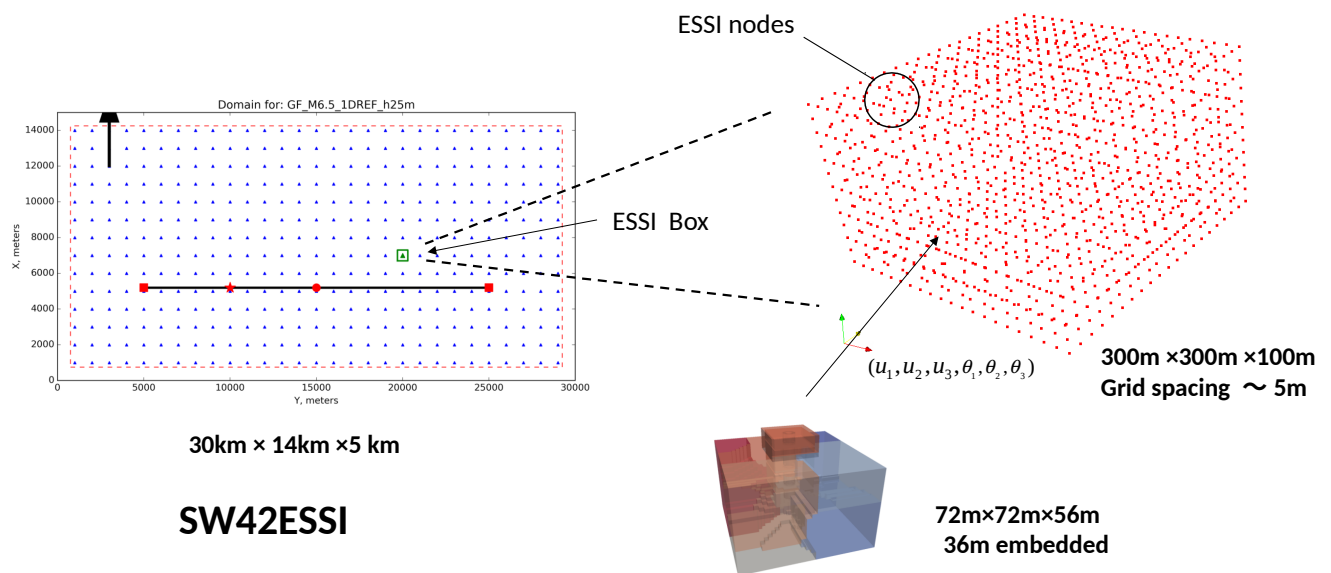


Figure 6.63: Illustration of transition from SW4 to Real-ESSI.

Free field 3D model, 3C motion, model with DRM

The Real-ESSI input files for this example are available [HERE](#). The compressed package of Real-ESSI input files for this example is available [HERE](#).

Results of free field DRM 3D Model under 3C motion are shown in figure 6.65.

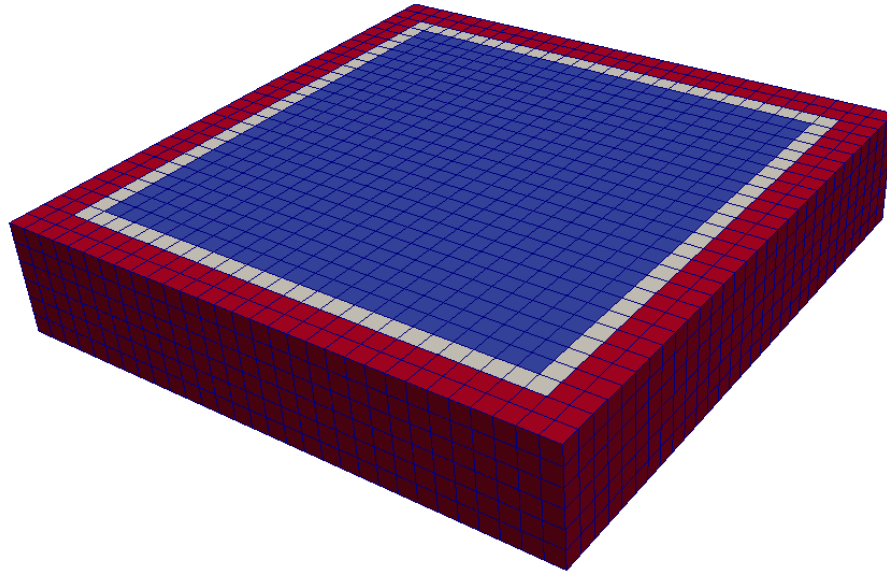


Figure 6.64: Simulation Model.

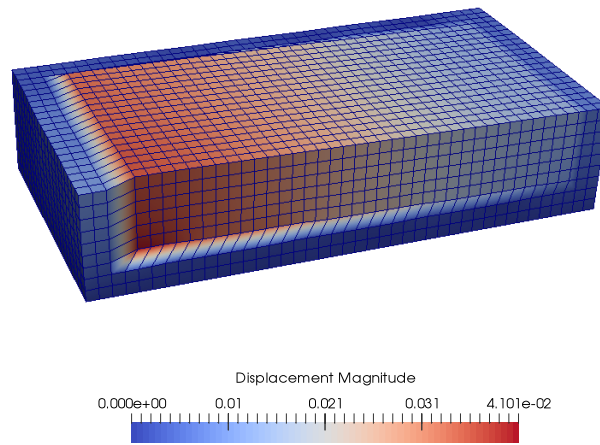


Figure 6.65: Simulation of 3D free field model under 3C seismic motion.

ESSI 3D building model, 3C motion, shell model with DRM

The Real-ESSI input files for this example are available [HERE](#). The compressed package of Real-ESSI input files for this example is available [HERE](#).

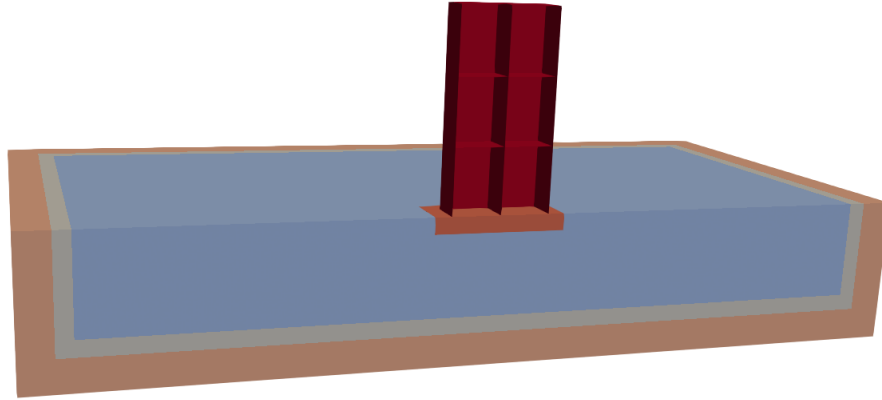


Figure 6.66: Simulation Model.

6.4 Day 3: Inelastic, Nonlinear Analysis

6.4.1 Single Element Models: Illustration of the Elastic-Plastic Behavior

von-Mises Perfectly Plastic Material Model.

The Real-ESSI input files for von-Mises perfectly plastic example are available [HERE](#). The compressed package of Real-ESSI input files for this example is available [HERE](#).

von-Mises Armstrong-Frederick Material Model.

The Real-ESSI input files for von-Mises Armstrong-Frederick example are available [HERE](#). The compressed package of Real-ESSI input files for this example is available [HERE](#).

The Modeling parameters are listed below:

- Left: von-Mises linear hardening material model
 - Mass Density, ρ , 0.0 kg/m^3
 - Young's modulus, E , 20 MPa
 - Poisson's ratio, ν , 0.0
 - von Mises radius, k , 100 kPa
 - kinematic hardening rate, K_{kine} , 2 MPa
 - isotropic hardening rate, K_{iso} , 0 Pa
- Right: Drucker-Prager nonlinear hardening material model
 - Mass Density, ρ , 0.0 kg/m^3
 - Young's modulus, E , 20 MPa
 - Poisson's ratio, ν , 0.0
 - Drucker-Prager, k , 0.179527
 - nonlinear kinematic hardening, H_a , 20 MPa
 - nonlinear kinematic hardening, C_r , 100
 - isotropic hardening rate, K_{iso} , 0 Pa
 - initial confining stress, p_0 , 1 Pa

Results are shown in Fig. 6.68.

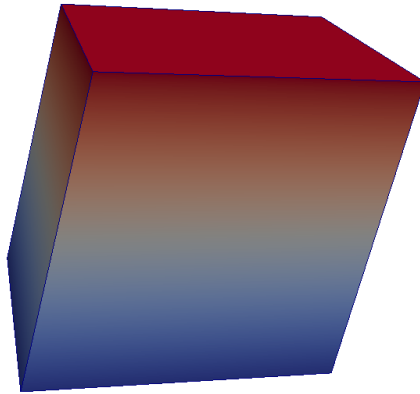


Figure 6.67: Simulation Model of Single Element.

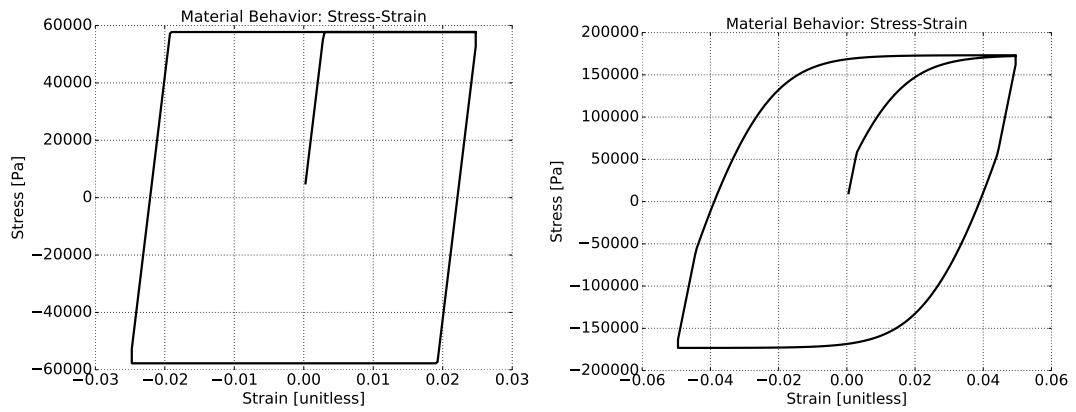


Figure 6.68: Simulation Results of Single Element.

von-Mises G/Gmax Material Model

The Real-ESSI input files for this example are available [HERE](#). The compressed package of Real-ESSI input files for this example is available [HERE](#).

The Modeling parameters are listed below:

- von-Mises G/Gmax material model
 - Mass density, ρ , 2000 kg/m^3
 - Young's modulus, E , 200 MPa
 - Poisson's ratio, ν , 0.1
 - Total number of shear modulus 9
 - G over Gmax, 1,0.995,0.966,0.873,0.787,0.467,0.320,0.109,0.063
 - Shear strain gamma, 0,1E-6,1E-5,5E-5,1E-4, 0.0005, 0.001, 0.005, 0.01

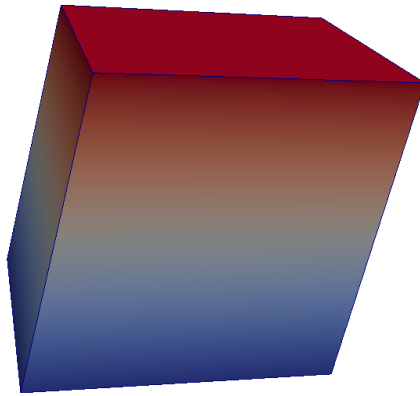
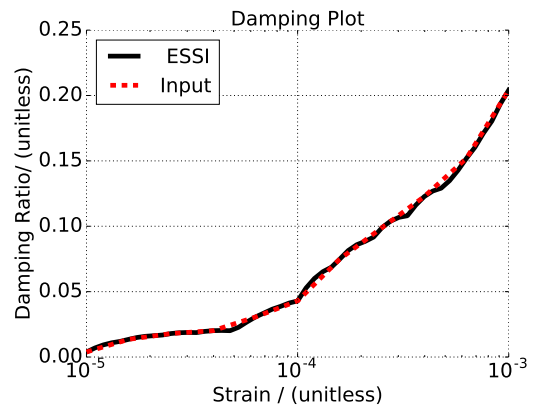
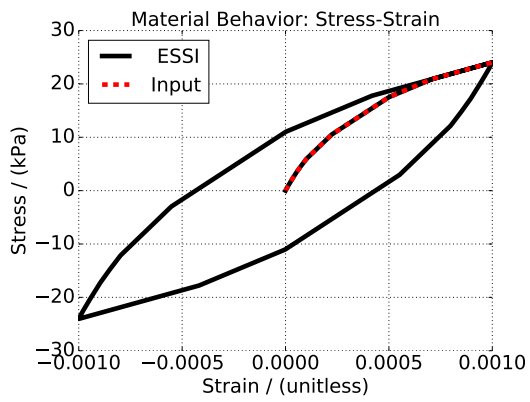
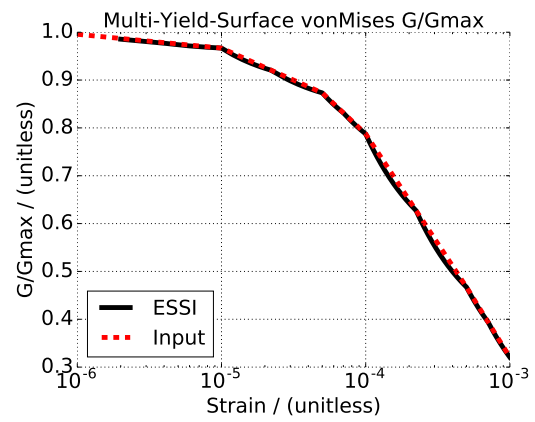
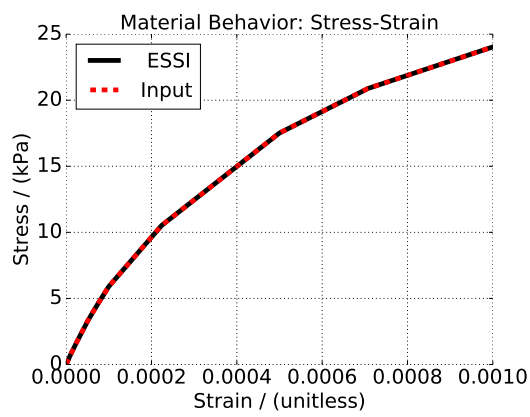


Figure 6.69: Simulation Model of Single Element.



Drucker-Prager Perfectly Plastic Material Model

The Real-ESSI input files for this Drucker-Prager perfectly plastic example are available [HERE](#). The compressed package of Real-ESSI input files for this example is available [HERE](#).

Drucker-Prager Armstrong-Frederick Non-Associated Material Model

The Real-ESSI input files for this Drucker-Prager Armstrong-Frederick example are available [HERE](#). The compressed package of Real-ESSI input files for this example is available [HERE](#).

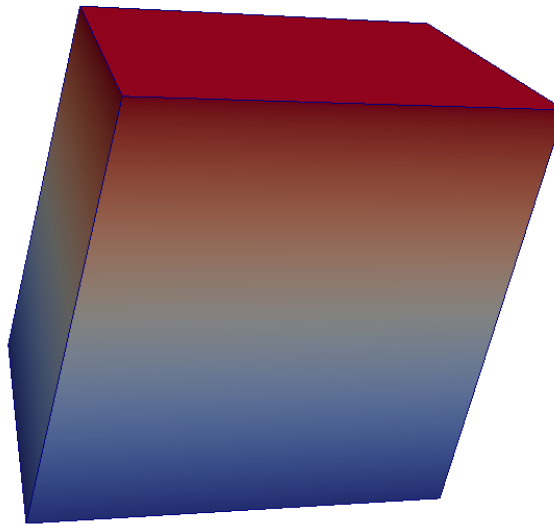


Figure 6.70: Simulation model, single element.

Results are shown in Fig. 6.71.

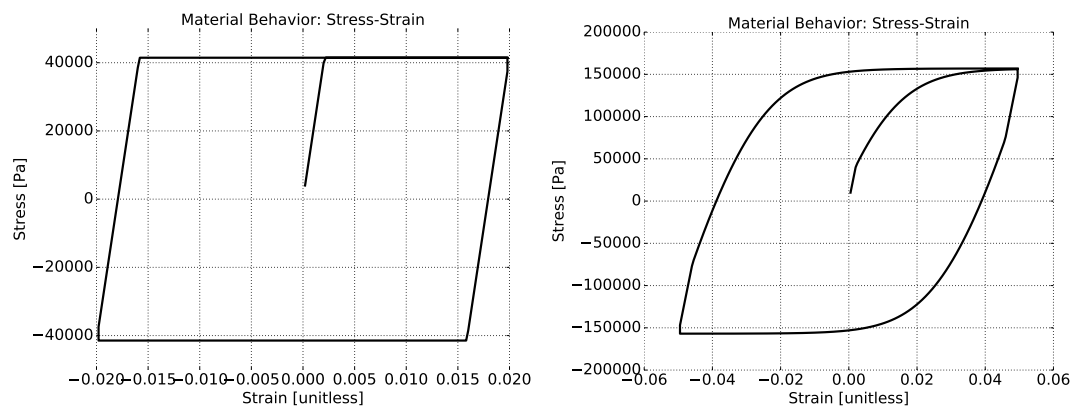


Figure 6.71: Simulation results for single element.

Drucker-Prager G/Gmax Non-Associated Material Model

The Real-ESSI input files for this example are available [HERE](#). The compressed package of Real-ESSI input files for this example is available [HERE](#).

The Modeling parameters are listed below:

- Drucker-Prager G/Gmax material model
 - Mass density, ρ , 2000 kg/m^3
 - Young's modulus, E , 200 MPa
 - Poisson's ratio, ν , 0.1
 - Initial confining stress, p_0 , 100 kPa
 - Reference pressure, p_{refer} , 100 kPa
 - Pressure exponential, n , 0.5
 - Cohesion, n , 1 kPa
 - Total number of Shear Modulus 9
 - G over Gmax, 1,0.995,0.966,0.873,0.787,0.467,0.320,0.109,0.063
 - Shear strain gamma, 0,1E-6,1E-5,5E-5,1E-4, 0.0005, 0.001, 0.005, 0.01

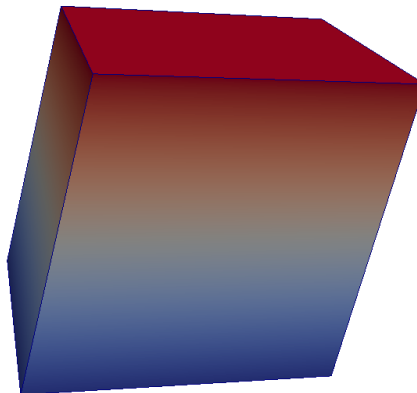


Figure 6.72: Simulation Model of Single Element.

Results are shown in Fig. [6.73](#).

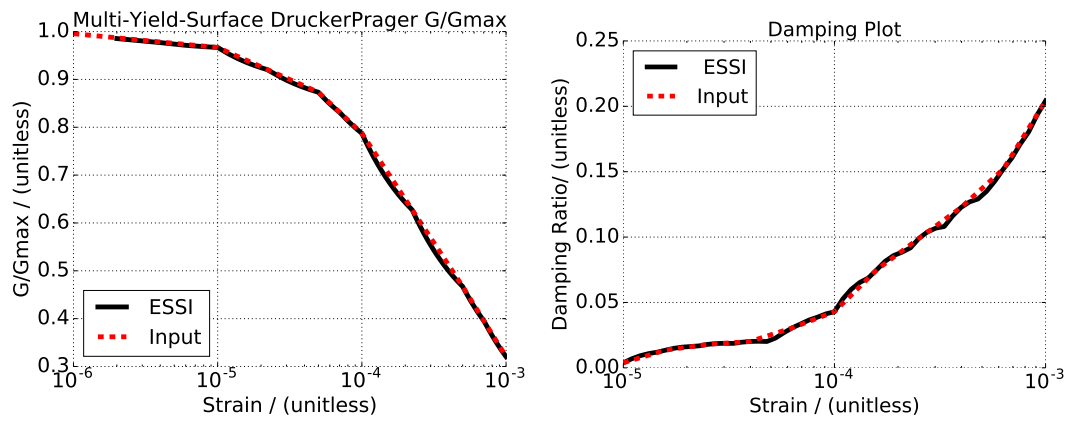


Figure 6.73: Simulation Results of Single Element.

6.4.2 Wave Propagation Through Elasto-plastic Soil

The Real-ESSI input files for this example are available [HERE](#). The compressed package of Real-ESSI input files for this example is available [HERE](#).



Figure 6.74: Wave Propagation through elastoplastic Soils.

The displacement series at the surface are plotted in time and frequency domain.

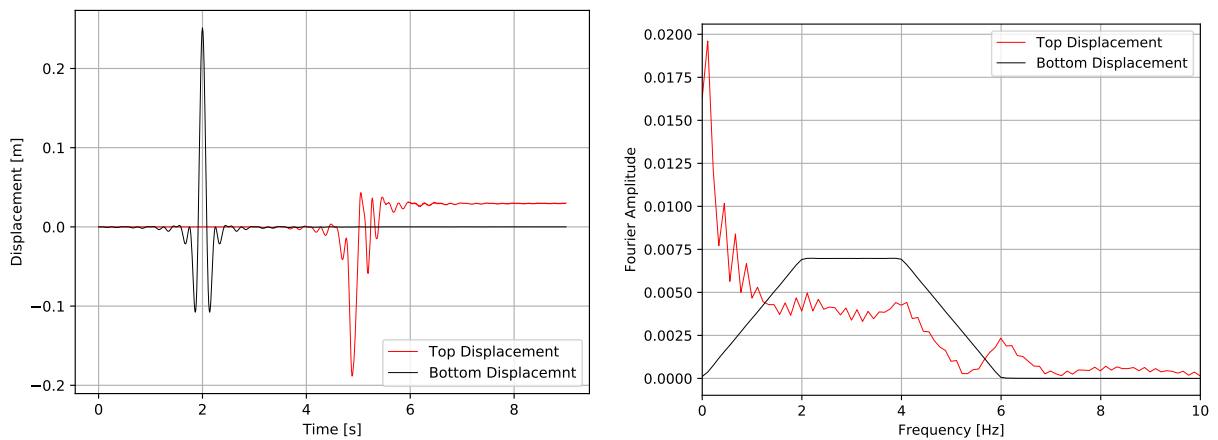


Figure 6.75: Simulation Results of Wave Propagation.

6.4.3 Contact/Interface/Joint Examples

Axial Behavior: Stress-Based Hard Contact/Interface/Joint Example

The Real-ESSI input files for hard contact/interface example are available [HERE](#). The compressed package of Real-ESSI input files for this example is available [HERE](#).

Axial Behavior: Stress-Based Soft Contact/Interface/Joint Example

The Real-ESSI input files for soft contact/interface example are available [HERE](#). The compressed package of Real-ESSI input files for this example is available [HERE](#).

The axial behavior of hard contact/interface and soft contact/interface is illustrated in Fig. 6.76.

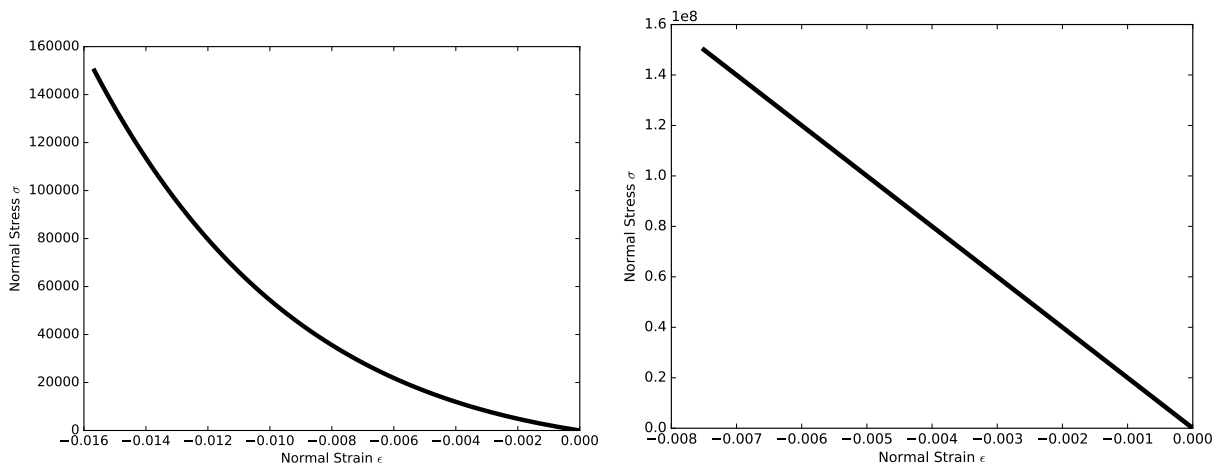


Figure 6.76: Simulation results for axial behavior of (left) soft contact/interface and (right) hard contact.

Shear behavior: Stress-Based Elastic Perfectly Plastic Contact/Interface/Joint

The Real-ESSI input files for the the elastic-perfectly plastic example are available [HERE](#). The compressed package of Real-ESSI input files for this example is available [HERE](#).

Shear behavior: Stress-Based Elastic-Hardening Contact/Interface/Joint

The Real-ESSI input files for the elastic-hardening contact/interface example are available [HERE](#). The compressed package of Real-ESSI input files for this example is available [HERE](#).

Shear behavior: Stress-Based Elastic-Hardening-Softening Contact/Interface/Joint

The Real-ESSI input files for the elastic-hardening-softening example are available [HERE](#). The compressed package of Real-ESSI input files for this example is available [HERE](#).

The shear behavior of elastic-perfectly plastic, elastic-hardening plastic, elastic and hardening and softening plastic is illustrated in Fig. [6.77](#).

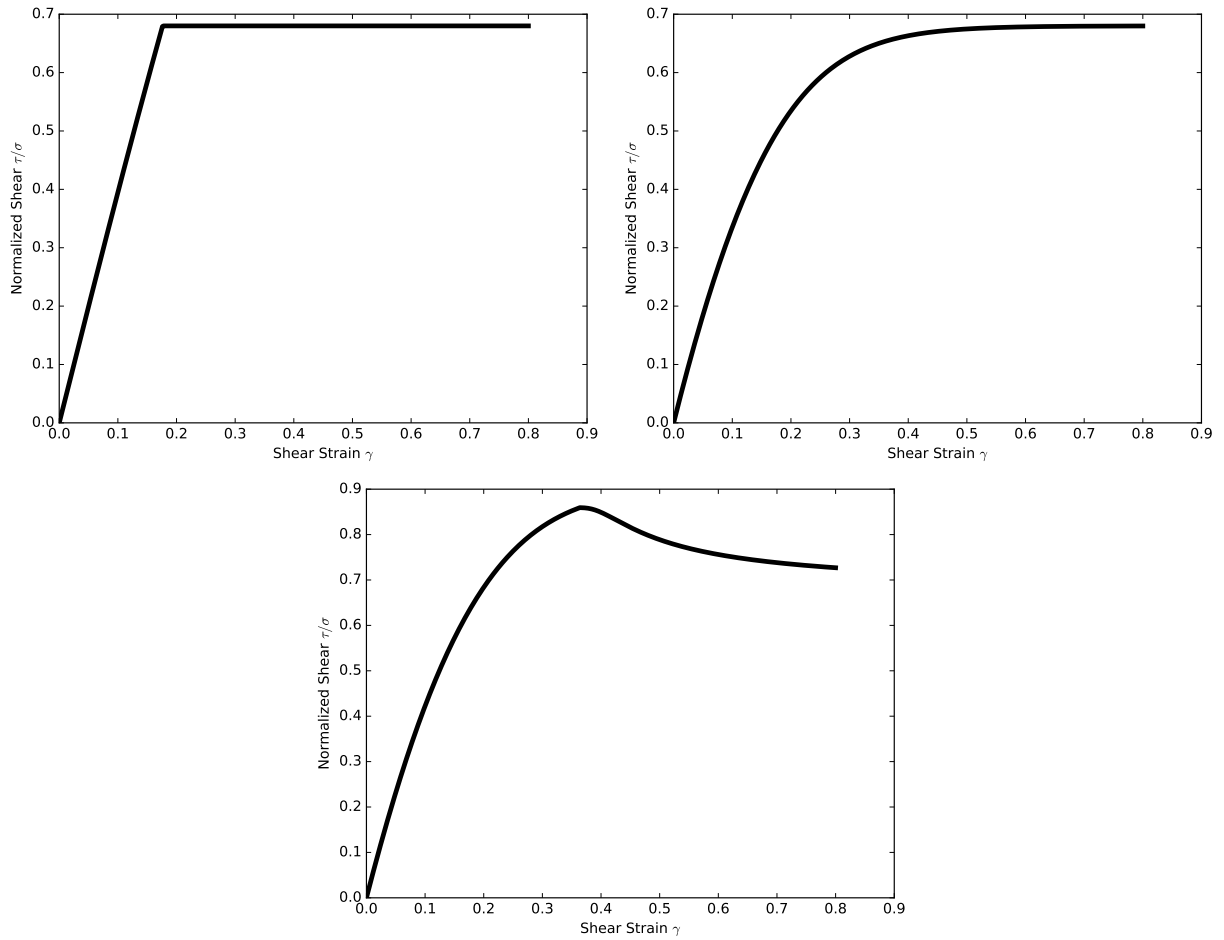


Figure 6.77: Simulation results for shear behavior for stress based contact elements: elastic-perfectly plastic, elastic-hardening plastic, elastic, hardening and softening plastic.

Force Based Contact/Interface/Joint Example: Base Isolator

The Real-ESSI input files for this example are available [HERE](#). The compressed package of Real-ESSI input files for this example is available [HERE](#).

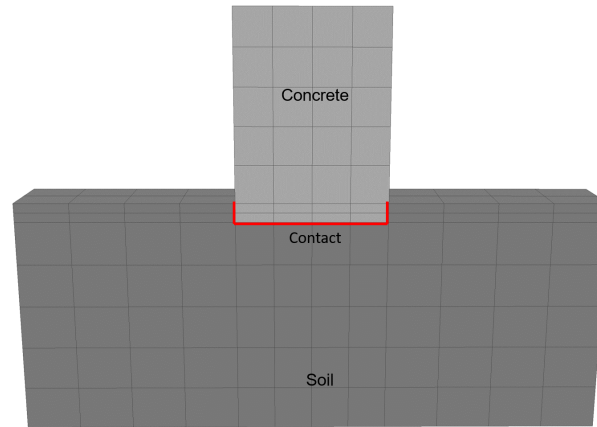


Figure 6.78: Simulation Model.

Results are show in Fig.6.79.

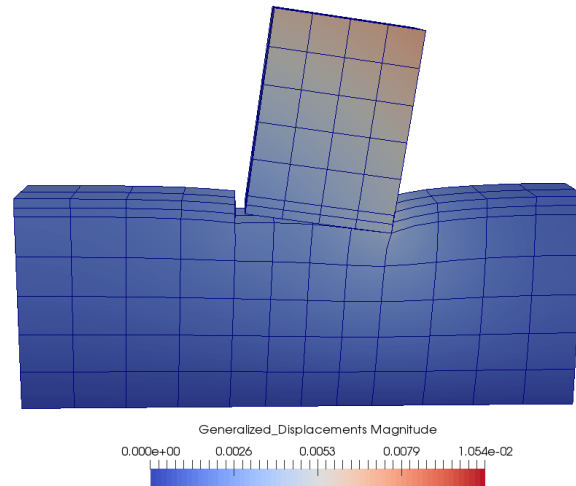


Figure 6.79: Simulation Results for Contact/Interface/Joint Examples.

6.4.4 Inelastic Frame Pushover

The Real-ESSI input files for this example are available [HERE](#). The compressed package of Real-ESSI input files for this example is available [HERE](#).

The Modeling parameters are listed below:

- Uniaxial concrete
 - Compressive strength, 24 MPa
 - Strain at compressive strength, 0.001752
 - Crushing strength, 0.0 Pa
 - Strain at compressive strength, 0.003168
 - lambda, 0.5
 - Tensile strength, 0 Pa
 - Tension softening stiffness, 0 Pa

- Uniaxial steel
 - Yield strength, 413.8 MPa
 - Young's modulus, 200 GPa
 - Strain hardening ratio, 0.01
 - R0, 18.0
 - cR1, 0.925
 - cR2, 0.15
 - a1, 0.0
 - a2, 55.0
 - a3, 0.0
 - a4, 55.0

Result is shown in Fig. [6.81](#).

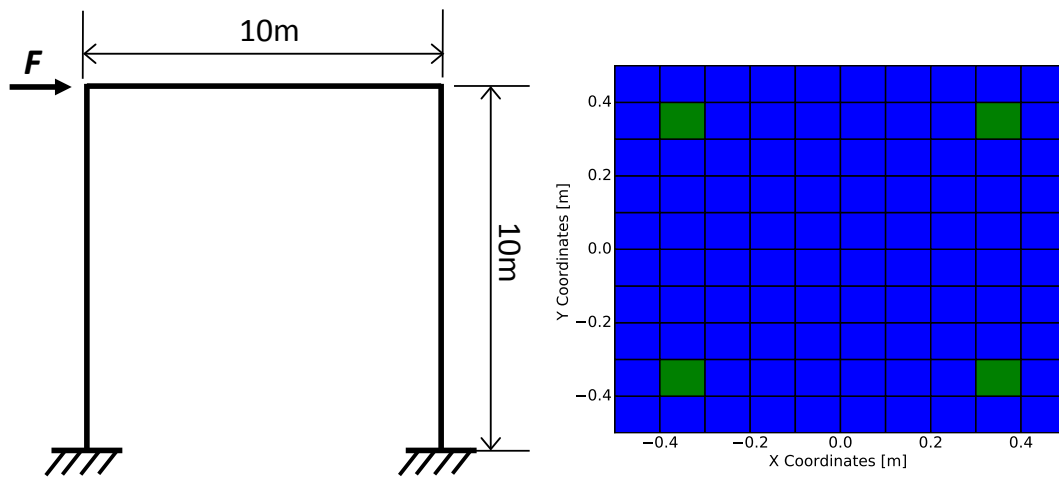


Figure 6.80: Model for pushover simulation and the cross section of fiber beam (concrete and reinforcement).

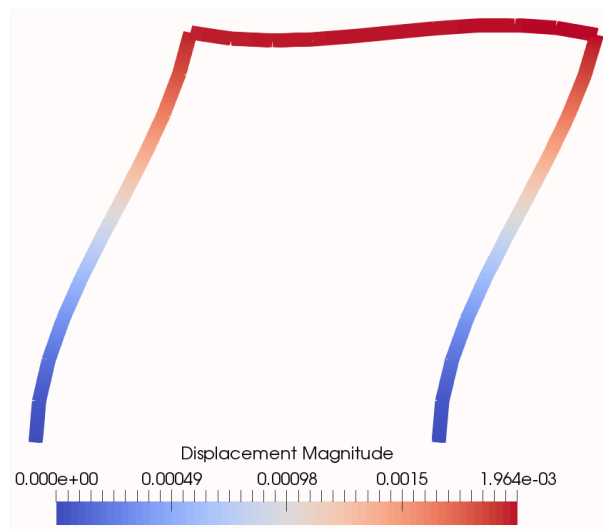


Figure 6.81: Results for fiber pushover.

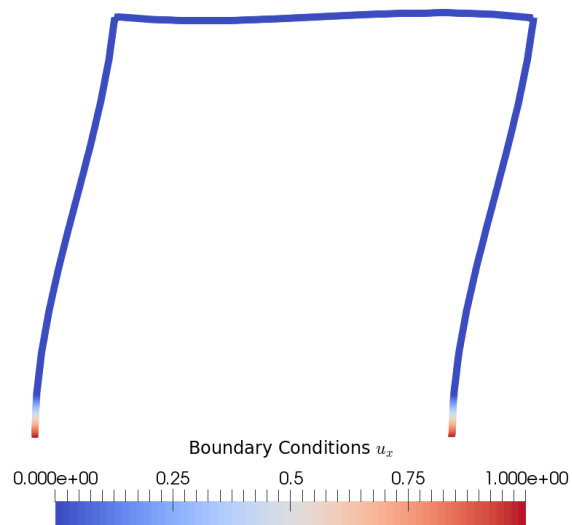


Figure 6.82: Boundary condition u_x for a fiber beam pushover.

6.4.5 Inelastic Wall Pushover

The Real-ESSI input files for this example are available [HERE](#). The compressed package of Real-ESSI input files for this example is available [HERE](#).

The Modeling parameters are listed below:

- Concrete Wall
 - Young's modulus, 36.9 GPa
 - Poisson's ratio, 0.2
 - Tensile yield strength, 5 MPa
 - Compressive yield strength, 56 MPa
 - Plastic deformation rate, 0.4
 - Damage parameter A_p , 0.1
 - Damage parameter A_n , 1.5
 - Damage parameter B_n , 0.75

- Uniaxial steel
 - Yield strength, 457.5 MPa
 - Young's modulus, 200 GPa
 - Strain hardening ratio, 0.011042
 - a_1 , 0.0
 - a_2 , 55.0
 - a_3 , 0.0
 - a_4 , 55.0

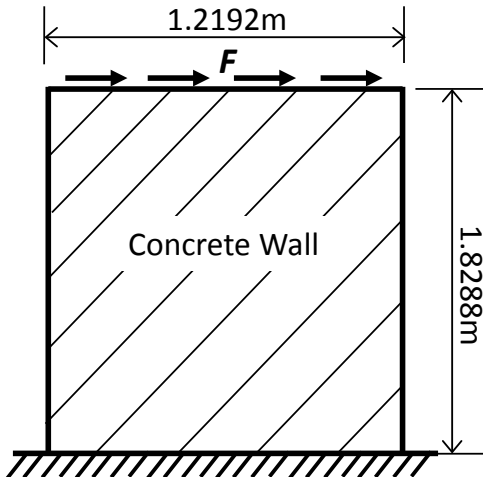


Figure 6.83: Model for wall element pushover.

6.4.6 Viscous Nonlinear behavior

The Real-ESSI input files for this example are available [HERE](#). The compressed package of Real-ESSI input files for this example is available [HERE](#).



Figure 6.84: Simulation Model.

Results are shown in Fig. 6.85 and Fig. 6.86.

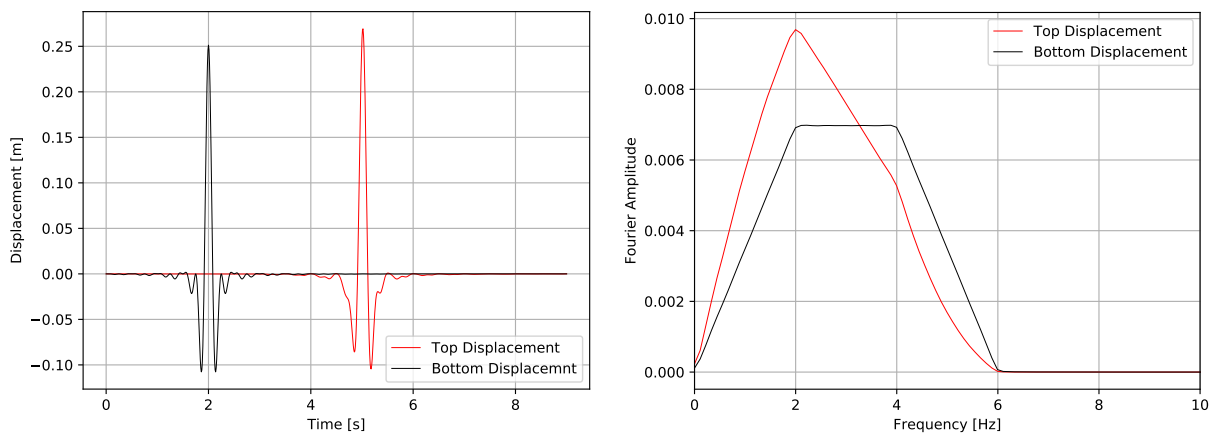


Figure 6.85: Results for low viscous damping.

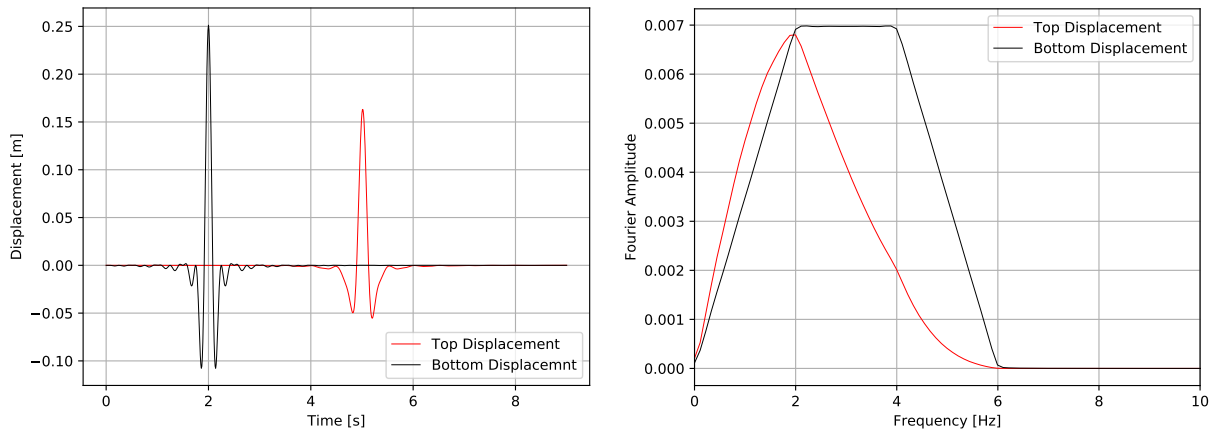


Figure 6.86: Results for high viscous.

6.4.7 Numerical Damping Example

The Real-ESSI input files for this example are available [HERE](#). The compressed package of Real-ESSI input files for this example is available [HERE](#).



Figure 6.87: Simulation Model.

Results are shown in Fig. 6.85 and Fig. 6.89 .

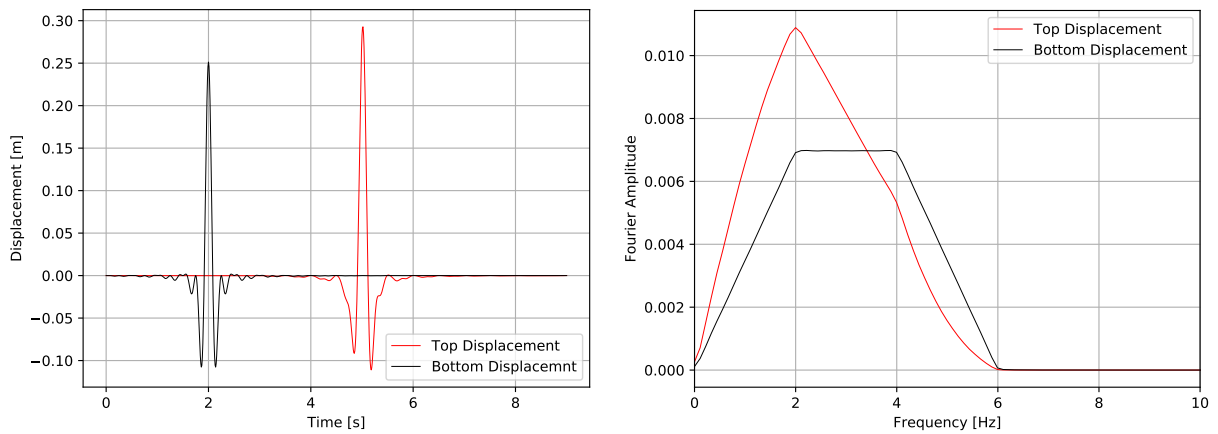


Figure 6.88: Results of low numerical damping.

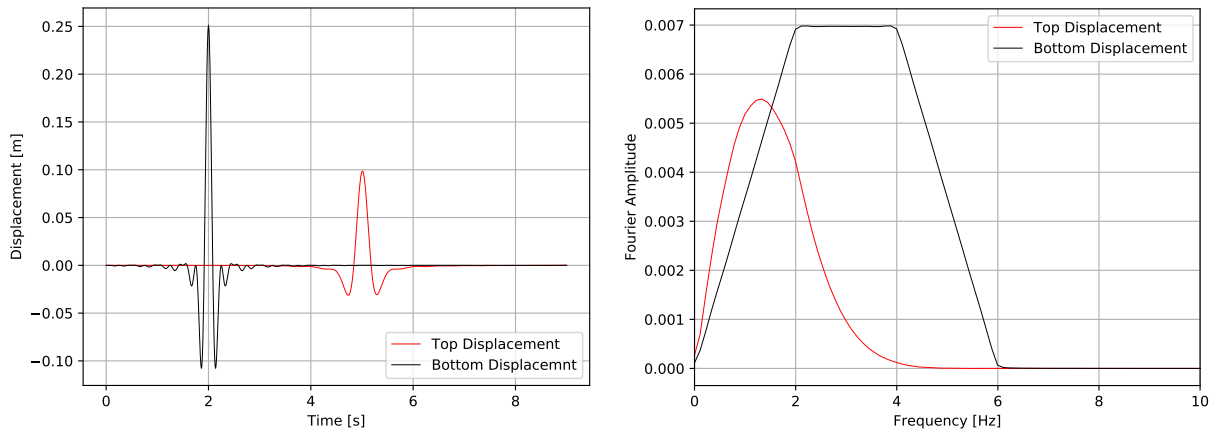


Figure 6.89: Results of high numerical damping.

6.4.8 Nuclear Power Plant Example with Nonlinearities

The Real-ESSI input files for this example are available [HERE](#). The compressed package of Real-ESSI input files for this example is available [HERE](#).

The Modeling parameters are listed below:

- Soil
 - Unit weight, γ , 21.4 kPa
 - Shear velocity, V_s , 500 m/s
 - Young's modulus, E , 1.3 GPa
 - Poisson's ratio, ν , 0.25
 - Shear strength, S_u , 650 kPa
 - von Mises radius, k , 60 kPa
 - kinematic hardening, H_a , 30 MPa
 - kinematic hardening, C_r , 25

- Structure
 - Unit weight, γ , 24 kPa
 - Young's modulus, E , 20 GPa
 - Poisson's ratio, ν , 0.21

- Contact/Interface/Joint
 - Initial axial stiffness, k_n^{init} , 1e9 N/m
 - Stiffening rate, S_r , 1000 /m
 - Maximum axial stiffness, k_n^{max} , 1e12 N/m
 - Shear stiffness, k_t , 1e7 N/m
 - Axial viscous damping, C_n , 100 N · s/m
 - Shear viscous damping, C_t , 100 N · s/m
 - Friction ratio, μ , 0.25

SIMULATION TIME: With 32 cores on AWS EC2 c4.8xlarge instance, the running time for this example is 30 hours.

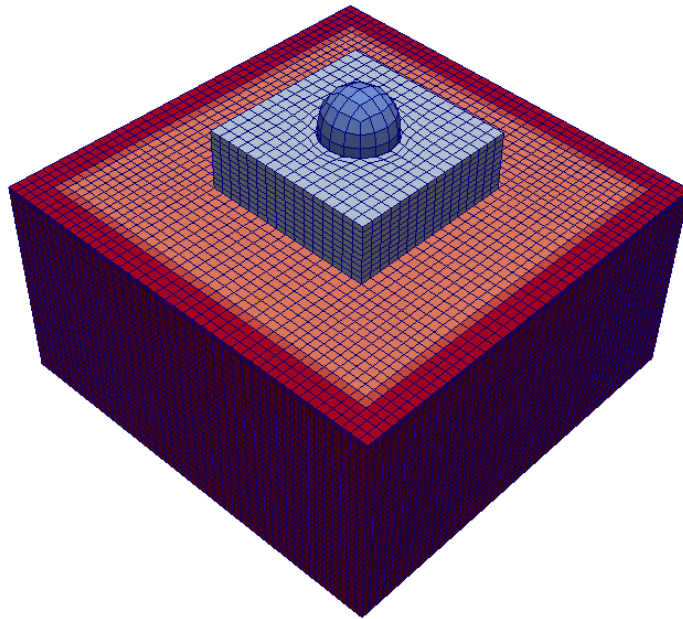


Figure 6.90: Simulation Model.

6.4.9 Buildings, ATC-144/FEMA-P-2091 Examples

The Real-ESSI building examples, models from FEMA-P-2091 report are available in Sections [509.2](#) (page [2676](#)), [509.4](#) (page [2684](#)), and [509.5](#) (page [2688](#)), in Lecture Notes by [Jeremić et al. \(1989-2025\)](#) ([Lecture Notes URL](#)).

Bibliography

B. Jeremić, Z. Yang, Z. Cheng, G. Jie, N. Tafazzoli, M. Preisig, P. Tasiopoulou, F. Pisanò, J. Abell, K. Watanabe, Y. Feng, S. K. Sinha, F. Behbehani, H. Yang, H. Wang, and K. D. Staszewska. *Non-linear Finite Elements: Modeling and Simulation of Earthquakes, Soils, Structures and their Interaction*. Self-Published-Online, University of California, Davis, CA, USA, 1989-2025. ISBN 978-0-692-19875-9. URL: <http://sokocalo.engr.ucdavis.edu/~jeremic/LectureNotes/>.